DEPARTMENT OF TRANSPORTATION

Environmental Impacts of Potassium Acetate as a Road Salt Alternative (Iowa State University evaluation)

Chris Rehmann, Principal Investigator
Institute for Transportation
Iowa State University

JULY 2022

Research Report
Final Report 2022-27B

To request this document in an alternative format, such as braille or large print, call 651-366-4718 or 1-800-657-3774 (Greater Minnesota) or email your request to ADArequest.dot@state.mn.us. Please request at least one week in advance.

Technical Report Documentation Page

1. Report No.	2.	3. Recipients Accession No.
MN 2022-27B		

4. Title and Subtitle	5. Report Date
Environmental Impacts of Potassium Acetate as a Road Salt Alternative (Iowa State University evaluation)	June 2022
	6.

7. Author(s)	8. Performing Organization Report No.
Chris Rehmann, Kaoru Ikuma, Masrur Mahedi, and Michael Perez	

9. Performing Organization Name and Address	10. Project/Task/Work Unit No.
Institute for Transportation Iowa State University 2711 S. Loop Drive, Suite 4700 Ames, IA 50010	11. Contract (C) or Grant (G) No. (c) 1034774

12. Sponsoring Organization Name and Address	13. Type of Report and Period Covered
Minnesota Department of Transportation Office of Research & Innovation 395 John Ireland Boulevard, MS 330 St. Paul, Minnesota 55155-1899	Final Report 14. Sponsoring Agency Code

15. Supplementary Notes

https://www.mndot.gov/research/reports/2022/202227B.pdf

See related report "Environmental Impacts of Potassium Acetate as a Road Salt Alternative (University of Minnesota evaluation)" by J. Gulliver at https://www.mndot.gov/research/reports/2022/202227A.pdf.

16. Abstract (Limit: 250 words)

The goal of this research project was to determine the environmental impact of potassium acetate (KAc) as a deicer, including its effects on water quality and the resulting toxicity to biota. The motivation for the research was the Minnesota Department of Transportation's (MnDOT's) exploratory use of KAc to significantly reduce the use of chloride-based deicers in controlling snow and ice on roads and the potential benefits, including reduced environmental effects.

This study evaluated the environmental impact of KAc as a deicer through field measurements, laboratory experiments, and modeling. Field sites, including bridges and tunnels, were selected to investigate a range of conditions, and sampling characterized KAc concentrations in soil and water as well as measured dissolved oxygen, biochemical oxygen demand, pH, and other water-quality parameters. Laboratory experiments investigated the persistence of KAc and its microbial toxicity at higher resolution than possible in field sampling.

To predict the spatial and temporal extent of KAc's environmental effects, models of the fate and transport of KAc in runoff to streams and lakes were constructed and evaluated. A detailed user's manual for the models is provided as an appendix in this report.

The researchers recommend that the two models, KAcStream and KAcLake, be used by MnDOT to guide its choice of sites and concentrations of KAc deicer applications. These models also allow for initial estimates of the environmental impact of KAc applications.

17. Document Analysis/Descriptors	18. Availability Statement
Acetates, Anti-icing, Deicing, Deicing chemicals, Potassium, Toxicity	No restrictions. Document available from: National Technical Information Services, Alexandria, Virginia 22312

19. Security Class (this report)	20. Security Class (this page)	21. No. of Pages	22. Price
Unclassified	Unclassified	102	

ENVIRONMENTAL IMPACTS OF POTASSIUM ACETATE AS A ROAD SALT ALTERNATIVE (IOWA STATE UNIVERSITY EVALUATION)

FINAL REPORT

Prepared by:

Chris Rehmann, Kaoru Ikuma, and Masrur Mahedi
Department of Civil, Construction, and Environmental Engineering
Iowa State University

Michael Perez
Department of Civil and Environmental Engineering
Auburn University

JULY 2022

Published by:

Minnesota Department of Transportation
Office of Research & Innovation
395 John Ireland Boulevard, MS 330
St. Paul, Minnesota 55155-1899

ACKNOWLEDGMENTS

The research team would like to thank the Minnesota Department of Transportation (MnDOT) for funding this project, as well as the project champions, Tara Carson and Nicklas Tiedeken, and the project coordinators, Thomas Johnson-Kaiser and Leif Halverson.

The research team also thanks the Technical Advisory Panel (TAP) members for their assistance and helpful guidance throughout the project: Christopher Cheney, maintenance superintendent; Perry Collins, District 1 operations engineer; Michael Hedlund, District 1 sub-area supervisor; Shannon Holland, traffic control supervisor; Laura Lyle, chief toxicologist; Nicholas Olson, District Metro project manager; Brent Rusco, Local Road Research Board (LRRB) research program manager; Robert Vasek, maintenance contracts; Brooke Asleson, Minnesota Pollution Control Agency; John Gulliver, University of Minnesota; and Jessica Wilson, city of Edina.

The team also thanks the members of the University of Minnesota research team, led by John Gulliver, for their help and productive collaboration—and, in particular, Chan Lan Chun, Kathryn Cassidy, Jerry Henneck, and Andy Erickson. Student and postdoctoral researchers at Iowa State University who contributed to this project included Masrur Mahedi, Yifei Ma, Rayla Pinto Vilar, Soo Bin Chun, and Calvin Maples.

TABLE OF CONTENTS

LIST OF FIGURES

LIST OF TABLES

ACRONYMS

FIELD EVALUATION SITES

BB	Blatnik Bridge
BC	Brewery Creek
CE	Central Entrance
KAc	potassium acetate (deicer application)
LS	Lake Superior
NaCl	sodium chloride (deicer application)
RP	Rice's Point

WATER AND SOIL QUALITY MEASUREMENTS

BOD	biochemical oxygen demand
DO	dissolved oxygen
DWEL	drinking water equivalent level
EC	electrical conductivity
IC	inorganic carbon
ICP-AES	inductively coupled plasma atomic emission spectroscopy
MCL	maximum contaminant level
MDL	minimum detection limit
SOUR	specific oxygen uptake rate
SOM	soil organic matter
TC	total dissolved carbon
TOC	total organic carbon
WLT	water leach test

EXECUTIVE SUMMARY

PROJECT GOAL, PROBLEM STATEMENT, AND BACKGROUND

The overarching goal of this research project was to determine the environmental impact of potassium acetate (KAc) as a deicer, including its effects on water quality and the resulting toxicity to biota, which is the animal and plant life of a particular region, habitat, or geological period. The motivation for the proposed research was the Minnesota Department of Transportation's (MnDOT's) exploratory use of KAc to significantly reduce the use of chloride-based deicers in controlling snow and ice on roads and the potential benefits, such as lower maintenance costs and reduced environmental effects.

The benefits of using most deicers are greatly reduced by their adverse environmental effects. Given that salt components, and particularly chlorides, don't readily adsorb onto soil or naturally degrade, they are highly mobile in surface runoff. Also, given that chloride causes corrosion and harms soil and water quality, MnDOT has investigated and experimented with alternative deicers. KAc is an appealing option because—unlike chloride-based deicers—it degrades in the environment.

In the Minneapolis-St. Paul metropolitan area, increases in the average chloride concentrations in nearby lakes have been strongly correlated with rock salt use in winter road maintenance (Novotny et al. 2008). Up to 70% of road salt applied in the area ended up in nearby lakes as well as in the groundwater. Other chemical deicers, such as glycol and glycerin, which are easily transported in runoff, have also harmed receiving waters. Ethylene and propylene glycol deicers, which have endocrine disrupting properties, have been shown to inhibit plant growth (Fay and Shi 2012).

Acetate-based deicers offer a promising alternative because they can be rapidly degraded and may have lower direct toxicity than other deicers. The half-life of acetate ranges from less than 2 d in soil at 7°C (Defourny 2000) to 21 d on airport surfaces at 4°C (Revitt and Worrall 2003) to 35 d in the unsaturated zone (French et al. 2001). However, a concern with acetate deicers is that they result in higher biochemical oxygen demand (BOD) in receiving waters, which leads to lower dissolved oxygen (DO) and toxicity related to hypoxia (Fay and Shi 2012).

BRIEF RESEARCH DESCRIPTION

This project assessed KAc's persistence in soil and water, its effects on water quality, and its toxicity to microorganisms. This assessment was addressed with field measurements, laboratory experiments, and modeling.

Between the Iowa State University (ISU) and University of Minnesota (U of M) teams, field sites were selected to investigate a range of conditions, and sampling characterized KAc concentrations in soil and water as well as measured dissolved oxygen (DO), BOD, pH, and other water-quality parameters. Laboratory experiments investigated the persistence of KAc and its microbial toxicity at higher resolution than possible in the field sampling.

Two models of the fate and transport of KAc in runoff to streams and lakes were constructed: KAcStream predicted the decrease in DO concentrations caused by BOD from KAc in streams, and KAcLake estimated the spread of KAc in a lake. These models complemented the watershed modeling of the U of M team.

MAJOR FINDINGS

Results from field sampling in Duluth during the winters of 2019–2020 and 2020–2021 showed that, while KAc deicers affected some water-quality parameters, the observed effects were relatively small. When applied on its own without mixing with chloride-based deicers, the KAc deicer appeared to have little effect on the concentrations of aqueous nitrogen species (e.g., ammonia, nitrite, nitrate) and heavy metals. While KAc deicer application resulted in elevated total organic carbon (TOC) and sulfate concentrations, the elevated TOC was likely from the acetate in the deicer, and the CF7 KAc-based deicer (Cryotech) used by MnDOT has also been reported to include high sulfate concentrations.

Unsurprisingly, KAc deicer application led to greater potassium concentrations in runoff water. The runoff samples from KAc-applied areas also tended to have higher sodium and calcium concentrations, which was unexpected. Further discussion with MnDOT and city of Duluth staff revealed the likelihood that these areas still received some chloride-based deicer either directly or in the immediate vicinity, which may have resulted in the presence of Na, Ca, and Cl in the samples. However, these elevated concentrations of TOC, sulfate, Na, Ca, and Cl observed in runoff appeared to have limited impact on surface waters in the surrounding areas. Similarly, the application of KAc deicers resulted in limited effects on soil quality (i.e., only elevated potassium concentrations), especially compared to areas with chloride-based deicer application.

Contrary to some published studies, there was no observable aerobic biodegradation of KAc by representative surface water and soil microorganisms at room temperature up to 28 days. Soil slurries composed of soil from sites receiving KAc deicer application (e.g., the I-35, Rice's Point, and Blatnik Bridge sites) and Duluth surface waters from Lake Superior and Lester River showed no change in acetate concentrations even when exposed to pure KAc chemicals.

These observations suggest that KAc biodegradation is unlikely or will occur at a very slow rate around Duluth (i.e., by native microbial communities) under aerobic and spring/summer conditions. These results are supported by literature that indicates acetate, while used for critical cellular mechanisms, is often not biodegraded at all or, at most, removed at very slow rates under aerobic conditions. Furthermore, laboratory experiments with model bacterial species showed that the KAc deicer had limited impact on bacterial metabolism even at high concentrations (e.g., 3.5 g/L, which is similar to acetate concentrations measured in runoff water samples). However, the deicer resulted in slightly lower metabolism in model bacteria compared to comparable concentrations of pure KAc, pointing to the potential impact of deicer additives. These results suggest that the presence of KAc deicer (either as acetate or potassium) does not exhibit toxicity toward bacteria at the concentrations observed in the runoff samples.

Two models of KAc fate and transport in streams and lakes were developed. The KAcStream model provides a way to estimate the DO deficit from KAc. This deficit is likely to be small compared to the DO concentration at saturation. For a wide range of conditions tested in this project, the deficit was less than 2 mg/L, or 15% of the concentration at saturation. The KAcLake model provides a way to estimate the concentrations as a cloud of KAc spreads in a lake. KAc concentrations from runoff in lakes can reach high values initially and drop sharply because of spreading in three dimensions. Initial simulations using these models suggest that the direct impact of KAc on dissolved oxygen levels in streams and lakes would be relatively small overall. The models were made available to MnDOT as an openly accessible MATLAB Runtime application, in which initial conditions can be manipulated by users to better predict KAc fate and transport in aquatic environments of interest.

CONCLUSIONS AND RECOMMENDATIONS

The results from this project indicate that, while KAc deicers can have immediate impacts on water quality from field application, these impacts appear to be relatively small especially to larger bodies of water. Although larger fauna were not assessed, the impact of KAc on aerobic bacteria appeared to be small. The fate and transport models further suggest that the impact of KAc deicers on DO levels in the water would be limited. However, these impacts would likely be magnified in sensitive water bodies, so caution should be exercised before applying KAc deicers in these areas.

The researchers recommend that MnDOT use the two models, KAcStream and KAcLake, to guide its choice of sites and concentrations of KAc deicer applications. These models allow for initial estimates of the environmental impact of KAc applications.

CHAPTER 1: INTRODUCTION

This research project was motivated by MnDOT's exploratory use of potassium acetate (KAc) to significantly reduce the use of chloride-based deicers to control snow and ice on roads and the potential benefits, such as lower maintenance costs and reduced environmental effects. Given that chloride causes corrosion and harms soil and water quality, MnDOT has investigated and experimented with alternative deicers. KAc is an appealing option because—unlike chloride-based deicers—it degrades in the environment. In collaboration with another research project team, at the University of Minnesota Twin Cities/Duluth, this research team evaluated the environmental impacts of KAc use in Duluth.

The benefits of using most deicers are greatly reduced by their adverse environmental effects. Given that salt components, and particularly chlorides, don't readily adsorb onto soil or naturally degrade, they are highly mobile in surface runoff.

In the Minneapolis-St. Paul metropolitan area, increases in the average chloride concentrations in nearby lakes were strongly correlated with rock salt use in winter road maintenance (Novotny et al. 2008). Up to 70% of road salt applied in the area ended up in nearby lakes as well as in the groundwater. Other chemical deicers, such as glycol and glycerin, which are easily transported in runoff, have also harmed receiving waters. Ethylene and propylene glycol deicers, which have endocrine disrupting properties, have also inhibited plant growth (Fay and Shi 2012).

Acetate-based deicers offer a promising alternative because they can be rapidly degraded and may have lower direct toxicity than other deicers. The half-life of acetate ranges from less than 2 d in soil at 7°C (Defourny 2000) to 21 d on airport surfaces at 4°C (Revitt and Worrall 2003) to 35 d in the unsaturated zone (French et al. 2001). However, a concern with acetate deicers is that they result in higher biochemical oxygen demand (BOD) in receiving waters, which leads to lower dissolved oxygen (DO) and toxicity related to hypoxia (Fay and Shi 2012).

Also, low temperatures during winter can reduce microbial activity that leads to degradation. Nevertheless, transport of KAc through soil may be small: simulations accounting for retardation and degradation suggest that less than 1% of infiltrated water would reach a water table 4 m deep in three weeks (French et al. 2001).

This study evaluated the environmental impact of KAc as a deicer for use by MnDOT through field measurements, laboratory experiments, and modeling. The specific KAc deicer evaluated was Cryotech CF7. Field sites, including bridges and tunnels, were selected to investigate a range of conditions, and sampling characterized KAc concentrations in soil and water as well as measured DO, BOD, pH, and other water quality parameters. Results from two winters are discussed in Chapters 2 and 3.

Laboratory experiments investigated the persistence of KAc and its microbial toxicity at higher resolution than possible in the field sampling. Results from the laboratory experiments are reported in Chapter 4.

To predict the spatial and temporal extent of KAc's environmental effects, a model of the fate and transport of KAc in runoff to streams and lakes was constructed and evaluated. The model is reported in Chapter 5, and a detailed user's manual for the model is provided in an appendix.

Chapter 6 presents the overall project conclusions and summarizes the major findings and recommendations.

Appendix A contains a user's manual for the models KAcStream and KAcLake. Appendix B has the standard operating procedure for the field sampling. Appendix C provides details on characterizing the size of a contaminant cloud in a lake.

CHAPTER 2: FIRST FIELD ASSESSMENT OF THE POTASSIUM ACETATE DEICER

2.1 OBJECTIVES

The research team implemented a field assessment plan during the first sampling season of winter 2019–2020 when KAc was applied in Duluth; both water and soil samples were collected from the identified sites during the season. The sampling plan was coordinated and carried out in collaboration with the University of Minnesota (U of M) team. The research team from Iowa State University (ISU), along with researchers from the University of Minnesota Duluth (UMD), collected runoff and soil samples and conducted analyses of pH, electrical conductivity (EC), and concentrations of total organic carbon (TOC), inorganic carbon (IC), sulfate (SO_4), ammonia (NH_3), nitrate-N + nitrite-N, nitrite-N, nitrate-N, potassium (K), calcium (Ca), magnesium (Mg), sodium (Na), aluminum (Al), iron (Fe), cadmium (Cd), nickel (Ni), lead (Pb), and zinc (Zn). Additional data from the same water samples is being reported on by the U of M/UMD team, including acetate concentrations and five-day BODs.

2.2 SITE SELECTION AND SAMPLING METHODS

2.2.1 Locations

The ISU and UMD research teams collected road runoff from three sites along I-35, three sites along Central Entrance, and two sites by Blatnik Bridge (Figure 2.1), of which some sites were control sites receiving chloride-based deicers and some were test sites with KAc application.

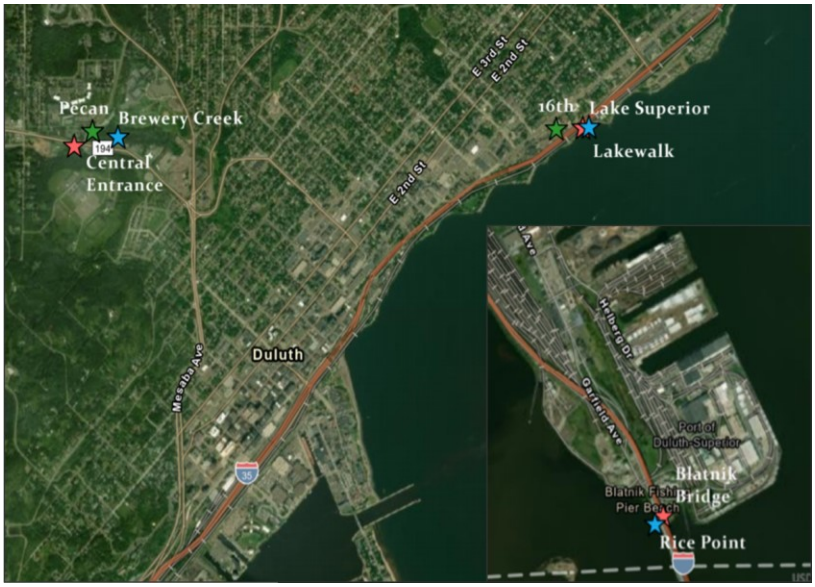

Imagery ©2019, Map data ©2019, Google Earth
Red stars = KAc samples, green stars = sodium chloride samples, and blue stars= samples in receiving waters

Figure 2.1. Sampling sites in Duluth, Minnesota

In addition, soil samples were collected at sites immediately adjacent to roads on which chloride-based and KAc deicers were applied. Specifically, soil sampling focused on the three sites along the Central Entrance route as well as the site below Blatnik Bridge because soil at these sites were safest to access.

2.2.2 Sampling Times

During winter 2019–2020, the research team from ISU conducted four visits to the sampling sites in Duluth (Table 2.1).

Table 2.1. Field visit schedule during winter 2019–2020

Date	Duration (Days)	Runoff Samples	Soil Samples	Activity
11/21/2019	3	✓		Installation of automated water samplers
12/19/2019	2	✓		Collection of grab runoff samples
02/01/2020	2	✓		Collection of automated and grab runoff samples
03/12/2020	2	✓	✓	Collection of automated and grab samples; collection of soil samples

The field visits were intended to collect runoff samples and soil samples from each of the sampling locations. In addition, the research team obtained runoff samples collected by the UMD team.

2.2.3 Sampling Methods

To collect the surface runoff samples, two automated water samplers (Teledyne ISCO 6712) were deployed. These were in the KAc sites at the Central Entrance and Lakewalk. The samplers were housed in a lockbox and powered by a 12V deep-cycle marine battery, which was charged by a solar panel mounted on the top of the housing (Figure 2.2).

© 2022 Teledyne ISCO

(a) **(b)**

(c)

Figure 2.2. (a) ISCO 6712 sampler, (b) sampler tray, and (c) sampler housing with the research teams from ISU and UMD

The samplers were programmed on an 8-hour time interval to accumulate a 0.75 L (25.36 oz) runoff sample each day. Each sample was collected in a separate ISCO pie bottle. To account for low flow of runoff during most of the sampling events, the researchers collected composite samples. A total of 24 pie bottles were held in a single sampler at a time.

In addition, grab samples were collected from Brewery Creek, Lake Superior, and Rice's Point, which were the other three test areas (previous Figure 2.1). Samples were collected in buckets and were immediately measured for pH, temperature, and DO using a portable Yellow Springs Instruments (YSI) device (Figure 2.3).

(a) (b)

Figure 2.3. (a) Surface water sample collection, and (b) measurement of pH, temperature, and DO at the Brewery Creek and Rice's Point locations

When the streams were frozen, the researchers used a metal pick to break the ice layer. For the collection of the Blatnik Bridge samples, initially, it was decided to use the drainage pipes to for sampling purposes. However, the drainage pipes were not connected with the bridge deck outlet due to frequent clogging of pipes by runoff debris. Therefore, a 55-gallon plastic barrel was installed just below the bridge deck outlet to collect the bridge runoff (Figure 2.4).

Figure 2.4. Runoff collection for Blatnik Bridge site

The barrel was only able to catch a little runoff due to varying wind speed and wind direction. As such, it was possible to collect only three bridge runoff samples during the winter 2019–2020 sampling season.

2.2.4 Runoff Sample Processing

The collected runoff samples were transported to the Natural Resources Research Institute (NRRI) at UMD where the samples were processed for further analyses. All samples were initially filtered through a piece of cloth (approximately 150-µm pore size) to remove any visible debris and soil particles. Next, subsamples were acidified with 10% trace metal-grade nitric acid to a pH lower than 2 and stored in 50

mL acid-washed centrifuge tubes for metal analysis. Another non-acidified subsample was stored for nutrient analysis. In addition, an aliquot of the collected samples was pressure filtered through 0.2-µm pore sized membranes into acid-washed centrifuge tubes (Cetin et al. 2012). A portion of the filtered samples was acidified, and another non-acidified portion was immediately frozen for nutrient analyses. Thus, each collected runoff sample was processed into four aliquots, (1) non-filtered and non-acidified, (2) non-filtered and acidified, (3) filtered and non-acidified, and (4) filtered and acidified, as specified by the U.S. Environmental Agency (EPA) methods used for each analyte.

2.2.5 Soil Sample Collection

Soil samples were collected along the roadway sections where KAc and NaCl were applied to evaluate the physical and environmental changes in soils exposed to deicers. For the collection of soil samples, a handheld soil sampler probe was used. It was only possible to collect the soil samples in March 2020 during the first field sampling campaign as the research team was unable to push the sampler into the soil when the ground was completely frozen in the earlier months of sampling. In March 2020, the soil was partially thawed, which allowed the collection of samples up to the depth of 4 to 5 in.

Soil samples were collected from the Central Entrance (KAc) and Pecan Street (NaCl) sites. Snow was piled along the roadsides of 6th Street, Lakewalk, and beneath the Blatnik Bridge, and hence the sampling from these locations was restricted. Soil samples were collected from nine points from each of the sampling sites (Figure 2.5).

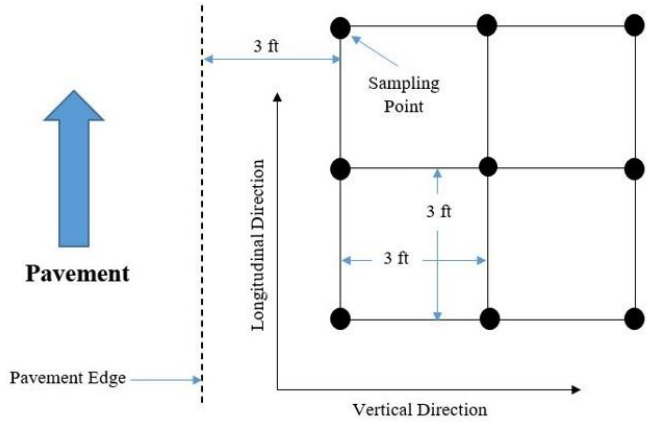

Figure 2.5. Soil sampling schematic

Samples were collected in grids, with three rows along the pavement direction. A sample spacing of 3 ft was maintained between the sampling points. An interval of 3 ft was also allowed between the pavement (sidewalk) edge and the first sampling row.

2.2.6 Soil Sample Processing

Soil samples were used to perform the batch water leach tests (WLTs) in accordance with ASTM D4793 *Standard Test Method for Sequential Batch Extraction of Waste with Water*. A liquid to solid (L/S) ratio

of 10 was used to simulate the representative field conditions (Kosson et al. 2002). The influent solution for WLTs was nanopure water. The mixtures were rotated at 29 rpm for 180.25 h (Figure 2.6).

Figure 2.6. Shaker used for the preparation of soil leachate

Once equilibrium was established, pH and EC of the supernatant fluid were measured. Next, the samples were centrifuged for 15 minutes at 3,000 rpm. The solutions were then filtered through 0.2-µm pore sized membranes using acid-washed pressure filter holders and plastic syringes. The filtered extract was acidified with 10% trace metal-grade nitric acid to a pH lower than 2 and stored at 4°C.

2.3 LABORATORY ANALYSES

The acidified runoff and soil samples were analyzed for effluent metal concentrations using inductively coupled plasma atomic emission spectroscopy (ICP-AES). The solution concentrations of K, Ca, Mg, Na, Al, Fe, Cd, Ni, Pb, and Zn were measured in this study. The ICP-AES equipment was calibrated with known concentrations of multi-element standards. Due to a wide range of metal concentrations, multiple calibration curves were prepared. Checking standards and blanks were analyzed every nine samples to verify the calibration curves. The minimum detection limits (MDLs) of ICP-AES for Ca, Mg, Na, K, Al, Fe, Cd, Ni, Pb, and Zn were 0.004 mg/L, 0.0012 mg/L, 0.03 mg/L, 0.008 mg/L, 0.0018 mg/L, 0.0012 mg/L, 0.001 mg/L, 0.0007 mg/L, 0.019 mg/L, and 0.0003 mg/L, respectively.

Dissolved inorganic and organic carbon concentrations in non-acidified samples were measured using a Shimadzu TOC-V analyzer. The instrument was calibrated using standard sodium bicarbonate ($NaHCO_3$) and sodium carbonate (Na_2CO_3) solutions for inorganic carbon measurements and potassium hydrogen phthalate ($C_8H_5KO_4$) solutions for organic carbon measurements. Sulfate measurements on non-acidified samples were carried out using a SEAL Analytical Limited AQ_2 analyzer, following the EPA-123-A Rev. 5 method. The method detection limit for the sulfate was 1 mg SO_4/L. In addition, the SEQL AQ2 analyzer was used to measure the effluent concentrations (non-acidified samples) of nitrate-N + nitrite-N, nitrite-N, and ammonia concentrations, following EPA-114-A Rev. 10 for nitrite/nitrate, EPA-115-A for nitrite, and EPA-129-A Rev. 8 for ammonia. Chloride concentrations were measured following the EPA-105-A Rev.5 method. The detection limits were 0.03 mg N/L, 0.0008 mg N/L, 0.05 mg N/L, and 0.3 mg/L for nitrite/nitrate, nitrite, ammonia, and chloride, respectively.

2.4 RESULTS AND DISCUSSION

2.4.1 I-35 Sites

I-35 sites provided different runoff samples with NaCl or KAc deicer application in addition to Lake Superior (LS) samples from the Lakewalk.

2.4.1.1 Nutrient Concentrations

Figure 2.7(a) shows the total dissolved carbon (TC) concentrations in the surface water runoff collected from the I-35 sites.

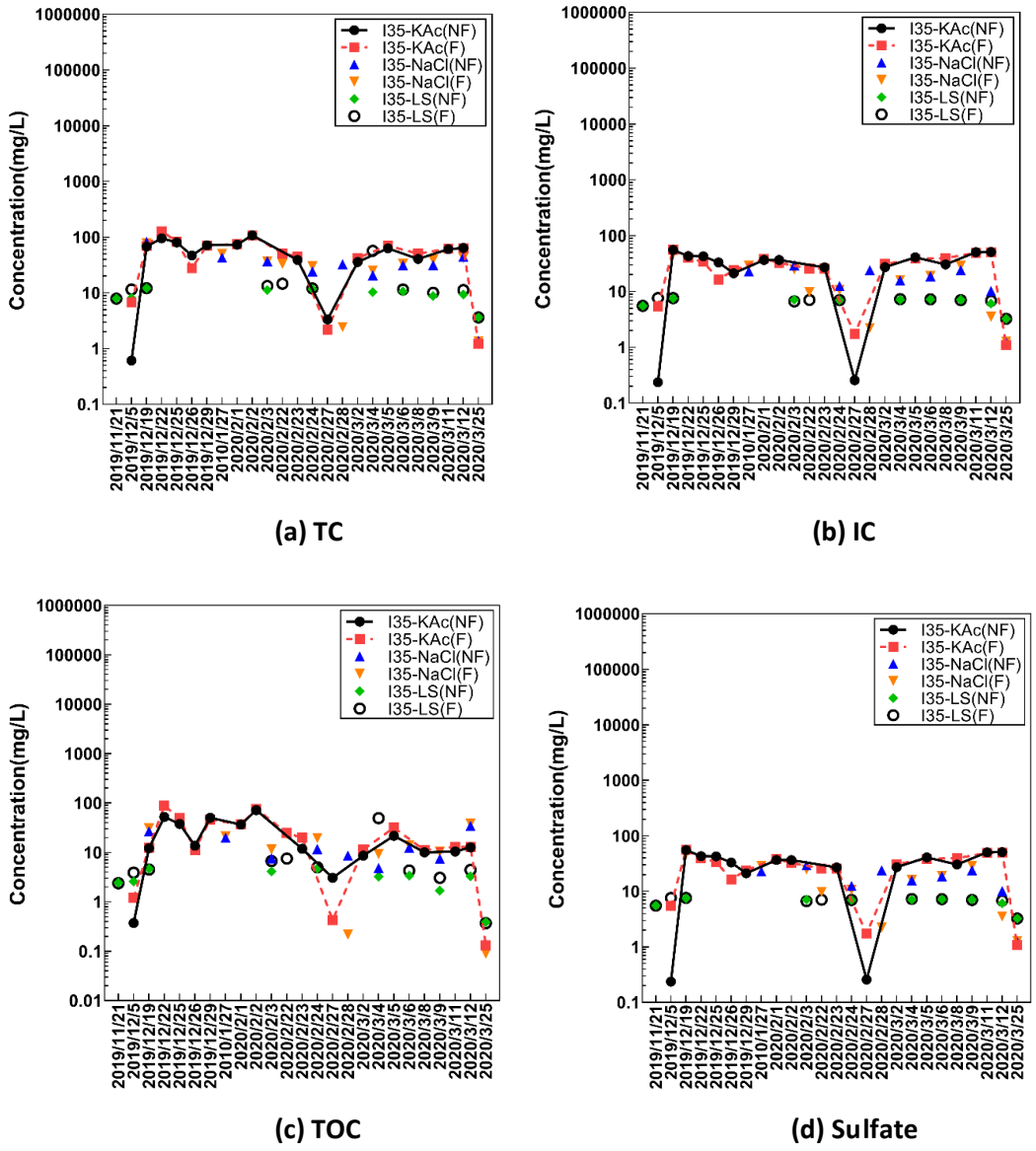

Figure 2.7. Concentrations of (a) TC, (b) IC, (c) TOC, and (d) SO_4 in the surface water collected from I-35 sites

The TC concentrations in the LS samples varied within the range of 3.27 to 17.6 mg/L. The NaCl and KAc sites had higher levels of TC compared to LS. The maximum concentrations of TC in the samples from the NaCl and KAc sites were observed in early February 2020. For the KAc site, three peak concentrations of TC were found during December 2019 and January 2020 and February 2020. As shown in Figure 2.7(b), the peaks agreed with the corresponding runoff concentrations of IC. Conversely, similar peaks were observed in the TOC concentrations curves (Figure 2.7(c)). Thus, the peaks in TC and TOC concentrations likely corresponded to the applications of KAc. The use of KAc increased the runoff concentrations of TOC, which also contributed to the eluate concentrations of TC. In addition, both the filtered and unfiltered samples had similar concentrations of TC, IC, and TOC.

As shown in Figure 2.7(d), SO_4^{2-} concentrations in LS samples were between 2.6 mg/L and 8 mg/L. The concentrations of SO_4^{2-} in LS samples were almost constant except for the samples collected in mid-December 2019 and late February 2020. The concentrations of SO_4^{2-} in the runoff from NaCl and KAc sites were noticeably higher compared to LS. Moreover, the highest concentrations of SO_4^{2-} were observed for the KAc site. The CF7 KAc deicer indeed appeared to contain sulfates, leading to our observations of increased runoff concentrations of SO_4^{2-}. Furthermore, no significant variations in SO_4^{2-} concentrations were observed reliant on the filtration conditions.

The concentration of ammonia (NH_3), NO_x, NO_2^-, and NO_3^- in the collected runoff samples from the I-35 sites are illustrated in Figure 2.8.

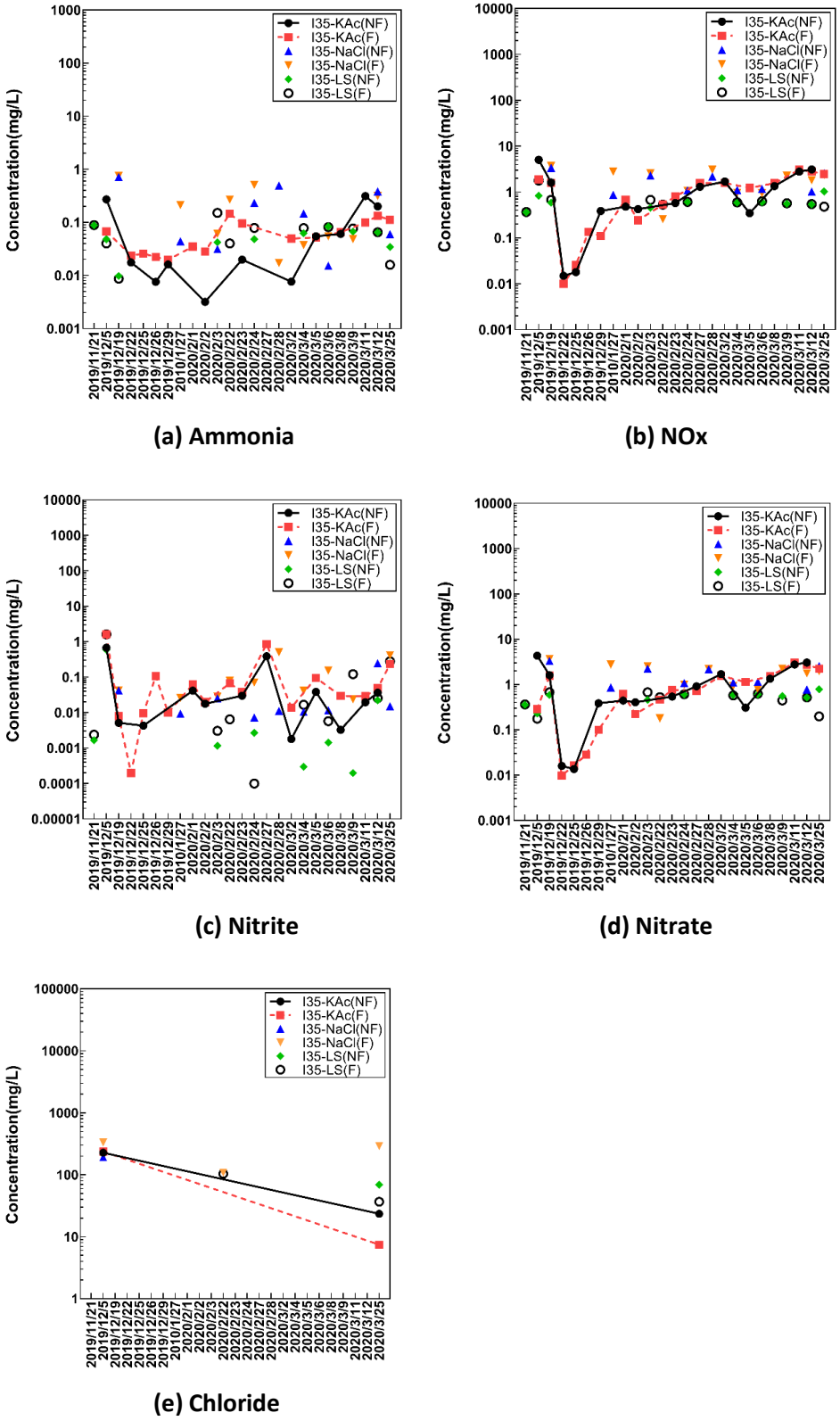

Figure 2.8. Concentrations of (a) ammonia (NH_3), (b) nitrite+nitrate (NO_x), (c) nitrite (NO_2), (d) nitrate (NO_3), and (e) chloride in the surface water collected from I-35 sites

For the sampling period of 2019–2020, no consistent trend in the concentrations of these nutrients was observed. Yet, it could be concluded that the NaCl site had slightly higher concentrations of NH_3, NO_x, and NO_3^- than those measured in the KAc runoff. The average concentrations of NH_3, NO_x, NO_2^-, and NO_3^- in the LS samples were 0.085 mg/L, 0.591 mg/L, 0.012mg/L, and 0.499 mg/L, respectively. The average NH_3, NO_x, NO_2^-, and NO_3^- concentrations in the KAc site samples were 0.054 mg/L, 1.145 mg/L, 0.095 mg/L, and 1.07 mg/L. The maximum contaminant levels (MCLs) of NOx, NO_2^-, and NO_3^- for drinking water are 10 mg/L, 1 mg/L, and 10 mg/L, respectively (U.S. EPA 2018). In addition, 30 mg/L of ammonia was identified as the taste threshold value. As discussed earlier, the concentrations of NH_3, NO_x, NO_2^-, and NO_3^- measured in the collected samples were significantly lower than the U.S. EPA drinking water standards and health advisories. The chloride concentration in the KAc site samples varied within the range of 108.7 to 333.3mg/L. The KAc and NaCl sites had higher levels of chloride compare to LS samples. The chloride concentration of the KAc and LS site samples significantly dropped in late March 2020, while there was no sign of it in the NaCl site samples.

2.4.2 Primary Metal Concentrations

Figure 2.9(d) shows the K concentrations in the samples collected from the I-35 sites.

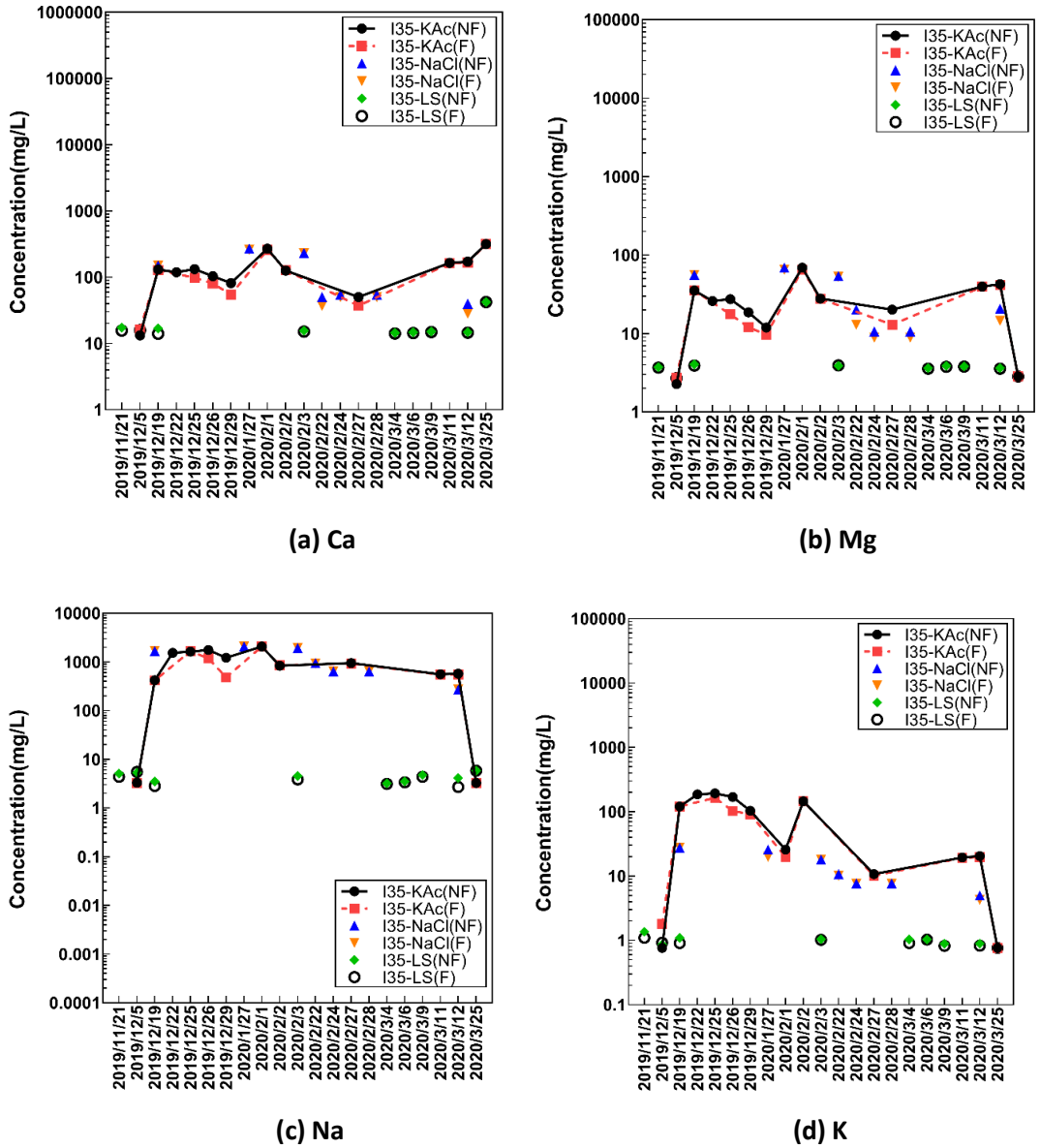

Figure 2.9. Metal concentrations in the surface water collected from I-35 sites (a) Ca, (b) Mg, (c) Na, and (d) K

The average concentration of K in the LS samples was 0.98 mg/L. The average K concentration in the samples collected from the NaCl site was 13.2 mg/L. The maximum concentrations of K were measured in the KAc samples (19–229 mg/L). The stormwater collection system located on the east side of Duluth Lakewalk collected the snowmelt water from I-35, where only KAc was applied. Therefore, the highest observed concentrations of K were likely due to the KAc used as the deicer. In addition, K concentrations in the runoff decreased in February 2020, which may have happened due to lower application rates of the deicer in later winter. Similarly, deicer applications likely ceased by late March as evidenced by the significant decrease in K concentrations in the March 25th water samples.

Figure 2.9(a) indicates that the Ca concentrations in the LS samples were nearly constant throughout the sampling period except for the samples collected in late March (14.5–16.5 mg/L). However, the

concentrations of Ca in the samples collected from the NaCl and KAc sites fluctuated depending on sampling time. In addition, concentrations of Ca in the runoff from the NaCl and KAc sites were 2 to 20 times higher than the concentrations in the LS samples. Similar observations were made for the measured concentrations of Mg (Figure 2.9(b)). The LS samples had nearly constant Mg concentrations varying between 2.27 mg/L and 4.7 mg/L. Higher concentrations of Mg were measured in the runoff from the NaCl and KAc sites. The concentrations of Mg also fluctuated depending on sampling time.

As shown in Figure 2.9(c), the Na concentrations in the LS samples were nearly constant over the sampling period of 2019–2020. The average concentration of Na in the LS samples was 4.10 mg/L. The Na concentrations in the NaCl and KAc runoff were approximately two to three orders of magnitude higher than those measured in the LS samples. The samples from the KAc site had Na concentrations similar to those at the NaCl site. The NaCl site was 16th Avenue E, where chloride-based deicers were applied above I-35. Samples were periodically collected from the upstream stormwater collection system. The KAc samples were acquired from the downstream stormwater collection system located on the east side of Duluth Lakewalk. The research team theorized that these stormwater collection systems could be connected, and, therefore, flow from the upstream NaCl site could have resulted in equivalent Na concentrations in downstream KAc site samples.

2.4.3 Heavy and Trace Metal Concentrations

Figure 2.10(a) shows the concentrations of Al in the samples from the I-35 sites.

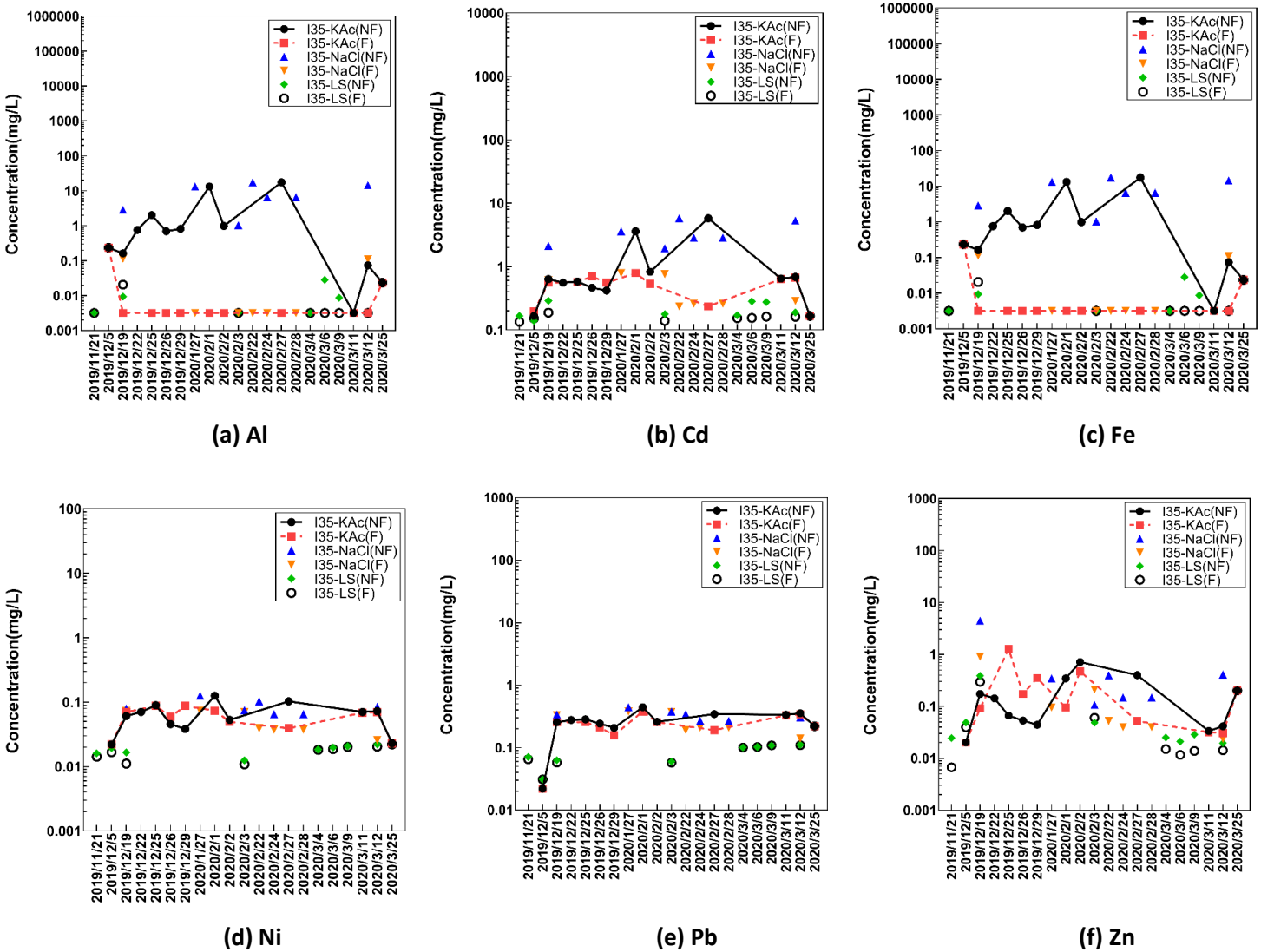

Figure 2.10. Metal concentrations in the surface water collected from I-35 sites: (a) Al, (b) Cd, (c) Fe, (d) Ni, (e) Pb, and (f) Zn

The average concentration of Al in the LS samples was 0.18 mg/L, which was below the MCL of 0.2 mg/L for drinking water. The Al concentrations in the runoff from the NaCl and KAc sites were above the MCL values. While no noticeable trend was observed in the runoff concentrations of Al, it could be concluded that the unfiltered samples had higher concentrations of Al compared to the filtered ones.

A similar observation was made for the runoff concentrations of Fe (Figure 2.10(b)). Fe concentrations in all filtered runoff samples were below the MCL of 0.3 mg/L.

It is well known that Al and Fe are the common elements presented in finer soil particles, and, in particular, clay (Barton and Karathanasis 2002). Thus, it was anticipated that clay particles were dispersed in the unfiltered samples, which released Al and Fe when the samples were acidified with 10% nitric acid. Thus, the concentrations of Al and Fe were higher in all the unfiltered samples.

The average concentration of Cd in the LS samples was 0.0082 mg/L, which was higher than the U.S. EPA specified MCL of 0.005 mg/L (Figure 2.10(c)). Cd concentrations in the LS samples were initially lower than 0.005 mg/L but increased noticeably after February 2020. However, the highest concentrations of Cd were measured in the collected runoff, regardless of the type of deicer applied, which points to increased runoff due to deicing in general leading to higher Cd levels instead of Cd directly coming from the deicers themselves.

As illustrated in Figure 2.10(d), the concentrations of Ni in the NaCl and KAc runoff were similar and higher than in the LS samples. However, the concentrations of Ni in the samples collected from the I-35 sites were well below the drinking water equivalent level (DWEL) of 0.7 mg/L.

Figure 2.10(e) shows that the concentrations of Pb in all the samples were always higher than the U.S. EPA specified MCL of 0.015 mg/L. The samples from deicer application sites all had higher Pb levels compared to the LS samples. These observations point to the likelihood that, similar to Cd, increased runoff from ice/snow melt due to deicer application on roads generally increased the concentrations of Ni and Pb rather than those metals being present in high concentrations in either type of deicer. On the other hand, Zn concentrations did not show any consistent trend when it was compared between the LS, NaCl, and KAc samples (Figure 2.10(f)).

2.4.4 Central Entrance Sites

Central Entrance sites included different runoff samples from NaCl and KAc deicer application points, as well as the Brewer Creek water samples.

2.4.4.1 Nutrient Concentrations

Figure 2.11(a) shows the TC concentrations in the surface water runoff collected from the Central Entrance (CE) sites.

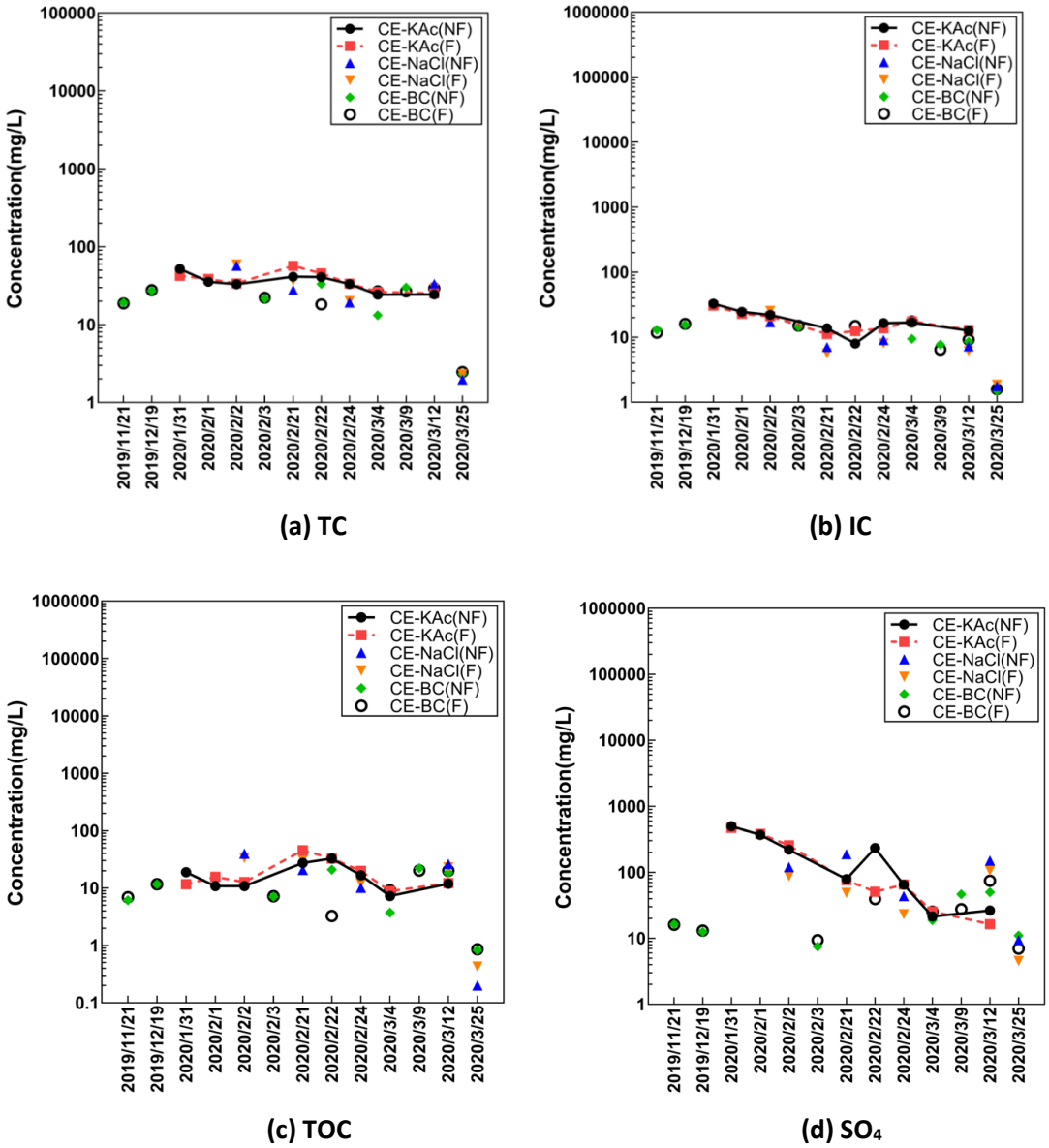

Figure 2.11. Concentrations of (a) TC, (b) IC, (c) TOC, and (d) SO_4 in the surface water collected from Central Entrance sites

The average TC concentration in the Brewery Creek (BC) samples was 19.30 mg/L. Thus, the TC concentrations in the BC samples were approximately two times higher compared to the LS samples. During January and February 2020, the NaCl and KAc sites had higher concentrations of TC compared to the BC samples. A peak concentration of TC in the KAc runoff was observed during February 2020 (57 mg/L). Compared to the corresponding IC and TOC concentrations of the samples, it was evident that the peak concentration in TC resulted from higher TOC concentrations (Figures 2.11(b) and (c)). The peak concentrations in TC and TOC may have occurred due to the KAc application as a deicer. For the NaCl site, TC, IC, and TOC concentrations gradually decreased after February 2020. Higher snowmelt volumes due to increased temperature may have diluted the runoff concentrations of TC, IC, and TOC. In

addition, no significant differences to TC, IC, or TOC concentrations were observed between the filtered and unfiltered samples.

As shown in Figure 2.11(d), the average SO_4 concentration in the BC samples was about 14.46 mg/L, which is approximately four times higher than that for the LS samples. The concentrations of SO_4 in the BC samples was almost constant except for the samples collected in late February and early March 2020. The concentrations of SO_4 in the runoff from the NaCl and KAc sites were noticeably higher compared to that for the BC samples. During late January 2020, higher concentrations of SO_4 were measured in the KAc runoff than those measured in the NaCl runoff. In addition, no significant variation in SO_4 concentrations was observed, depending on the filtration conditions.

The concentrations of ammonia (NH_3), NO_x, NO_2, and NO_3 in the samples from the CE sites are illustrated in Figure 2.12.

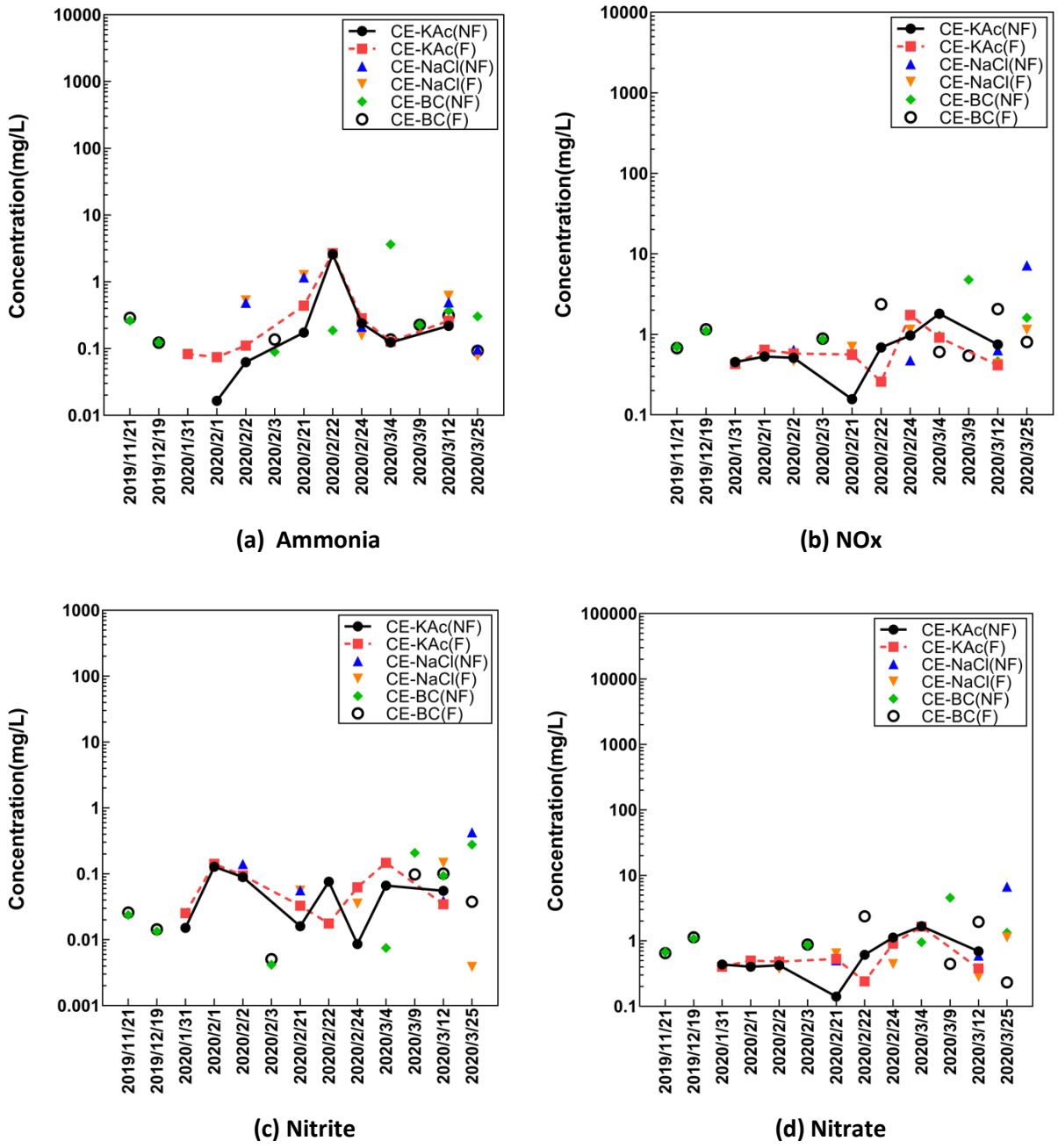

Figure 2.12. Concentrations of (a) ammonia (NH_3), (b) nitrite+nitrate (NO_x), (c) nitrite (NO_2), and (d) nitrate (NO_3) in the surface water collected from Central Entrance sites

For the sampling period of 2019–2020, no consistent trend in the concentrations of these nutrients was observed.

2.4.4.2 Primary Metal Concentrations

Figure 2.13(d) shows the K concentrations in the samples collected from the CE sites.

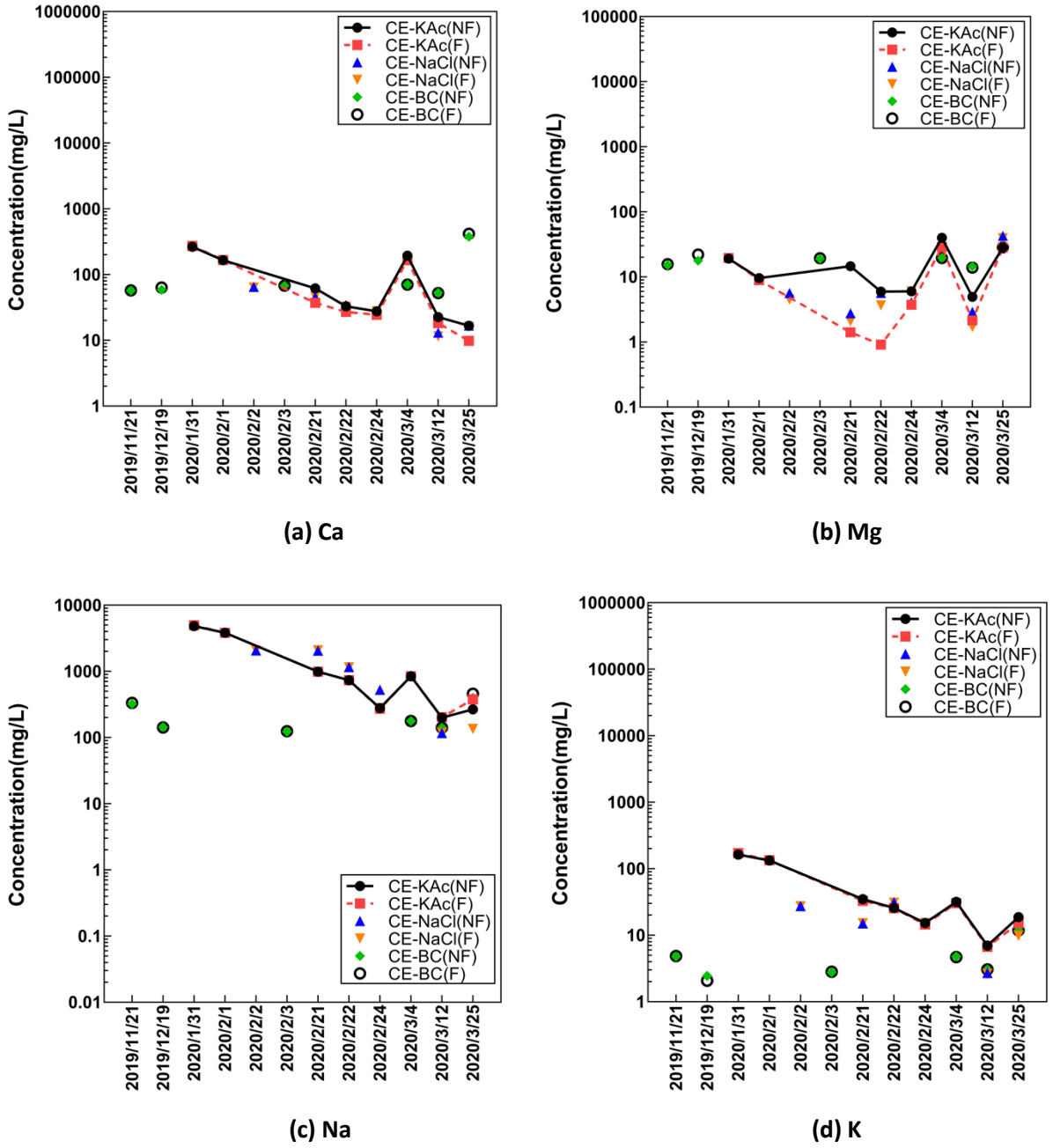

Figure 2.13. Metal concentrations in the surface water collected from Central Entrance sites (a) Ca, (b) Mg, (c) Na, and (d) K

The average concentration of K in the BC samples was 4.7 mg/L. The concentrations of K in the samples collected from the NaCl site were in the range of 2.6 mg/L to 31.2 mg/L, while K concentrations in the KAc runoff were between 6.7 mg/L and 171 mg/L. The peak K concentration for the KAc site was measured in January 2020. It was anticipated that a large amount of KAc was applied during January 2020 because of heavy snowfall events. The runoff concentrations of K decreased in late winter because MnDOT restriced the application of KAc. Similar to the KAc site, the runoff concentrations of K gradually

decreased throughout February and March 2020. The minimum concentrations of K were measured in March 2020 for both the NaCl and KAc sites.

Figure 2.13(a) indicates that the Ca concentrations in the BC samples were constant except for the late March data. The concentrations of Ca in the samples collected from the NaCl and KAc sites decreased during the Febuuary sampling time. Ca concentrations were lower in the runoff from the NaCl site. In contrast, the KAc site dissolved higher levels of Ca with two peaks in concentrations during January and February of 2020.

The average concentration of Mg in the BC samples was 18.9 mg/L, which is about four times higher than the concentrations measured in the LS samples (Figure 2.13(b)). Lower concentrations of Mg were measured in the runoff from NaCl and KAc sites. The concentrations of Mg also fluctuated depending on sampling time. In addition, unfiltered samples tended to have higher Mg concentrations, especially for the runoff samples from the KAc site.

As shown in Figure 2.13(c), the Na concentrations in BC samples fluctuated depending on sampling time. However, the average concentrations of Na in BC samples were 218.1 mg/L, which is approximately 43 times higher than the average Na concentrations measured in the Lake Superior samples. The Na concentrations in the runoff of NaCl and KAc sites were significantly higher. The highest concentrations of Na were measured in the runoff samples during January and February of 2020. In later winter, the runoff concentrations of Na gradually decreased, which may have happened due to lower application rates of deicer. As noted above, we plan to further analyze the correlations of deicer application rates and timelines with our data. Similar concentrations of Na were measured for both the NaCl and KAc sites. In addition, no significant differences in Na concentrations were observed between the filtered and unfiltered samples.

2.4.4.3 Heavy and Trace Metal Concentrations

Figure 2.14(a) shows the concentrations of Al in the collected samples from the CE sites.

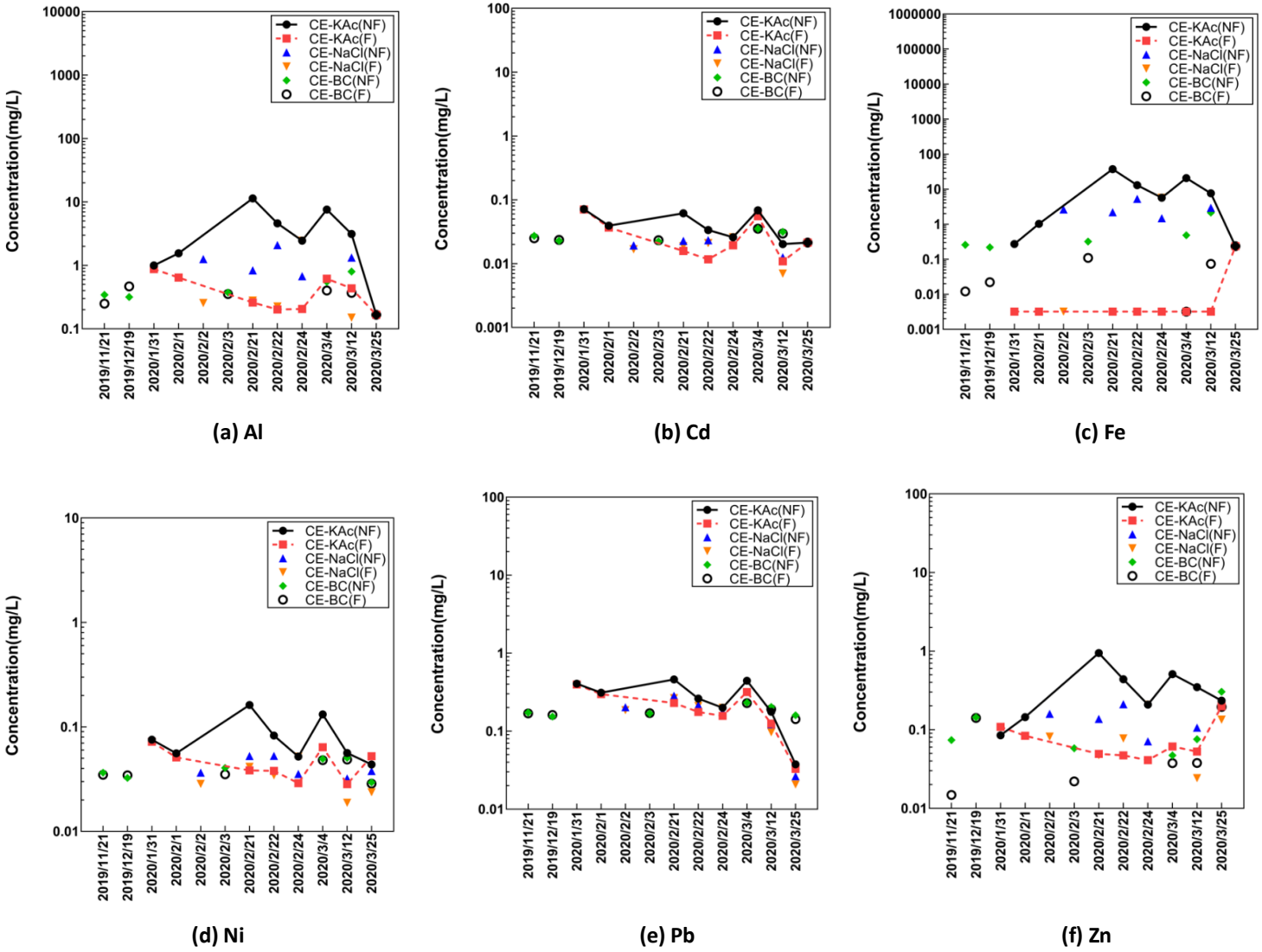

Figure 2.14. Metal concentrations in the surface water from Central Entrance sites (a) Al, (b) Cd, (c) Fe, (d) Ni, (e) Pb, and (f) Zn

The average concentration of Al in the BC samples was 0.41 mg/L, which was above the U.S. EPA specified MCL of 0.2 mg/L. Also, the average concentrations of Al in the BC samples were approximately 2.3 times higher than the average Al concentrations measured in the LS samples. Higher concentrations of Al were measured in unfiltered samples compared to those in filtered ones. In general, Al concentrations in the runoff from the NaCl and KAc sites were above the MCL values. The runoff from the KAc site had higher concentrations of Al. However, Al levels in the filtered runoff from the NaCl site decreased in the late winter of 2019–2020.

Fe concentrations in all the filtered samples from the CE sites were below the MCL of 0.3 mg/L (Figure 2.14(c)). Similar to Al, unfiltered samples had the highest concentrations of Fe due to the presence of dispersed clay particles. Almost all of the unfiltered samples exceeded the U.S. EPA specified permissible limit of 0.3 mg/L. Among the unfiltered samples, KAc runoff had higher concentrations of Fe compared to the BC and NaCl runoff samples.

The average concentration of Cd in the BC samples was 0.027 mg/L, which was higher than the U.S. EPA specified MCL of 0.005 mg/L (Figure 2.14(b)). Cd concentrations in the BC samples were initially lower but increased noticeably after February 2020. The Cd level in the runoff samples fluctuated, showing no consistent trend with sampling time. Slightly higher concentrations of Cd were measured in the runoff from the KAc site compared to those measured in the NaCl runoff.

The concentrations of Ni in the samples collected from the CE sites were well below the U.S. EPA provided DWEL of 0.7 mg/L (Figure 2.14(d)). The lowest concentrations of Ni were measured in the runoff from the NaCl site. The maximum concentrations of Ni were measured for the KAc site.

The concentrations of Pb in all the samples collected from the CE sites were always higher than the U.S. EPA specified MCL of 0.015 mg/L (Figure 2.14(e)). In general, runoff from the KAc site had higher concentrations of Pb compared to the samples collected from the NaCl site.

The CE site observations of Cd, Ni, and Pb concentrations being higher in the KAc site samples compared to the NaCl site samples are not in agreement with observations made in samples from the I-35 sites. Although it is difficult to pinpoint the exact reason, this discrepancy likely was due to the differences between the I-35 and CE sites, especially in vehicle traffic, speed limits, topography, and the probable differences in deicer application rates.

Zn concentrations did not show any consistent trend during the sampling period of 2019–2020 (Figure 2.14(f)). In general, the highest concentrations of Zn were measured in the runoff from the KAc site. Except for the unfiltered KAc runoff, similar concentrations of Zn were measured in the samples collected from the CE sites. In addition, the concentrations of Zn were always lower than the U.S. EPA specified MCL of 5 mg/L.

2.4.5 Blatnik Bridge Sites

Blatnik Bridge sites included above-bridge runoff collected (with KAc deicer applications) as well as Rice's Point (RP), (where Saint Louis Bay water enters Lake Superior) water samples collected under the bridge.

2.4.5.1 Nutrient Concentrations

Figure 2.15(a) shows the TC concentrations in the surface water runoff collected from the Blatnik Bridge (BB) sites.

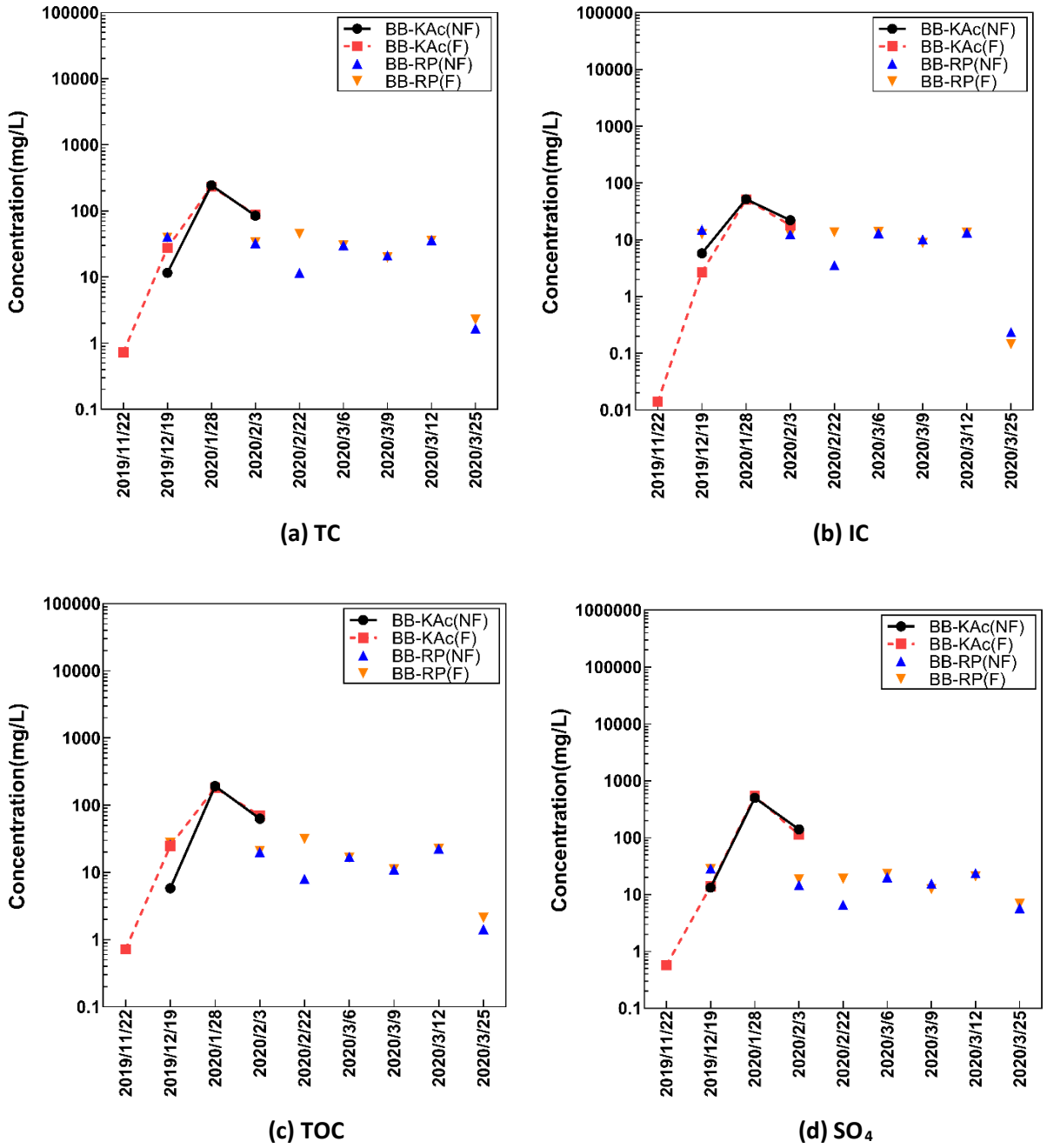

Figure 2.15. Concentrations of (a) TC, (b) IC, (c) TOC, and (d) SO_4 in the surface water collected from Blatnik Bridge sites

The average TC concentration in the samples obtained from RP was 28.6 mg/L with negligible variations with time. The average TC concentration measured in RP samples was nearly 2.5 and 1.4 times higher than the average TC concentrations measured in the LS and BC samples, respectively. As shown in Figures 2.15(b) and (c), the average IC and TOC concentrations were 10.9 mg/L and 18.4 mg/L, respectively. When was compared to the LS and BC samples, similar concentrations of IC were also

measured in the RP samples. Thus, the higher TC concentrations in the RP samples were due to higher TOC concentrations.

It was possible to acquire only three KAc runoff samples from the BB site. In particular, a sharp TC concentration peak of 240 mg/L was observed in January 2020. As shown in Figures 2.15(b) and (c), this high concentration in TC was contributed to by higher levels of both IC and TOC. However, the flatter IC peak indicated that higher organic carbon was the major contributor to the peak concentrations of TC. In addition, no significant differences of TC, IC, and TOC concentrations were observed between the filtered and unfiltered samples.

As shown in Figure 2.15(d), the average SO_4 concentration in the RP samples was 18.9 mg/L, which was the highest when compared to the LS and BC sample averages. The concentrations of SO_4 were almost constant throughout the sampling time. In December 2019, the SO_4 concentration in the bridge runoff was low (13.6 mg/L), while it had increased significantly in January and February of 2020 (538 mg/L and 139 mg/L, respectively). The researchers anticipated that given KAc is a liquid, and the application procedure was combined with other solid salts such as calcium sulfate, magnesium sulfate, and sodium sulfate. (Details of the deicers may be verified with MnDOT in future meetings.) Higher concentrations of Ca, Mg, and Na were also measured in the bridge runoff samples. Besides, no significant variations in the SO_4 concentrations were observed, depending on the filtration conditions.

The concentration of NH_3, NO_x, NO_2, and NO_3 in the samples collected from the BB sites are presented in Figure 2.16.

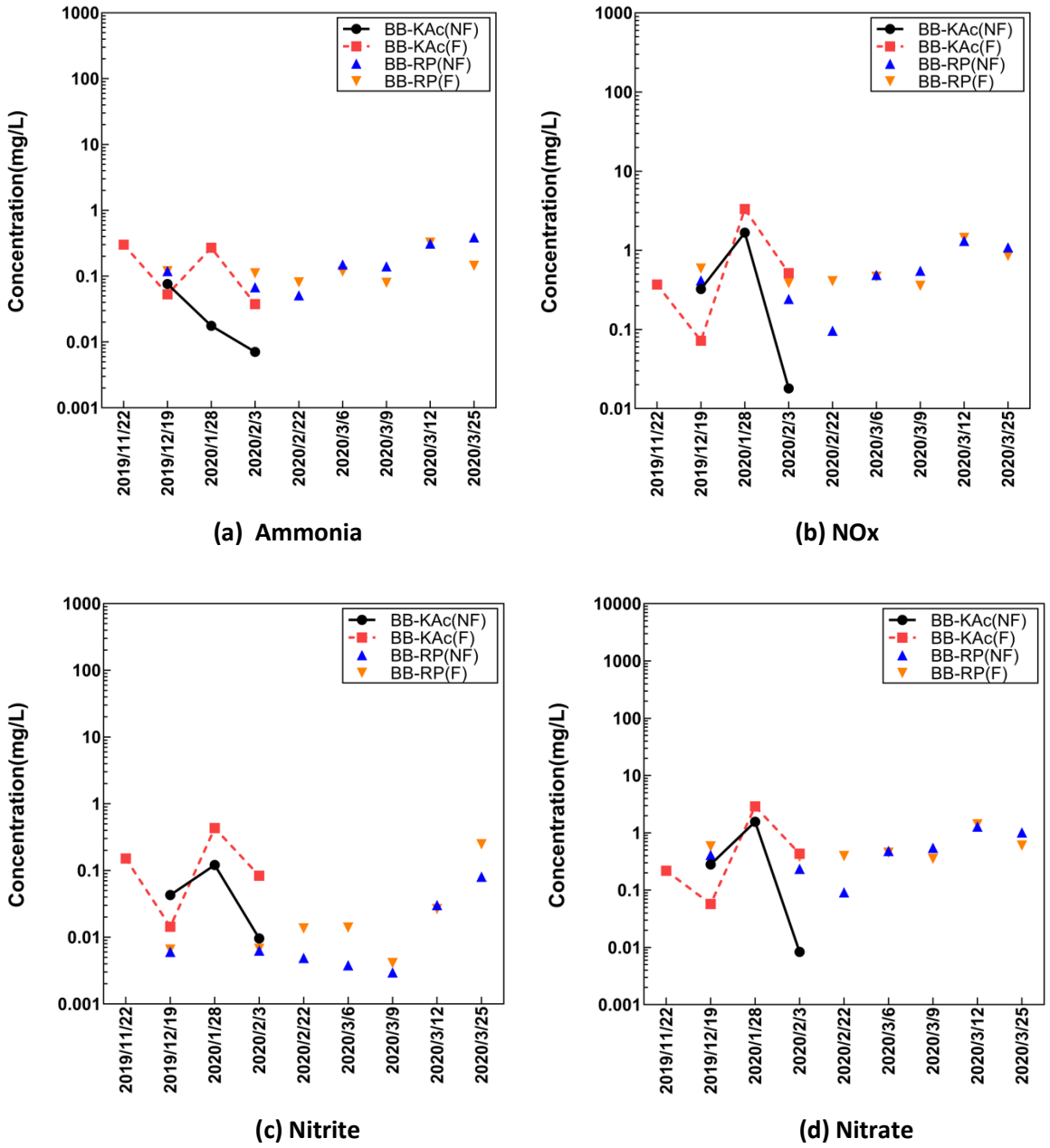

Figure 2.16. Concentrations of (a) ammonia (NH_3), (b) nitrite+nitrate (NO_x), (c) nitrite (NO_2) and (d) nitrate (NO_3) in the surface water collected from Blatnik Bridge sites

For the sampling period of 2019–2020, no trend in the temporal variation of these nutrients was observed. However, the concentrations of NO_x, NO_2, and NO_3 in the bridge runoff (KAc site) were slightly higher compared to those measured in RP samples. In general, filtered samples had higher concentrations of NH_3, NO_x, NO_2, and NO_3 than those in unfiltered samples.

2.4.5.2 Primary Metal Concentrations

Figure 2.17(d) shows the K concentrations in the samples collected from the BB sites.

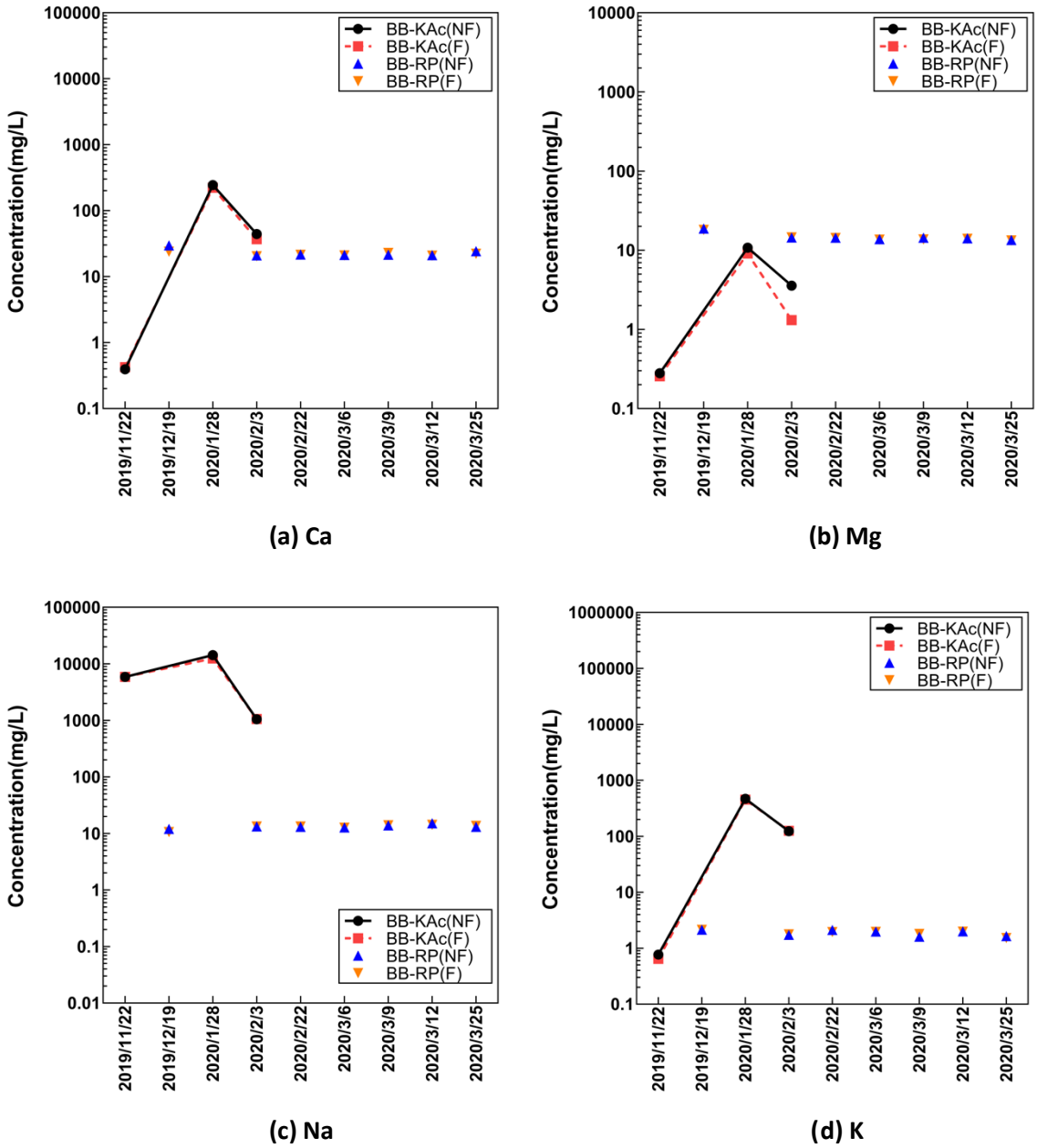

Figure 2.17. Metal concentrations in the surface water collected from Blatnik Bridge sites (a) Ca, (b) Mg, (c) Na, and (d) K

The average concentration of K in the RP samples was 2 mg/L. The concentrations of K in the LS and BC samples were 1 mg/L and 6.7 mg/L, respectively. K levels in the bridge runoff were significantly higher. K concentrations in the bridge runoff were 37 mg/L, 460 mg/L, and 124 mg/L during December 2019, January 2020, and February 2020, respectively. These high concentrations of K in the bridge runoff may have resulted due to the application of KAc as a deicer.

Figure 2.17(a) indicates that the Ca concentrations in the RP samples varied within the narrow range of 20 to 24 mg/L. Thus, the concentrations of Ca in the RP samples were slightly higher than in the LS

samples but lower compared to the BC samples. In December 2019, the Ca concentration in the bridge runoff was about 13 mg/L. However, in January 2020, the concentration of Ca in the bridge runoff was 234 mg/L. In February 2020, the Ca concentration in the bridge runoff decreased to about 40 mg/L.

The average concentration of Mg in the RP samples was 14.8 mg/L, which is higher than in the LS samples (Figure 2.17(b)). Conversely, Mg concentrations in RP samples were lower than the average Mg concentrations in the BC samples. The concentrations of Mg in bridge runoff were even smaller. Nonetheless, an increase in the Mg concentration in the bridge runoff was observed in January 2020. This could have happened due to the KAc application in combination with magnesium salts. In addition, unfiltered samples tended to have higher Mg concentrations, especially for the bridge runoff samples (KAc site).

As shown in Figure 2.17(c), the average Na concentration in the RP samples was 13 mg/L. Similar to Ca and Mg, the average concentration of Na in the RP samples was higher than that in the LS samples, but lower than that in the BC samples. During the sampling periods of January 2020 and February 2020, the concentrations of Na in the bridge runoff were 13,400 mg/L and 1055 mg/L, respectively. These concentrations of Na were the highest among all the samples collected in winter 2019–2020. Not surprisingly, during these winter seasons, KAc was often applied in combination with sodium salts at the Blatnik Bridge.

2.4.5.3 Heavy and Trace Metal Concentrations

Figure 2.18(a) shows the Al concentrations measured in the BB samples.

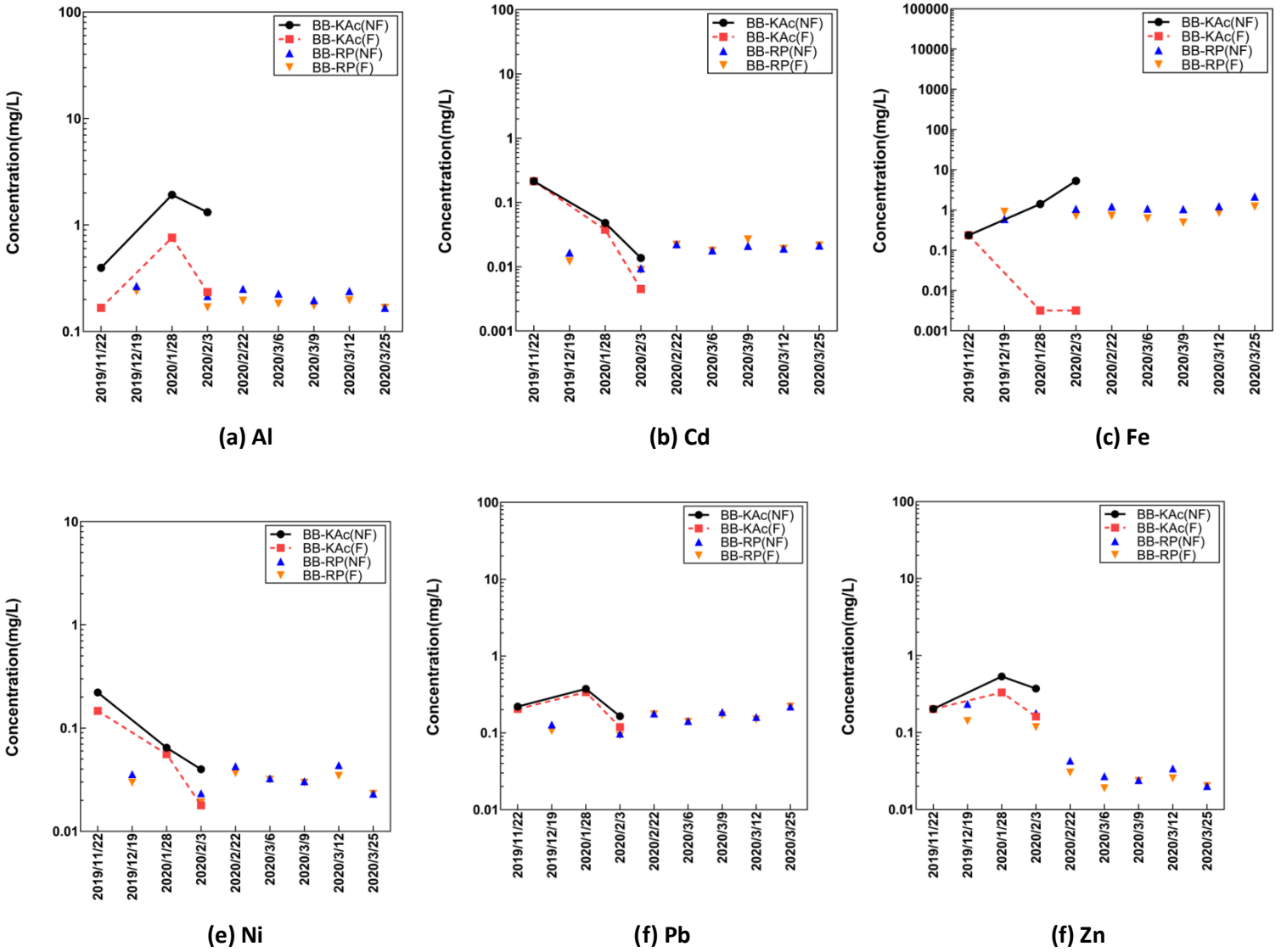

Figure 2.18. Metal concentrations in the surface water from Blatnik Bridge sites (a) Al, (b) Cd, (c) Fe, (d) Ni, (e) Pb, and (f) Zn

The average Al concentration in RP samples was 0.21 mg/L, which is above the U.S. EPA specified MCL of 0.2 mg/L. Thus, the average Al concentration in the RP samples was similar to the average Al concentration measured in the LS samples. Al levels in the RP samples were about half that in the BC samples. The maximum concentration of Al was observed in the bridge runoff during January 2020. In addition, higher levels of Al were always measured in unfiltered samples compared to those in filtered ones.

As shown in Figure 2.18(c), the average concentration of Fe in the RP samples was 1.0 mg/L. Similar to Al, the unfiltered samples had the highest concentrations of Fe due to the presence of dispersed clay particles. Filtered bridge runoff had Fe concentrations lower than the U.S. EPA specified MCL for Fe (0.3 mg/L). Among all the unfiltered samples, the maximum Fe concentration was measured in the bridge runoff in February 2020.

The average concentration of Cd in the RP samples was 0.018 mg/L, which was higher than the U.S. EPA specified MCL of 0.005 mg/L (Figure 2.18(b)). Cd concentrations in the RP samples were initially lower but increased after February 2020. The Cd levels in the runoff samples fluctuated. Slightly higher concentrations of Cd were measured in the bridge runoff during November 2019.

As illustrated in Figure 2.18 (d), the concentrations of Ni in the samples collected from the BB sites were well below the U.S. EPA provided DWEL of 0.7 mg/L. The lowest concentrations of Ni were measured in the bridge runoff. However, during November 2019, the highest concentration of Ni was measured in the bridge runoff (0.22 mg/L).

Figure 2.18(e) shows that the concentrations of Pb in all of the samples collected from the BB sites were always higher than the U.S. EPA specified MCL of 0.015 mg/L. The maximum concentration of Pb in the bridge runoff was 0.36 mg/L. The large fluctuations in these metal concentrations in the bridge runoff with the KAc treatment further supports the observations made for the I-35 sites, which pointed to the metals correlating generally to runoff events instead of specific deicers.

The concentrations of Zn measured in the BB samples are shown in Figure 2.18(f). Zn concentrations were always lower than the U.S. EPA specified MCL of 5 mg/L. In early winter, the RP samples had higher levels of Zn, which decreased progressively in the late winter of 2019–2020, pointing to no correlation between Zn and deicer applications. Zn concentrations in bridge runoff were low during December 2019. The maximum concentrations of Zn in the bridge runoff occurred in January 2020 (0.3-0.5 mg/L).

2.4.6 Soil Sample Results

The leachate from the collected soil samples was analyzed for pH, EC, and concentrations of SO_4, Ca, Na, K, Mg, Al, Fe, Cd, Ni, and Pb. Effluent concentrations of nitrate-N + nitrite-N, nitrite-N, and ammonia were not quantified since the results from surface runoff did not show any significant change over the sampling season of 2019–2020. In addition, the concentrations of these nutrients were close to the instrument detection limits. The soil samples were not analyzed for total organic and inorganic carbon

concentrations. Soil organic residues were visible in the samples. Therefore, it would not be possible to conclude if the variations of soil carbon concentrations were due to the KAc deicer application.

2.4.6.1 pH, Electrical Conductivity (EC), and Sulfate

Figure 2.19 shows the pH, EC, and sulfate concentrations of the soil samples collected from the CE sites.

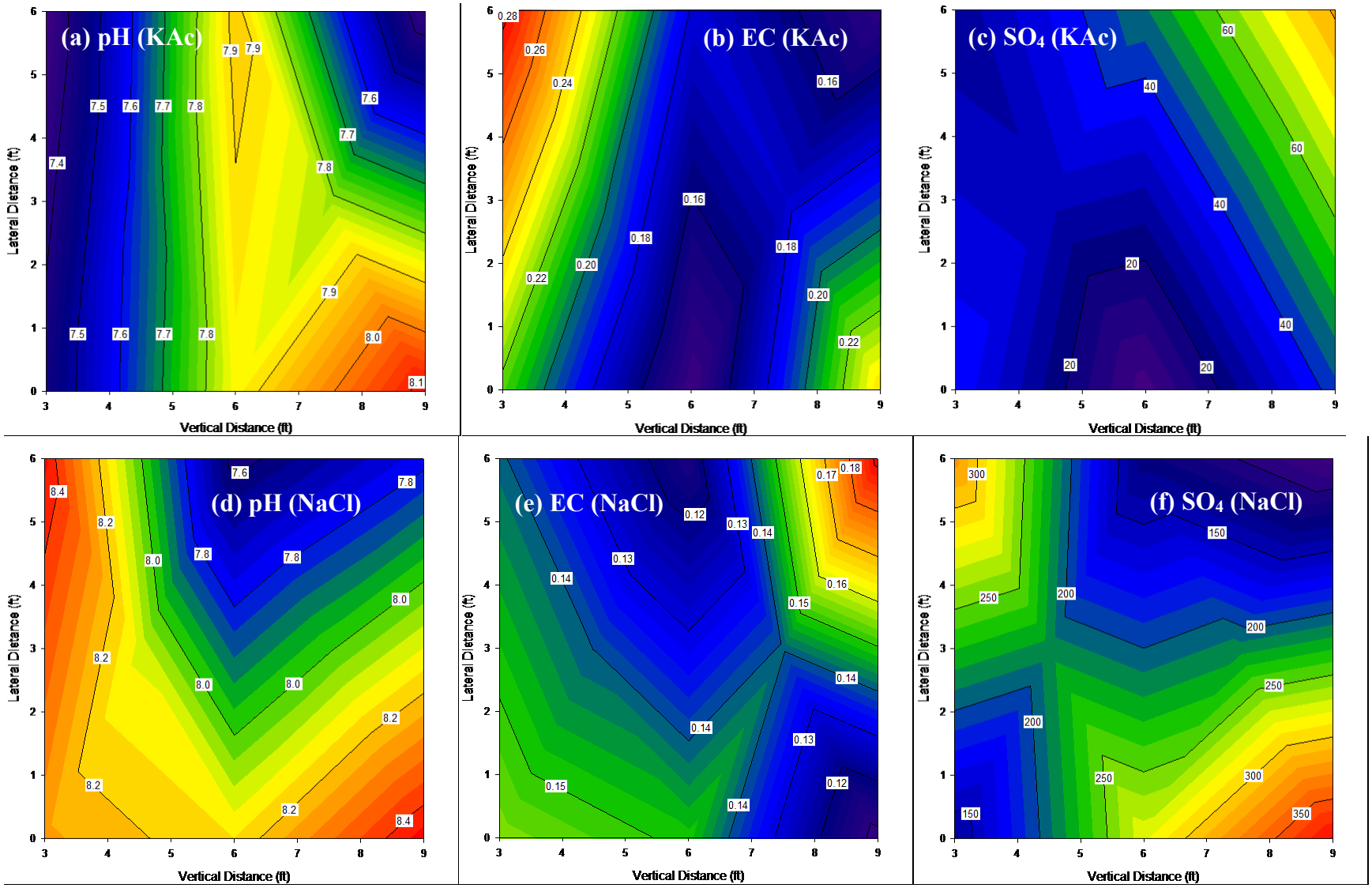

EC values are in mS/cm and SO_4 concentrations are in mg/L

Figure 2.19. Central Entrance (KAc site) soil (a) pH, (b) EC, (c) SO_4 concentrations, and Pecan Street (NaCl site) soil (d) pH, (e) EC, and (f) SO_4

As shown in Figure 2.19(a), the KAc site had relatively lower pH values next to the pavement section, likely due to the near-neutral pH of the CF7 deicer. Soil pH values increased as the distance from the roadway increased. Conversely, for the NaCl site, soil samples collected next to the pavement section had higher pH values (Figure 2.19(d)). Unlike the liquid KAc deicer, application of solid NaCl likely did not affect the runoff and soil pH as readily. With an increase in distance from the pavement edge, soil pH values tended to decrease in the NaCl site.

As shown in Figure 2.19(b), higher values of EC were measured for the soil samples collected next to the KAc pavement section. With an increase in distance from the pavement edge, EC values generally decreased. In contrast, the NaCl site showed lower values of EC compared to those measured in the KAc site (Figure 2.19(e)). Generally speaking, lower values of EC were measured next to the pavement section in the NaCl site.

Lower concentrations of SO_4 were measured in the soil samples collected from the KAc site than those measured in the samples obtained from the NaCl site (Figures 2.19(c) and (f)). In addition, the concentrations of SO_4 in the KAc soil samples increased with an increase in distance from the pavement edge. For the NaCl site, higher concentrations of SO_4 were measured near the pavement edge.

2.4.6.2 Soil Metal Concentrations

The leached concentrations of metals from the soil samples are illustrated in Figure 2.20.

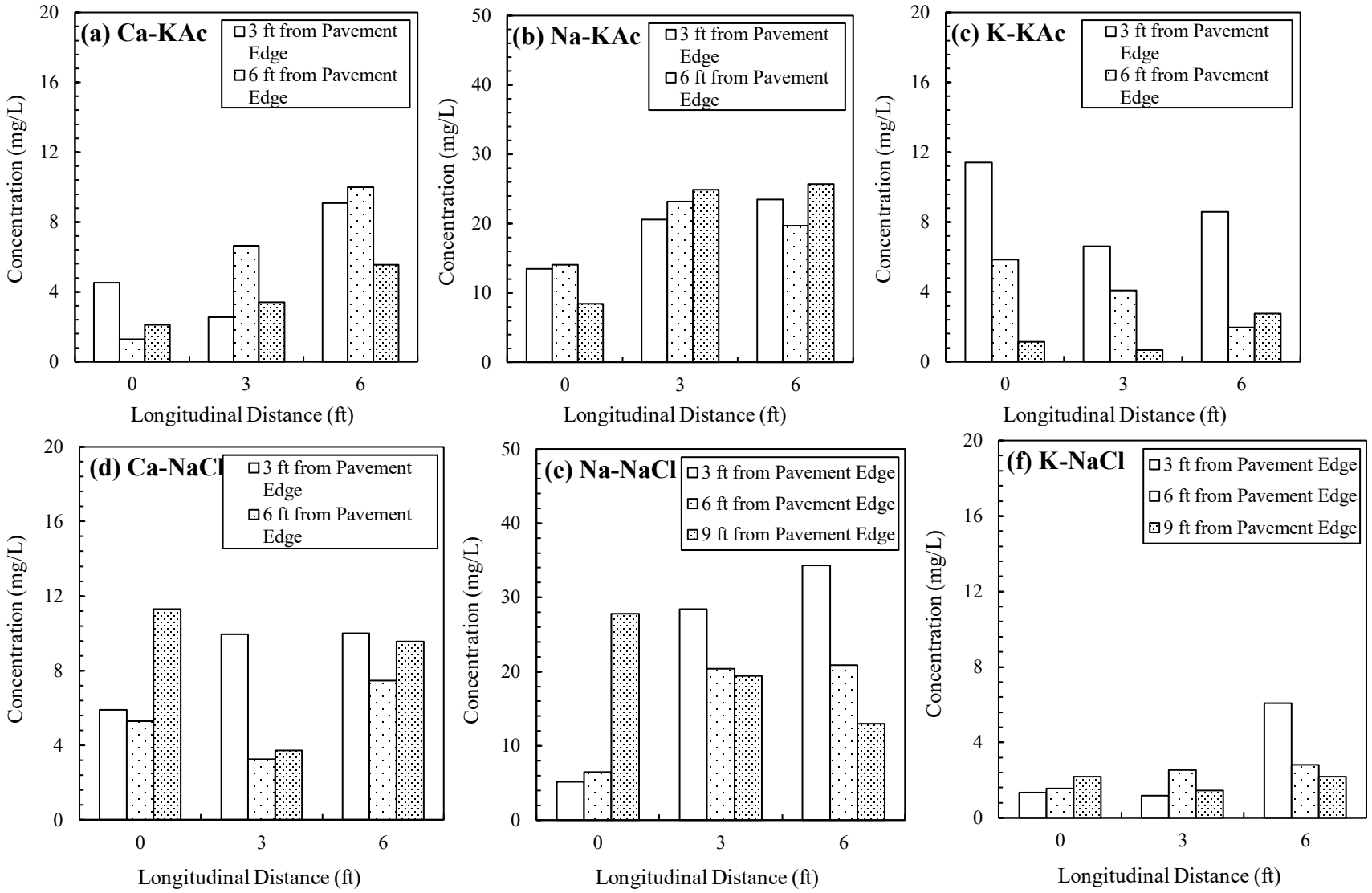

Figure 2.20. KAc site soil concentrations of (a) Ca, (b) Na, (c) K, and NaCl site soil concentrations of (d) Ca, (e) Na, (f) K

The soil concentrations of K were significantly higher in the KAc site samples compared to those measured in the NaCl site samples (Figures 2.20 (c) and (f)). K concentrations in the KAc site samples were in the range of 0.6 to 12 mg/L, whereas K concentrations in the NaCl site samples were between 1.3 mg/L and 6 mg/L. Unsurprisingly, higher concentrations of K were measure in proximity to the assessed KAc pavement section.

As observed from Figure 2.20, higher concentrations of Ca were measured in the soil samples collected from the NaCl site. The Ca concentrations in the KAc site soil samples were lower. In addition, smaller concentrations of Ca were measured next to the KAc pavement section. For the NaCl site, Ca concentrations fluctuated with the distance from the pavement section.

As shown in Figure 2.20(b), Na concentrations in the soil samples collected from the KAc site were in the range of 8 to 26 mg/L. The concentrations of Na in the NaCl site soil samples were between 5 mg/L and 35 mg/L (Figure 2.20(e)). Generally speaking, for both the KAc and NaCl sites, lower concentrations of Na were measured next to the pavement sections.

Figure 2.21 shows the soil concentrations of Mg, Al, and Fe.

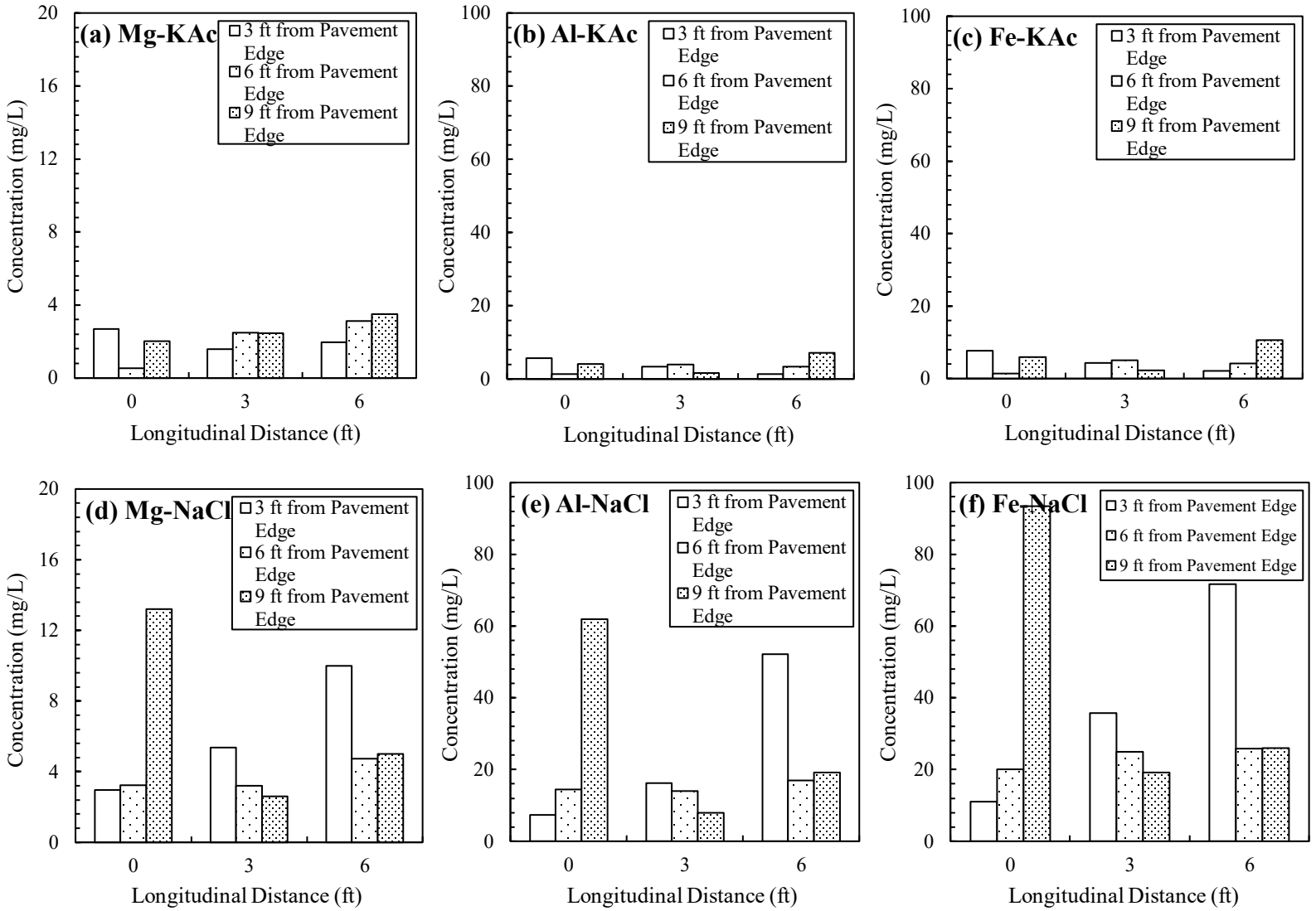

Figure 2.21. KAc site soil concentrations of (a) Mg, (b) Al, (c) Fe, and NaCl site soil concentrations of (d) Mg, (e) Al, (f) Fe

While no clear trend was observed between the soil concentrations of these elements and the distance from the pavement edge, the soil samples from the NaCl site had significantly higher levels of Mg, Al, and Fe. For instance, the Mg, Al, and Fe concentrations of KAc site soil samples were in the range of 0.5 to 3.5 mg/L, 1.3 to 7.1 mg/L, and 1.4 to 10.6 mg/L, respectively. The ranges of Mg, Al, and Fe concentrations in the NaCl site soil samples were 2.6 to 5.4 mg/L, 8 to 62 mg/L, and 11 to 94 mg/L, respectively. While the rationale for the variations remains unknown, it is likely that the variations in soil mineralogy could be a possible reason for the observed behavior.

Similarly, the soil samples collected from the NaCl site had higher concentrations of Cd, Ni, and Pb (Figure 2.22).

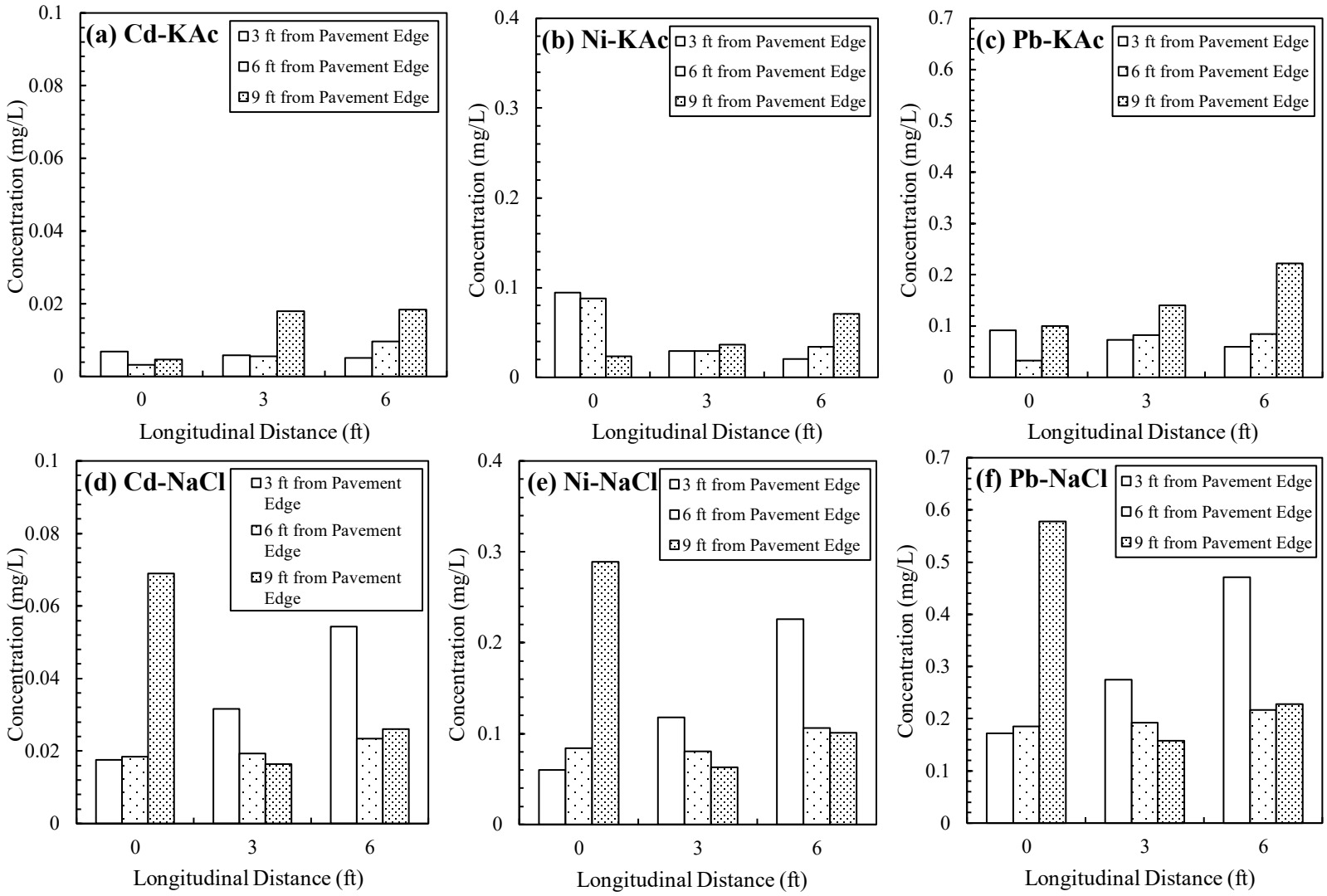

Figure 2.22. KAc site soil concentrations of (a) Cd, (b) Ni, (c) Pb, and NaCl site soil concentrations of (d) Cd, (e) Ni, (f) Pb

The researchers theorized that the soil concentrations of these elements resulted from the exhaust of vehicles. CE sites had a sidewalk, and the soil samples were collected 3 ft, 6 ft, and 9 ft from the outer edge of the sidewalk. Conversely, Pecan Street did not have a sidewalk. Hence, the soil sampling points in the KAc site were further away from the pavement, which may have resulted in lower concentrations of Cd, Ni, and Pb in the soil samples collected from the KAc site.

Figure 2.23 shows the water extractable concentrations of Zn measured in soil collected from the KAc and NaCl sites.

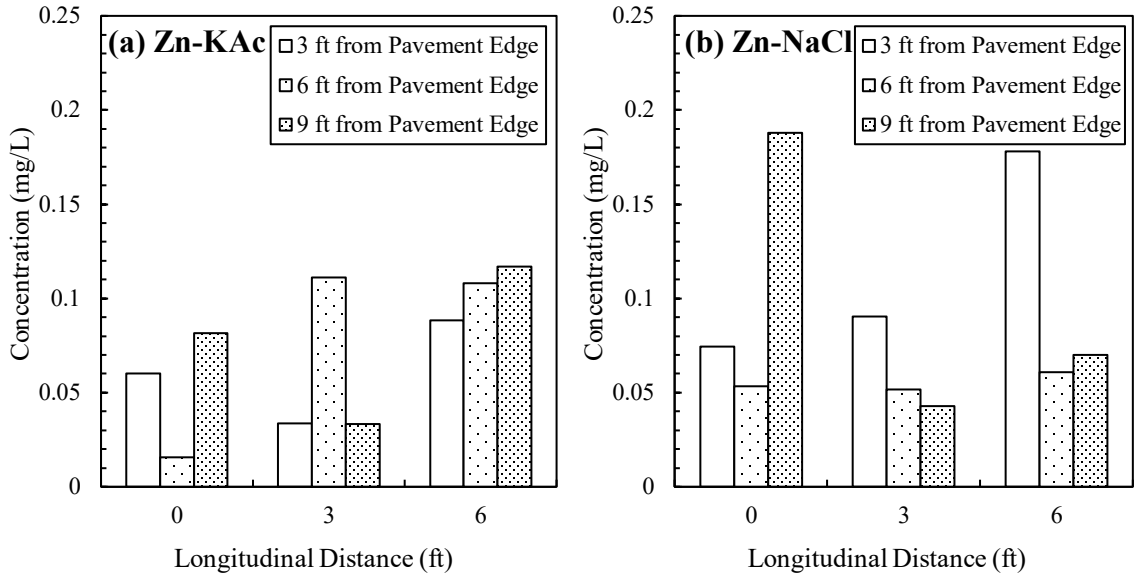

Figure 2.23. Concentrations of Zn measured in the soil leachate collected from (a) KAc site, and (b) NaCl site

As depicted in Figure 2.23, soil samples from the NaCl site had relatively higher concentrations of Zn than those measured from the KAc site. The concentrations of Zn in the KAc site soil samples were between 0.03 mg/L and 0.12 mg/L, whereas Zn concentrations were in the range of 0.04 to 0.19 mg/L in NaCl site soil samples. Relatively, higher concentrations of Zn were measured at a greater distance from the edge of a pavement.

CHAPTER 3: SECOND FIELD ASSESSMENT OF THE POTASSIUM ACETATE DEICER

3.1 OBJECTIVES

The research team, in collaboration with the UMD team, conducted a second field sampling campaign in Duluth during winter 2020–2021. The goal of this field assessment was to further understand the environmental impact of KAc deicers in runoff and surface water surrounding Duluth.

3.2 SITE SELECTING AND PLANNING

3.2.1 Sampling Schedule and Major Changes to First Sampling Season

Sampling during winter 2020–2021 in Duluth (Figure 3.1) was coordinated between ISU and UMD in which at least one of the research teams collected runoff and surface water samples between December 2020 and March 2021.

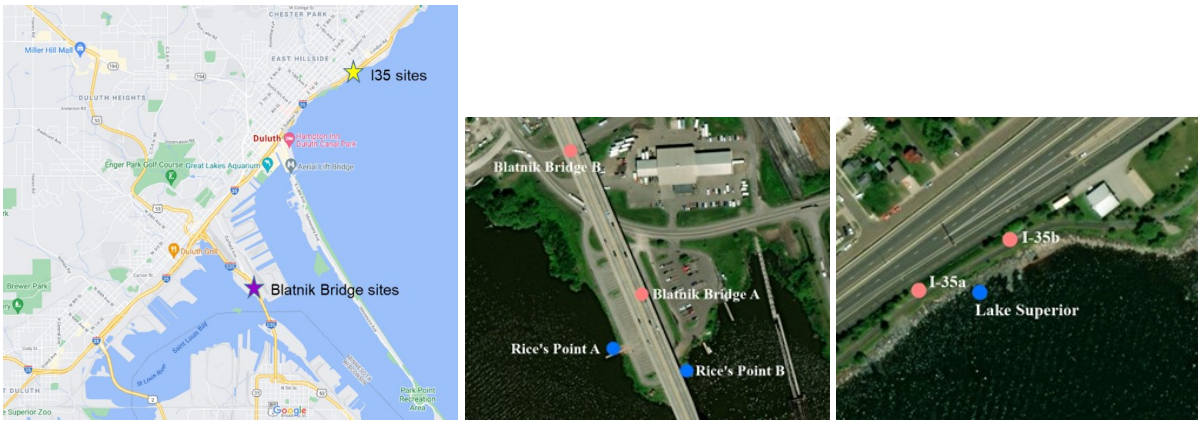

(a) **(b)** **(c)**

Maps and satellite images taken from Google maps and modified, Map data ©2020

Figure 3.1. (a) Map of I-35 and Blatnik Bridge sites, (b) Rice's Point and Blatnik Bridge sites, and (c) I-35 sites

Logistical limitations due to the COVID-19 pandemic hindered travel of the ISU research team to Duluth; however, the UMD team generously sent runoff samples that they were able to collect so that the ISU research team had a more complete data set. The 2020–2021 winter season was unusually warm, and sampling started later (December) and ended earlier (March) than originally planned.

Field sampling and analyses followed the procedures from the first sampling campaign with the following exception. Due to limited travel to the sites by the ISU team due to the pandemic, the researchers decided to not collect and analyze soil samples during the winter 2020–2021 season. According to the soil sample characterization results (Chapter 2), the KAc deicer application appeared to have minimal impact on soil parameters (pH, EC, and metal concentrations). These observations were taken into account when the decision was made.

Additionally, although measurements for chloride, sulfate, and metals were taken in the second sampling season, the data appeared to significantly deviate from expected values upon comparisons with data collected by the UMD research team. For quality control, the researchers obtained third-party data for these analytes (processed through the ISU Water Quality Research Laboratory) and found that the team's data were indeed 1–2 orders of magnitude lower compared to their values. The most likely reasons for these discrepancies were instrumental and/or human error. As the water samples were well past their holding times outlined in the standard methods used, the team was not able to conduct follow-on measurements of the samples to correct the initial data. Instead, this report includes only the data for nitrate, ammonia, and TOC. These data were collected and passed quality control tests.

3.3 RESULTS AND DISCUSSION

3.3.1 I-35 Sites

The concentrations of nitrogen species in runoff and surface water samples were low (Figure 3.2(a) and (b)).

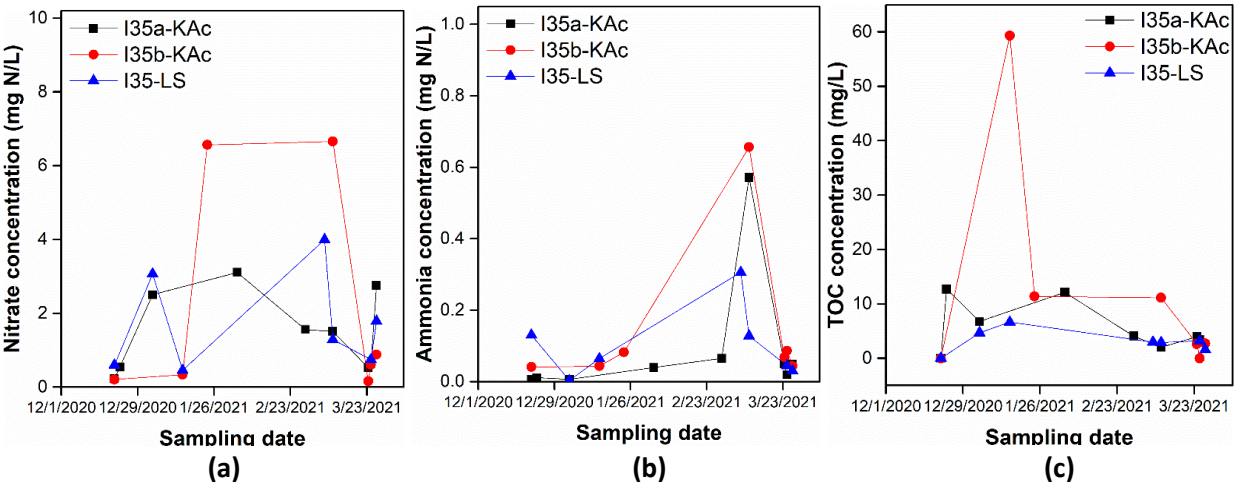

Figure 3.2. Concentrations of (a) nitrate, (b) ammonia, and (c) TOC in the runoff and surface water samples collected from I-35 sites

Nitrate concentrations observed were highest in I35b-KAc samples at ~7 mg N/L and all measurements were similar to those observed in the first field sampling campaign (winter 2019–2020). Ammonia concentrations were lower than 0.8 mg N/L, also following trends observed in the first field sampling campaign. There was an observable peak in ammonia concentrations in early March in all I-35 samples, which may have corresponded to additional snow melt presence in the samples due to increased temperatures in the Duluth area (Figure 3.3).

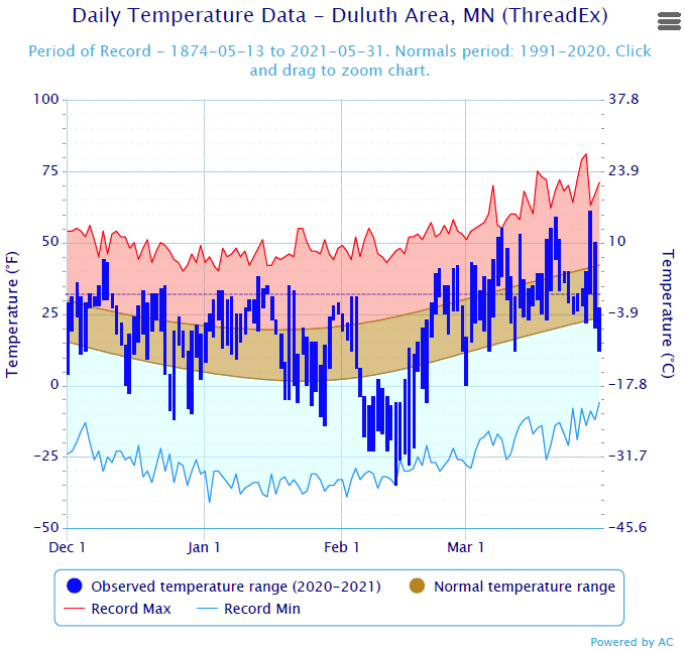

National Oceanic and Atmospheric Administration

Figure 3.3. Temperature recordings for Duluth from December 1, 2020 through March 31, 2021

TOC concentrations were generally low in the I-35 samples (below 20 mg/L; previous Figure 3.2(c)) with concentrations similar to those observed in the first field sampling campaign. One spike in TOC concentrations was observed in the I35a-KAc runoff sample from January 15, 2021. Although there may have also been a spike in the other KAc site along I-35, a sample was not collected on the same day for that site. No corresponding increase in TOC was seen in the Lake Superior water.

3.3.2 Blatnik Bridge Sites

The results from water chemistry analyses of runoff samples collected from the BB area (Figure 3.4) showed generally similar trends as the I-35 samples.

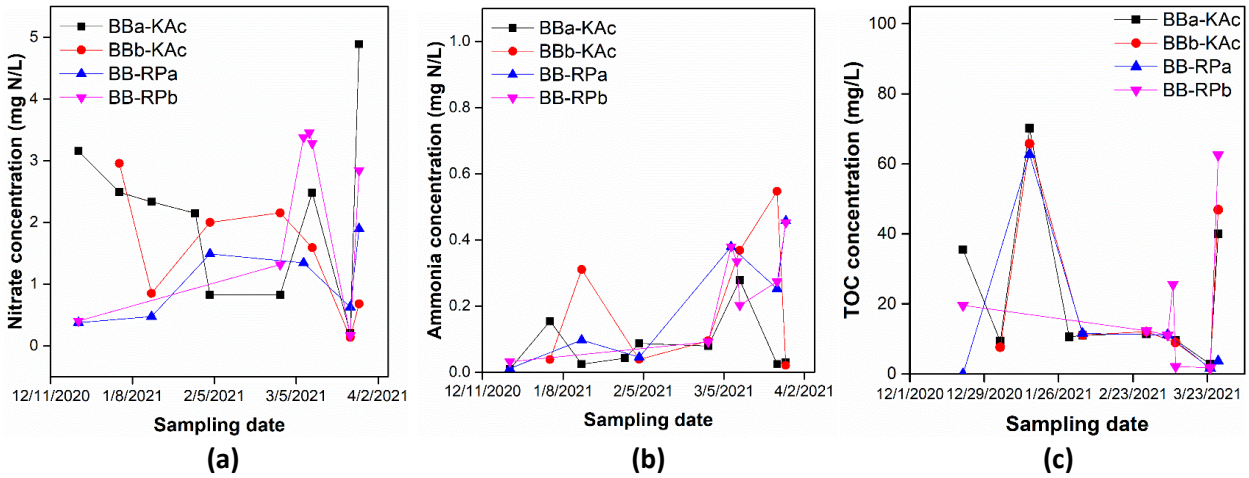

Figure 3.4. Concentrations of (a) nitrate, (b) ammonia, and (c) TOC in the runoff and surface water samples collected from Blatnik Bridge sites

Nitrogen species concentrations were low for both nitrate and ammonia (Figure 3.4(a) and (b)) with peaks observed toward the end of the sampling period (mid to late March). TOC concentrations were 70 mg/L at most with peaks observed on January 15, 2021 and toward late March.

CHAPTER 4: ASSESMENT OF FATE OF POTASSIUM ACETATE WITH LABORATORY EXPERIMENTS

4.1 OBJECTIVE

The researchers evaluated the persistence of acetate in soil and water using soil slurry reactors with representative soil and surface waters collected from Duluth. The toxicity was also analyzed by testing the tolerance of *Escherichia coli* to different pure KAc and deicer concentrations through the determination of specific oxygen uptake rates (SOURs).

4.2 METHODS

4.2.1 Soil Slurry Reactor Tests

Water and soil samples were collected from Duluth during the second field sampling campaign (winter 2020–2021). The soil samples were collected from the sidewalk of I-35, Rice's Point A (RP-A), Blatnik Bridge A (BB-A), and Blatnik Bridge B (BB-B) (Figure 4.1).

(a) **(b)** **(c)**

Images taken from Google maps and annotated, Map data ©2020

Figure 4.1. Water and soil sampling sites for Chapter 4: (a) Rice's Point and Blatnik Bridge sites, (b) I-35 sites, and (c) Lester River site

The water samples were collected from Lester River and Lake Superior (Figure 4.1). Lester River water acted as a "pristine" water body control; whereas, Lake Superior water was expected to have experienced prior KAc applications. Lake Superior and Lester River water had pH values of 7.91 and 7.74, respectively, upon collection.

Soil slurry reactors were designed to test the effects of the KAc deicer on soil and water microbial activities (Figure 4.2).

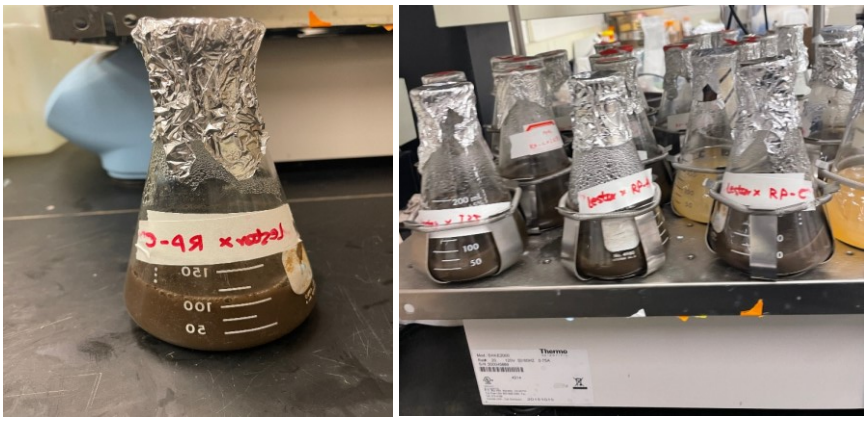

(a) (b)

Figure 4.2. (a) Slurry reactor and (b) slurry reactors on the shaker

To complement the UMD research team's effort on KAc degradation in water samples, the ISU team tested the effects on both soil and water. It was expected that, as soil typically has greater microbial biomass per volume than surface water, any negative impacts from the deicer would be observed to a lesser degree.

Both autoclaved (sterile) and non-autoclaved soil samples were used; slurries with autoclaved soil were used to measure both the short-term adsorption of KAc onto soil (which occurs within 2–4 hours) and longer-term biodegradation by the surface water microbial communities, in contrast to the non-autoclaved soil slurries that measured the combination of adsorption, biodegradation by water microbes, and biodegradation by soil microbes.

All soil samples were screened to pass the 2 mm mesh sieve. Soil subsamples were autoclaved for 45 min at 121°C three separate times to ensure adequate sterilization. Duplicate reactors were prepared for each group shown in Table 4.1.

Table 4.1. Experimental matrix for soil slurry setups

Non-Autoclaved Soil Slurry Reactor	Autoclaved Soil Slurry Reactor
I35+Lester River+10% Deicer	I35+Lester River+10% Deicer
I35+Lake Superior+10% Deicer	I35+Lake Superior+10% Deicer
RP-A+Lester River+10% Deicer	RP-A+Lester River+10% Deicer
RP-A+Lake Superior+10% Deicer	RP-A+Lake Superior+10% Deicer
BB-A+Lester River+10% Deicer	BB-A+Lester River+10% Deicer
BB-A+Lake Superior+10% Deicer	BB-A+Lake Superior+10% Deicer
BB-B+Lester River+10% Deicer	BB-B+Lester River+10% Deicer
BB-B+Lake Superior+10% Deicer	BB-B+Lake Superior+10% Deicer
Lester River+10% Deicer	–
Lake Superior+10% Deicer	–

I35, RP-A, BB-A, and BB-B indicate soil samples; whereas, Lester River and Lake Superior indicate water samples used

Soil and water samples were mixed in each slurry to achieve a 20% weight per volume (w/v) soil sample in lake/river water (i.e., 20 g soil sample in 100 mL water). The CF7 deicer solution was added to each reactor at 10% volume/volume (v/v) to test a high application scenario. Based on the acetate measurements of the original CF7 solution, the 10% v/v additions of the deicer was expected to result in approximately 1.78 g/L acetate in the soil slurry reactors (i.e., undiluted CF7 contained 17.8 g/L acetate). Flasks were shaken at 150 rpm at room temperature for 10 days. At different time points, 3 mL samples were obtained to analyze the acetate concentrations in each reactor. All samples were filtered through a 0.45 μm filter and diluted 1:1 with 100 mM phosphoric acid prior to analysis. A Perkin Elmer AltusTM HPLC System at the Iowa State University Keck Metabolomics Research Laboratory was used to measure acetate concentrations in each sample.

4.2.2 Specific Oxygen Uptake Rate (SOUR) Tests

The SOURs of *E. coli* were tested under different deicer and pure KAc concentration exposure for the toxicity experiments following Standard Methods 2710B with modifications as described below. The SOUR test is a method routinely used to assess the stability of bacterial activity. This method measures the oxygen uptake rates of a population of bacteria in an aqueous suspension containing nutrients, typically with and without toxic compounds.

The water samples used for this experiment were collected from the Duluth area during the second field campaign. Three water samples were prepared for this testing: St. Louis Bay, Lester River, and Lake Superior water.

Pure *E. coli* cultures were grown in a lysogeny broth until the late log phase (final density of 2×10^{10} to 5×10^{10} CFU/mL) prior to SOUR tests. 30 mL of cells were harvested per condition, washed twice, and transferred to a BOD bottle. A surface water sample (approximately 250 mL) was added into the BOD bottle, along with a test volume of deicer or pure KAc (Table 4.2) and a glucose solution to achieve a final glucose concentration in the BOD bottle of 1 g/L.

Table 4.2. SOUR test experimental sets

Solution Applied	Deicer volume ratio (% v/v)	Pure KAc
Concentration in BOD Bottle	10%, 6.67%, 3.33%, 0% (Expected equivalent acetate concentrations of 1.78, 1.19, 0.59, and 0 g/L, respectively)	20 g/L, 12 g/L, 6 g/L, 0 g/L (Equivalent acetate concentrations of 7.97, 4.78, 2.39, and 0 g/L, respectively)

Additional control experiments were designed to compare the oxygen consumption with and without *E. coli* presence to determine the baseline oxygen consumption observed in the surface water samples. Upon measuring the changes in DO concentrations in each BOD bottle, the SOUR results (mg O_2/min/CFU) were calculated using equation (1):

$$\text{SOUR} = \frac{\text{Slope (mg O}_2\text{/L/min)} \times 1000 \text{ (mL/L)}}{\text{Cell density (CFU/mL)}} \quad \textbf{(1)}$$

where slope indicates the slope of DO readings along the time period (mg O_2/L/min), and cell density (CFU/mL) was calculated using the optical density reading of *E. coli* at the late log phase.

4.3 RESULTS AND DISCUSSION

4.3.1 Soil Slurry Reactors

The acetate concentration in the autoclaved soil slurry reactors were monitored at 0, 4, and 24 hours and 2, 7, 10, and 28 days. The time zero acetate concentrations for all conditions were similar (~3,500 mg/L; Figure 4.3).

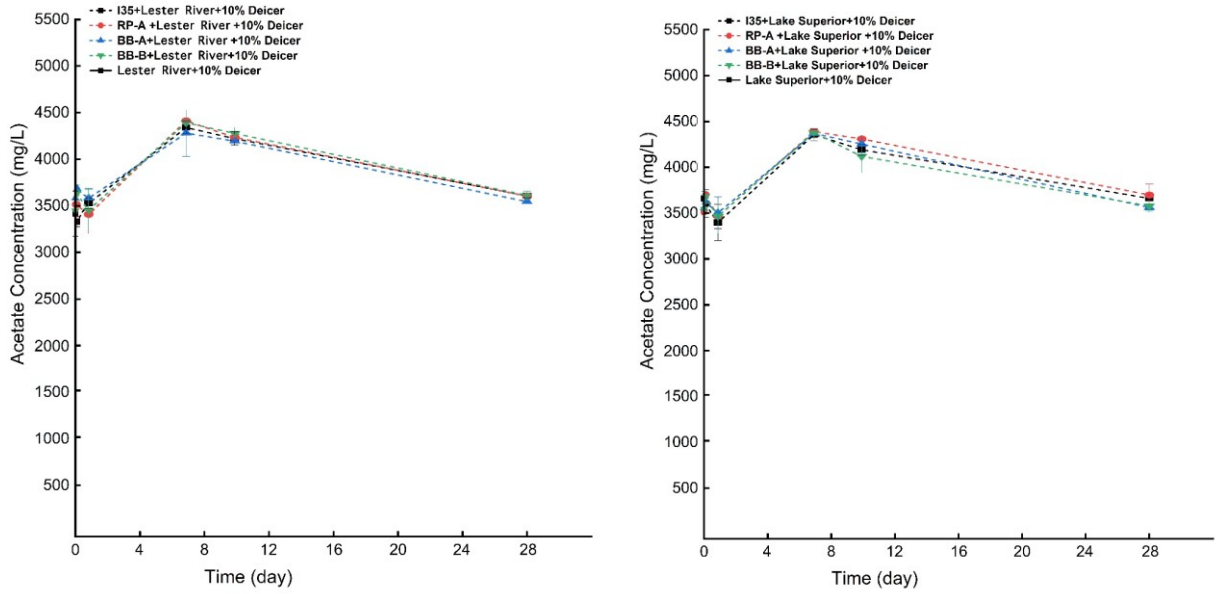

(a) **(b)**

Figure 4.3. Acetate concentration in autoclaved soil slurry reactors with (a) Lester River water and (b) Lake Superior water over 28 days

Although the expected acetate concentrations upon the 10% v/v CF7 deicer addition was 1,780 mg/L based on the direct acetate measurements of the original deicer solution, it is likely that the additives present in CF7 interfered with the acetate measurements of the concentrated solution, resulting in an underestimation.

Acetate concentrations appeared to increase by about 1,000 mg/L between day 1 and 7 in all soil slurry reactors. This increase may be due to acetate-like moieties in soil organic matter (SOM) leaching into the aqueous phase over the first few days of the testing. Results from slurries with autoclaved soil suggest that no observable acetate adsorption onto soil occurred during the test period. Aerobic acetate biodegradation by the water microbiomes in the soil slurry reactors was not observed even after 28 days

(previous Figure 4.3). Although there was a small decrease (by ~500 mg/L) in acetate concentrations between 7 and 28 days, the concentrations remained similar to or higher than the initial acetate levels. Therefore, it is likely that these fluctuations in acetate measurements were due to complex interactions between the soil and the SOM instead of adsorption or biodegradation of the CF7 deicer. The pH of the reactors ranged between 9.24 and 9.39 in the soil slurries before deicer addition and between 9.17 and 9.30 10 days after deicer addition, suggesting that deicer application resulted in a negligible shift in pH.

The acetate concentration in the non-autoclaved soil slurry reactors was monitored at 0, 4, 9, 12, and 24 hours and 2, 3, 7, 10, and 28 days. The Lester River and Lake Superior water samples with 10% v/v deicer additions without soil were monitored as the controls (Figure 4.4).

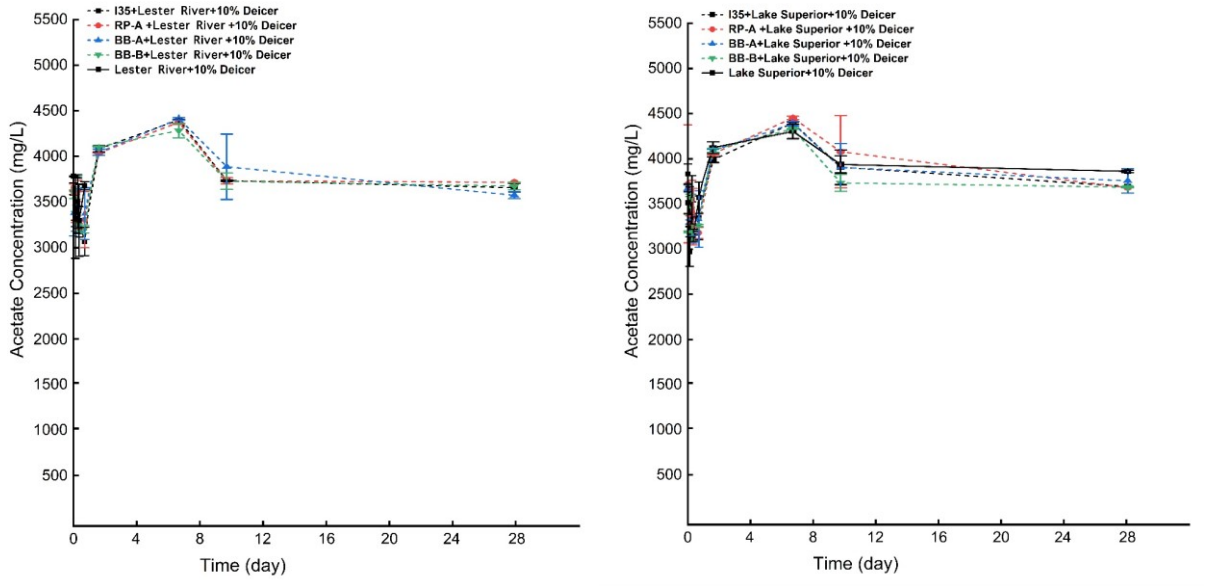

(a) **(b)**

Figure 4.4. Acetate concentration in non-autoclaved soil slurry reactors with (a) Lester River water and (b) Lake Superior water over 28 days

Initial acetate concentrations in the non-autoclaved soil slurries were similar to those in the autoclaved soils (~3,500 mg/L), further suggesting that the CF7 deicer contained larger concentrations of acetate than the researchers' original measurements indicated (i.e., the original deicer may contain ~35 g acetate/L). Increases in acetate concentrations were observed between days 1 and 7 as previously discussed for the autoclaved soil slurries. Similar to that shown in Figure 4.3, there was no observable aerobic biodegradation of acetate by the soil and water microbiomes (Figure 4.4); the small decrease in aqueous acetate concentrations observed between days 7 and 10 was likely due to sorption of SOM instead of the CF7 deicer. The soil slurry pH values were similar to those measured in the autoclaved reactors with values shifting less than 0.25 due to deicer addition.

The observed lack of acetate biodegradation over 28 days was unsurprising, specifically under the conditions tested including the use of native microbial communities from around the Duluth area. Acetate as an organic ion (CH_3COO) is small but important to all types of cells, especially as a precursor

to acetyl coenzyme A (CoA). In fact, under aerobic conditions, most bacteria are slow in removing acetate from the environment, but, instead, circulate acetate in and out of the cell while changing its form from acetate to acetyl CoA (Pinhal et al. 2019). There is likely a slow removal of acetate under these conditions given that bacterial cells require storage or usage of acetyl CoA due to changes in bioenergy levels, which may have been observed if the experiments were run for many more weeks. However, acetate utilization by bacteria (although not degradation) may readily occur under anoxic or anaerobic conditions, especially if methane-producing microorganisms are present; these conditions are not likely in moving surface water bodies but can be seen in swamps and particularly stagnant waters.

4.3.2 SOURs

The raw DO consumption data for all deicer conditions are shown in Figure 4.5.

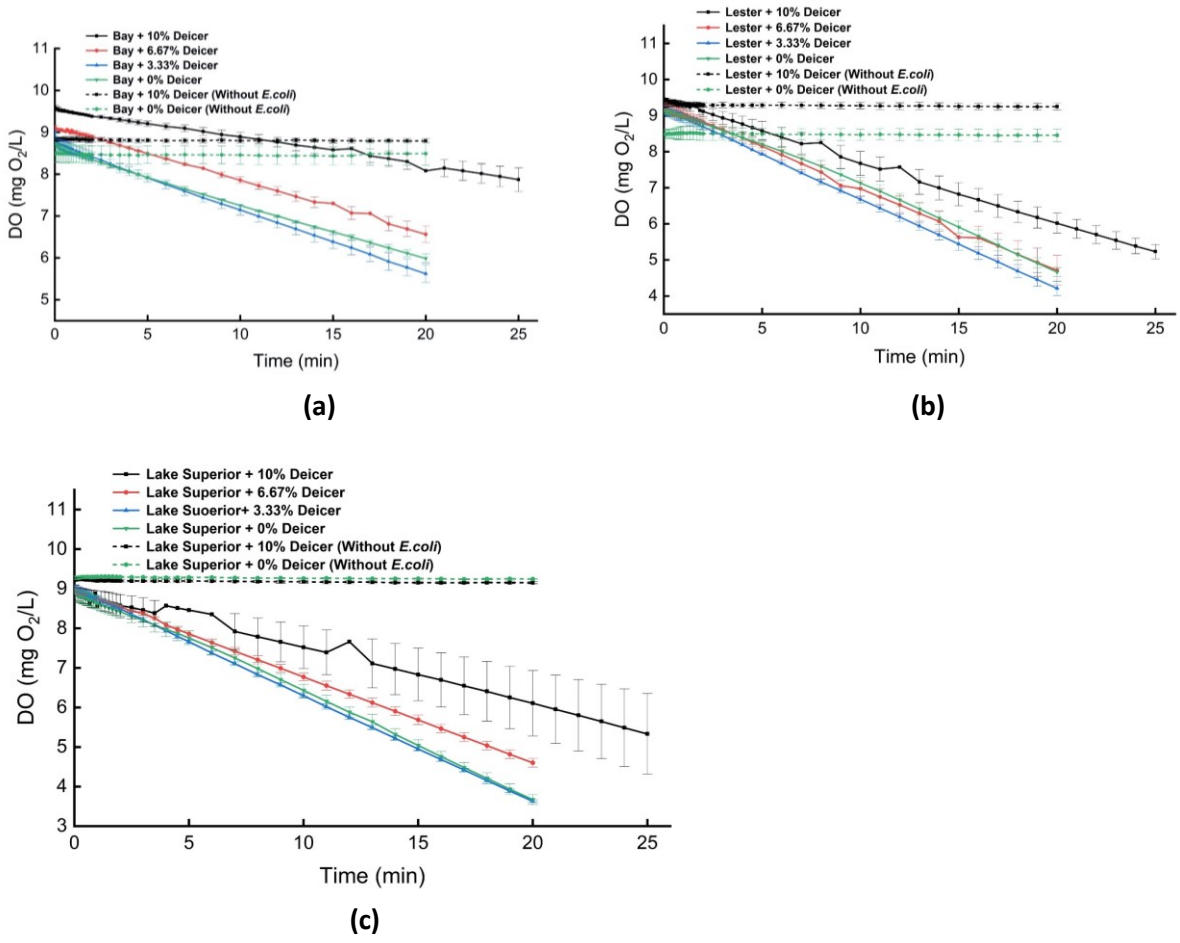

Figure 4.5. Change in DO concentrations over time in (a) St. Louis Bay water with deicer, (b) Lester River water with deicer, and (c) Lake Superior water with deicer

The results from the control sample experiments without *E. coli* indicated that limited oxygen consumption occurred in the water samples alone. DO consumption appeared to be impacted by deicer additions with some dose dependence (SOUR analysis discussed below). Generally, higher deicer applications resulted in greater variability in the DO measurements over time (e.g., 10% deicer additions

to Lake Superior water), likely due to the biological variability in the response to the inhibitory effects of the CF7 deicer.

The raw DO consumption data of pure KAc-added conditions are shown in Figure 4.6.

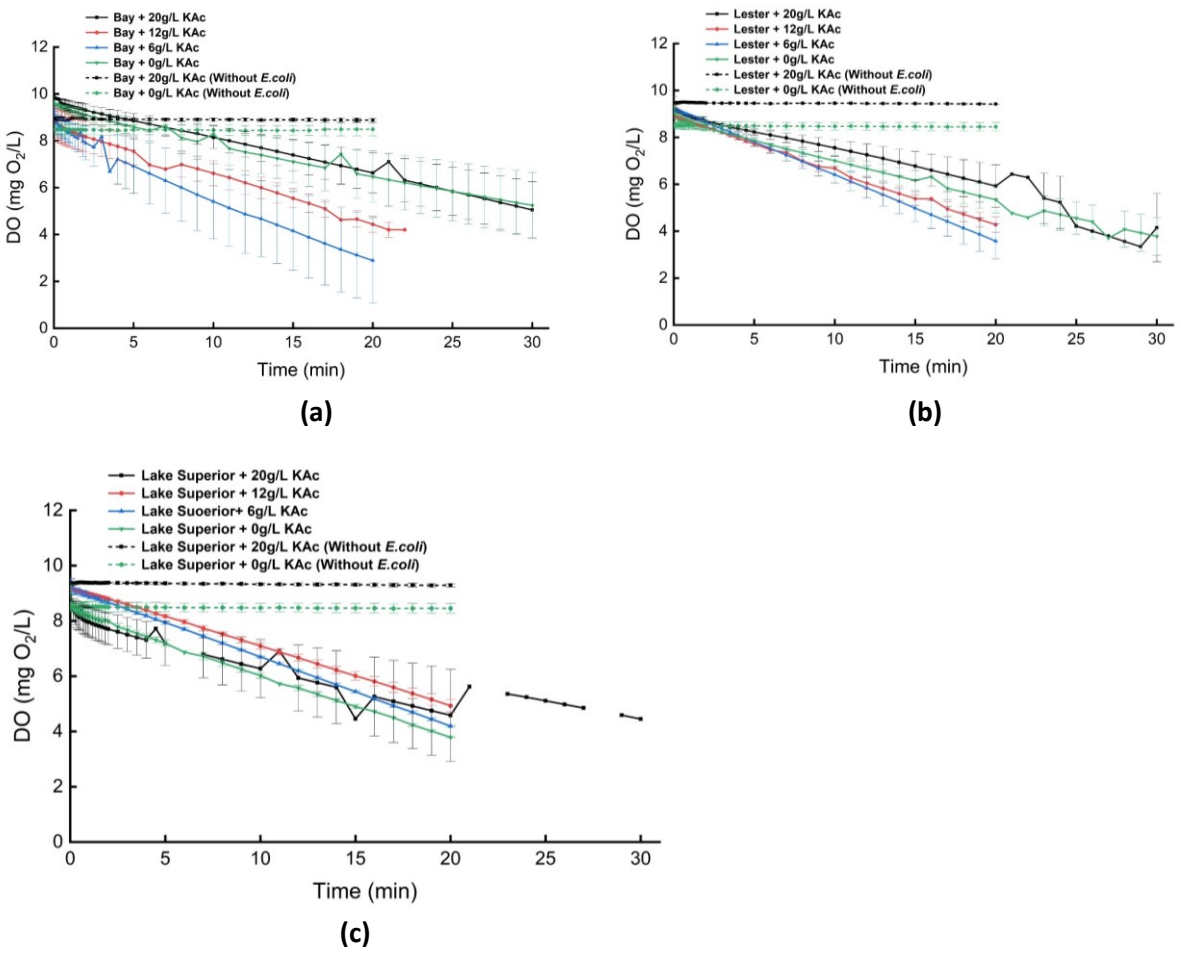

Figure 4.6. (a) St. Louis Bay water with pure KAc, (b) Lester River water with pure KAc, and (c) Lake Superior water with pure KAc

Again, the water samples with no *E. coli* showed minimal DO consumption with or without the KAc addition. The effects of the KAc addition on DO consumption were less observable compared to the effects of the CF7 deicer. Larger variability was observed in the KAc experiments, possibly due to greater heterogeneity in the biological replicates of *E. coli* used.

Addition of the highest deicer dose (10% v/v with a likely acetate concentration of ~3.5 g/L) resulted in slightly lower SOURs in the St. Louis Bay water samples but not in the other samples (Figure 4.7(a)).

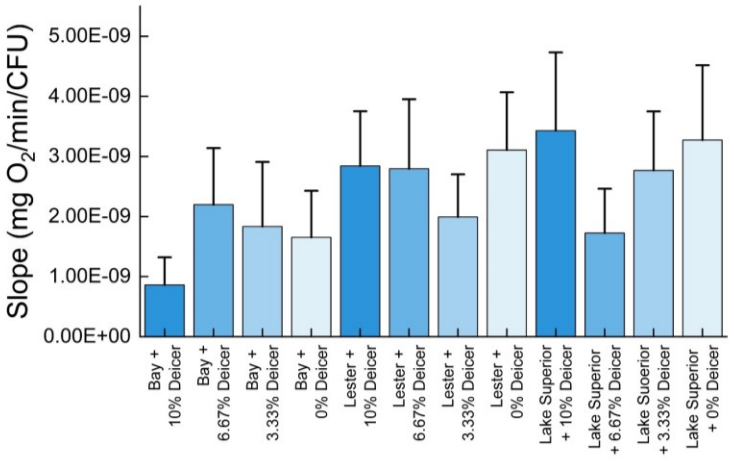

(a)

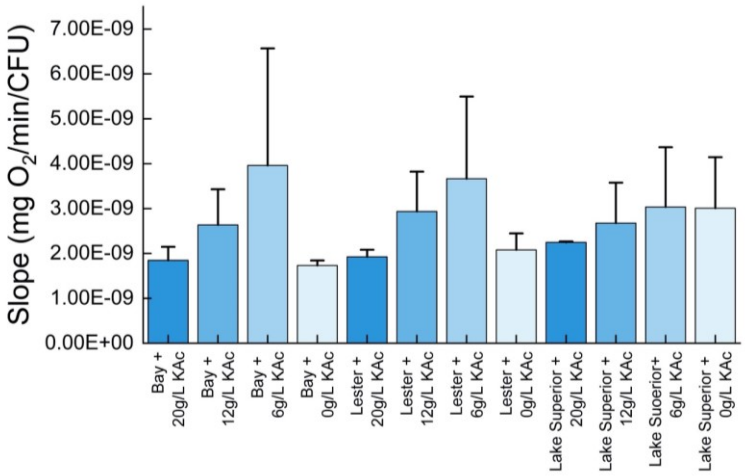

(b)

Figure 4.7. SOURs of (a) deicer added groups and (b) pure KAc added groups

This suggests that the presence of concentrated deicer may affect the microbial activity of *E. coli* in some waters, potentially dependent on water chemistry parameters. On the other hand, the presence of concentrated pure KAc (20 g/L) appeared to have limited negative impacts on the microbial activity of *E. coli* in the aqueous phase (Figure 4.7(b)).

In fact, additions of lower pure KAc concentrations resulted in slight increases in SOURs, suggesting that KAc can be used as nutrients by *E. coli*, thereby increasing DO consumption. However, this slight increase in SOURs was only observed in lower KAc concentrations; 20 g/L additions resulted in similar SOURs as the no-KAc controls.

These results suggest that the pure KAc in the aqueous phase must reach a very high concentration to exhibit any negative impact on bacterial activities. However, it should be noted that the SOURs differences observed were not statistically significant ($p>0.05$). Although it is possible that the slight

differences observed may become significant upon scaling up to water body/watershed levels, the research results suggest that the CF7 deicer has limited impact on bacterial activity in surface waters.

Based on acetate measurements of the CF7 deicer in the soil slurries, the KAc concentration of the highest deicer dose-added group (10%) was close to 3.5 g acetate/L (2.3 g potassium/L assuming complete dissociation); as such, the 6 g/L pure KAc dose (i.e., 3.6 g acetate/L and 2.4 g potassium/L) samples were the closest comparison (previous Figure 4.7). The deicer-added samples had lower SOURs than pure KAc-added samples despite lower theoretical KAc concentrations ($p=0.02$).

These observations suggest that the deicer has a greater negative impact on bacterial activity than pure KAc, possibly due to the additives, such as the corrosion inhibitors found in the CF7 deicer. Also note that the levels of potassium tested showed little to low toxicity to *E. coli*.

CHAPTER 5: PREDICTION OF THE FATE AND TRANSPORT OF POTASSIUM ACETATE

5.1 OBJECTIVES

The research team developed a predictive model for fate and transport of KAc in lakes and streams. The intent was to estimate the likely extent of KAc effects in generic waterbodies, while the model will not be able to capture the intricacies of flow in every specific waterbody in Minnesota. This modeling complements that of the U of M team, which involves the movement of KAc throughout a watershed. Results of the model and the insights gained regarding fate and transport in a stream or lake can be implemented in the watershed model. The model was developed, parameterized, and evaluated.

5.2 NOMENCLATURE

a	=	coefficient in the relation between dispersion coefficient and cloud size
B	=	width of a channel cross section
BOD	=	biochemical oxygen demand
b	=	exponent in the relation between dispersion coefficient and cloud size
C	=	concentration
C_0	=	concentration at the runoff point
D	=	dissolved oxygen deficit
DO	=	dissolved oxygen
f_r	=	fraction of KAc running off from road surface
f_s	=	fraction of active ingredient in the deicer solution
H	=	channel depth
K	=	dispersion coefficient for a river
K_x	=	dispersion coefficient in the x-direction for a lake
K_y	=	dispersion coefficient in the y-direction for a lake
K_z	=	vertical eddy diffusivity
k_1	=	biodegradation rate
k_2	=	reaeration rate
L	=	concentration of oxidizable organic matter
L_0	=	concentration of oxidizable organic matter at the runoff point
L_c	=	length scale of contaminant cloud
L_r	=	length of lanes contributing to runoff
L_u	=	ultimate BOD
M	=	mass of contaminant
N	=	number of lanes contributing to runoff
Q	=	discharge
R	=	KAc application rate
r	=	$\left(x^2 + y^2\right)^{1/2}$

T = runoff duration
T_w = water temperature
t = time
U = mean velocity
u_* = shear velocity
v = $\left(U^2 + 4\lambda K\right)^{1/2}$
x = streamwise coordinate
y = horizontal coordinate
z = vertical coordinate
α = $3^{2b/(2-b)}\left(4a\right)^{2/(2-b)}$
β = $\left[\left(U/2K\right)^2 + \lambda/K\right]^{1/2}$
θ = temperature coefficient, 1.0241
λ = removal rate coefficient
ρ_s = density of the deicer solution
σ = measure of the size of a contaminant cloud
σ_{ma} = major axis of a contaminant cloud
σ_{mi} = minor axis of a contaminant cloud
σ_x^2 = spatial variance in the *x*-direction
τ = integration variable

5.3 EFFECTS OF KAC IN STREAMS

5.3.1 Developing the Model

5.3.1.1 Fate and Transport

Modeling the fate and transport of a contaminant in a stream employs generic one-dimensional advection-dispersion-reaction equations similar to those in Rutherford (1994) and Gulliver (2007). For an idealized stream of unchanging geometry, the concentration C can be computed as a function of time t and downstream distance x using equation (2):

$$\frac{\partial C}{\partial t} + U\frac{\partial C}{\partial x} = K\frac{\partial^2 C}{\partial x^2} - \lambda C \qquad \textbf{(2)}$$

where U is mean velocity, K is the longitudinal dispersion coefficient, and λ is the removal rate coefficient. Equation (2) applies to any contaminant undergoing one-dimensional transport and first-order decay. For runoff of concentration C_0 at a point ($x = 0$) over a duration T, the concentration from equation (2) is as follows:

$$C = \frac{C_0}{2}\exp\left(\frac{Ux}{2K}\right)\left\{e^{-\beta x}\left[\operatorname{erfc}\left(\frac{x-vt}{2\sqrt{Kt}}\right)-\operatorname{erfc}\left(\frac{x-v(t-T)}{2\sqrt{K(t-T)}}\right)\right]\right.$$
$$\left. + e^{\beta x}\left[\operatorname{erfc}\left(\frac{x+vt}{2\sqrt{Kt}}\right)-\operatorname{erfc}\left(\frac{x+v(t-T)}{2\sqrt{K(t-T)}}\right)\right]\right\} \quad \textbf{(3)}$$

where $v = \left(U^2 + 4\lambda K\right)^{1/2}$ and $\beta = \left[\left(U/2K\right)^2 + \lambda/K\right]^{1/2}$.

5.3.1.2 Dissolved Oxygen and Biochemical Oxygen Demand

Biodegradation of KAc leads to BOD. The BOD from acetate deicers is considered high (>100,000 mg/L) and likely to deplete oxygen in surface water (Weiss and Gulliver 2019). For example, Corsi et al. (2012) measured the BOD at 5 d to be 196,000 mg/L and determined the variation of the BOD with time at 5°C and 20°C. Revitt and Worrall (2003) showed that the BOD from KAc followed a first-order process as follows:

$$\mathrm{BOD} = L_u\left(1 - e^{-k_1 t}\right) \quad \textbf{(4)}$$

where L_u is the ultimate BOD and k_1 is the biodegradation rate. Laboratory experiments yielded values of k_1 of 0.048, 0.033, and 0.036 d^{-1} for temperatures of 1, 4, and 8°C. Weiss and Gulliver (2019) noted the curious trend of k_1 with temperature; Revitt and Worrall (2003) stated that, while the biodegradation rates for two glycol-based deicers decreased with temperature, the rate for Clearway, a KAc-based deicer, showed no clear trend.

These observations suggest that the concentrations of KAc can be related to the BOD and the amount, *L,* of oxidizable organic matter. This relationship is determined, theoretically, with a stoichiometric ratio (Chapra 1997 §19.4). BOD and dissolved oxygen in streams is modeled by adapting equation (2). For example, Bravo (1997) modified the Streeter-Phelps equations (e.g., Chapra 1997 §§21-22) to include dispersion as follows:

$$\frac{\partial L}{\partial t} + U\frac{\partial L}{\partial x} = K\frac{\partial^2 L}{\partial x^2} - k_1 L \quad \textbf{(5)}$$

$$\frac{\partial D}{\partial t} + U\frac{\partial D}{\partial x} = K\frac{\partial^2 D}{\partial x^2} + k_1 L - k_2 D \quad \textbf{(6)}$$

where *D* is the dissolved oxygen deficit (i.e., the difference between the concentrations of oxygen at saturation and at the current conditions) and k_2 is the reaeration rate.

The similarity between equations (2) and (5) indicates that, for the same runoff conditions, BOD can be computed with an equation analogous to equation (3)—that is, change *C* and C_0 to *L* and L_0 and λ to k_1. The dissolved oxygen deficit was estimated by ignoring dispersion as follows:

$$D = k_1 e^{-k_2 t} \int_0^t e^{k_2 t} L\left(x - U(t-\tau), \tau\right) d\tau \quad \textbf{(7)}$$

A key point to recognize from either equation (6) or equation (7) is that, if degradation does not occur (i.e., $k_1 = 0$) and the initial DO deficit is zero, the DO deficit will be zero downstream.

5.3.1.3 Assumptions

The model outlined in the previous subsections employs a few assumptions to make the calculations tractable:

- Flow and transport are one-dimensional
- Transport follows the advection-dispersion equation
- Temperature, pH, and other water properties are constant

The first assumption reduces the number of dimensions to be considered in computing concentrations. While the velocity in a channel varies with position in the cross-section, and, while near a source or spill site, the mixing occurs in all three directions, the model considers only variations in the streamwise, or *x*, direction. This assumption reduces characterizing the flow to determining the discharge and the cross-sectional area of the channel. Typically for mixing problems, vertical mixing is considered only near the source, and transverse mixing is considered until the contaminant is fully mixed across the channel. In fact, the one-dimensional approach is used in many river mixing applications, including the spill alerting system ICWater (Bahadur and Samuels 2015).

The advection-dispersion-reaction equation employed in the model assumes a mechanism for the transport. An equation such as equation (2) arises from an analysis of shear dispersion or spreading caused by parts of a contaminant cloud experiencing different velocities as they mix across the cross section (Fischer et al. 1979, Ch. 4).

Assumption 2 is related to assumption 1 in that the theory of shear dispersion requires a certain amount of time to pass before it strictly applies; in other words, the contaminant cloud must leave the "advective zone" near the source and reach the far field. Because of this requirement and the presence of other mechanisms of dispersion (e.g., trapping in recirculation zones), the advection-dispersion model underpredicts both the spreading of a contaminant cloud and the persistent skewness of the cloud (Gonzalez-Pinzon et al. 2013). An approach that relaxes some of the assumptions behind the advection-dispersion model while requiring little more data is the enhanced one-dimensional model of Reichert and Wanner (1991), and its solution by Schmalle and Rehmann (2014).

The current model does not account for variations in temperature, pH, or other properties of the surface water. Previous measurements have indicated a lack of clear temperature dependence of the biodegradation rate coefficient k_1 (Revitt and Worrall 2003). Results from Chapter 4 indicated no observable degradation over a 28-day period in soil or Lake Superior water at room temperature. At temperatures near freezing, degradation rates are small: Revitt and Worrall (2003) measured rate coefficients of 0.048, 0.033, and 0.036 d^{-1} at temperatures of 1, 4, and 8°C, respectively. For the

calculations below, the research team used k_1 = 0.05 d^{-1} to represent the maximum value of the degradation rate measured by Revitt and Worrall (2003) and the worst case for oxygen depletion.

5.3.2 Parameterizing the Model

The stream model outlined in the previous subsections requires several parameters to be specified (Table 5.1).

Table 5.1. Parameters for the model, with the range of values to be considered and the sources of data or approach for estimating values listed

Parameter	Range	Source/approach
Discharge *Q*	0.02–20 m^3/s	Axler et al. 2009, MN DNR
Stream width *B*	1–30 m	Estimate
Water depth *H*	0.3–0.8 m	Manning's equation (*n* = 0.03, rectangular)
Mean velocity *U*	0.3–0.9 m/s	Ratio of discharge and cross-sectional area
Shear velocity u_*	0.013–0.13 m/s	Average of U / u_* from Rutherford 1994
Dispersion coefficient *K*	0.1–75 m^2/s	Koussis and Rodriguez-Mirasol 1998
Removal rate coefficient λ	k_1 (KAc), 0 (NaCl)	Explanation in text
Biodegradation rate k_1	0.03–0.05 d^{-1}	Revitt and Worrall 2003
Reaeration rate k_2	4–16 d^{-1}	Covar 1976, *T* = 0°C
Input acetate concentration	10–3,500 mg/L	IA/MN year 1 field sampling

Parameters describing physical transport—i.e., the mean velocity and dispersion coefficient—can be computed from estimates of the discharge, *Q,* and stream geometry. Both vary widely across Minnesota and between seasons (Figure 5.1).

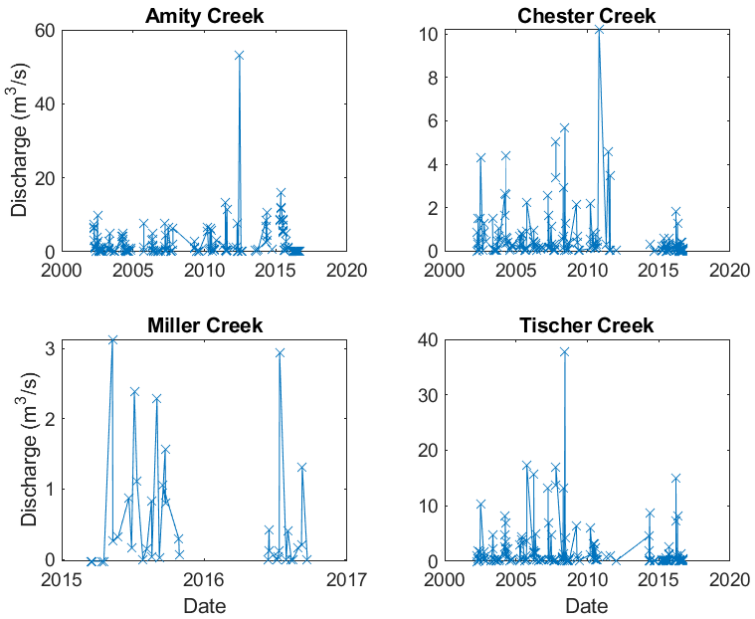

Data from Axler et al. 2020; vertical scales differ among subplots

Figure 5.1. Discharge in Duluth-area streams

The ranges for *Q* and width *B* in Table 5.1 reflect estimates for winter for streams near Duluth based on the ranges observed between October and April (Table 5.2).

Table 5.2. Summary of discharge and chloride concentration reported in Duluth-area streams for October 2002 through April 2016

Stream	Discharge (m^3/s)			Chloride concentration (mg/L)		
	Minimum	Average	Maximum	Minimum	Average	Maximum
Amity Creek	0.03	2.7	8.8	4	25	75
Chester Creek	0.02	1.0	10.2	22	110	1,210
Miller Creek	0.06	0.2	0.3	62	145	367
Tischer Creek	0.00	2.6	17.2	17	124	860

Data from Axler et al. 2009

The depth, *H,* is calculated from Manning's equation (e.g., Henderson 1966), and mean velocity is computed as $U = Q/BH$. In this way, the model was developed for streams with flow and geometry representative of streams near Duluth.

Many empirical formulas for the dispersion coefficient have been proposed. An evaluation of 11 formulas showed that, for small streams ($B/H < 30$), the formulas from Iwasa and Aya (1991), Liu (1977), and Koussis and Rodriguez-Mirasol (1998) performed best (Rehmann et al. 2021). Because the estimates were similar, the research team used the last of these formulas to estimate *K* as follows:

$$K = 0.6u_* \frac{B^2}{H} \quad \textbf{(8)}$$

where u_* is the shear velocity estimated with $U / u_* = 8$, which is the average of data compiled in Rutherford (1994). These estimates included the effect of channel slope through the use of Manning's equation.

The next class of parameters to be considered involves degradation and removal. In general, the removal rate for KAc would reflect the combined effects of mechanisms such as biodegradation, photolysis, hydrolysis, sorption, etc. However, information on the environmental fate of acetic acid suggests that the prime removal mechanism is biodegradation (NIH 2020). Therefore, the removal rate λ for KAc was taken to be equal to the biodegradation rate k_1, which ranges from 0.03 to 0.05 d^{-1} (Revitt and Worrall 2003).

The reaeration rate depends on the flow, temperature, turbulence intensity, and conditions at the free surface. The default approach in the model QUAL2K (Chapra et al. 2008) is the Covar (1976) scheme, which uses the depth and velocity to choose between the formulas of O'Connor and Dobbins (1958), Churchill et al. (1962), and Owens et al. (1964) as follows:

$$k_{2,20} = 3.93\frac{U^{0.5}}{H^{1.5}}, \quad k_{2,20} = 5.026\frac{U}{H^{1.67}}, \quad k_{2,20} = 5.32\frac{U^{0.67}}{H^{1.85}} \tag{9}$$

where $k_{2,20}$ is the reaeration rate at 20°C (d^{-1}) and U and H are in m/s and m, respectively. The effect of water temperature T_w. is assessed with the following:

$$k_2 = k_{2,20}\theta^{T_w - 20} \tag{10}$$

where θ = 1.0241 (Demars and Manson 2013). Note that Demars and Manson (2013) review the effects of temperature, bubbles, and turbulence on the coefficient θ in detail.

The remaining parameters for simulating the fate and transport of contaminants for this problem relate to the initial and boundary conditions. The initial condition is the acetate concentration before runoff enters the stream. Because acetate degrades, the initial concentration was assumed as zero. The boundary condition is the concentration of acetate entering the streams from runoff. As documented in Chapters 2 and 3, sampling by the Iowa and Minnesota teams during the first field season yielded acetate concentrations between about 10 and 3,500 mg/L.

5.3.3 Evaluating the Model

5.3.3.1 Tracer-Response Curves and Affected Lengths

The model predicts the tracer-response curves, or plots of concentrations vs. time at specified locations (Figure 5.2).

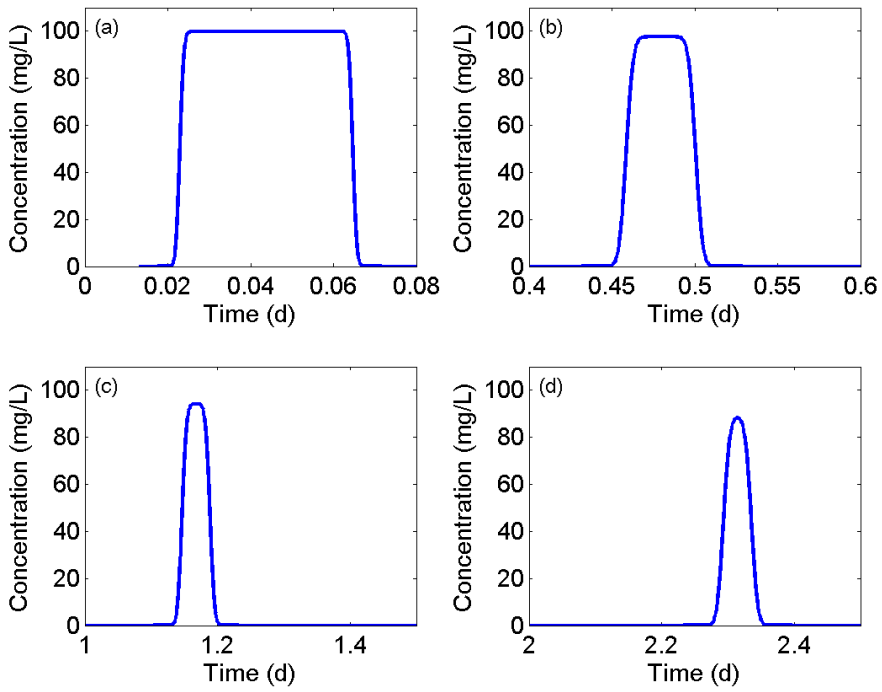

Flow rate Q = 0.5 m^3/s, channel width B = 3 m, and channel slope $S_0 = 10^{-3}$

Figure 5.2. Examples of tracer-response curves for runoff of C_0 = 100 mg/L for T = 1 h for downstream distances of (a) 1 km, (b), 20 km, (c) 50 km, and (d) 100 km

In this example, the tracer-response curve measured 1 km downstream of the runoff point resembles the boxcar shape of the input. At a distance of 20 km (or a travel time of about 0.5 d), the edges have dispersed noticeably, but the concentration has not decreased significantly below the input concentration of 100 mg/L. By 50 km, the concentration cloud has dispersed further, and, by 100 km (or 2.3 d of travel time), the concentration cloud resembles the tracer-response curve for an instantaneous input. Even after that travel, the concentration has decreased by only about 12%. At that point, the concentration obtains measurable values for about 2 h, or twice the runoff duration.

The model can also predict the length beyond which the concentration will not exceed a specified value. In the example shown with Figure 5.2, if the concentration threshold is set to 90 mg/L, Figures 5.2(c) and (d) show that the affected length is between 50 and 100 km; in fact, a full calculation gives the value 86 km.

The example in Figure 5.3 illustrates in more detail how the affected length varies with discharge and runoff duration.

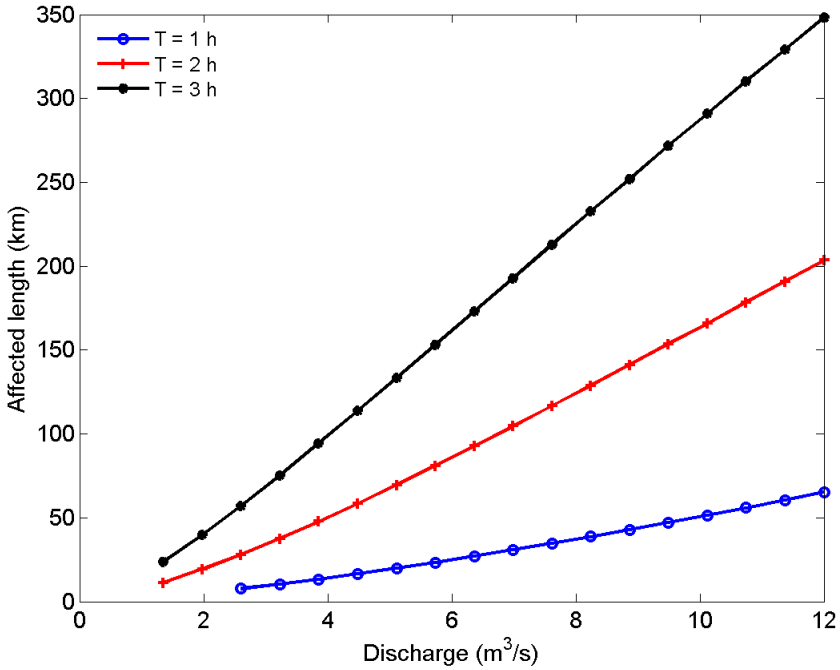

Channel width B is 20 m and channel slope S_0 is 10^{-3}

Figure 5.3. Examples of affected lengths computed for an input concentration C_0 of 20 mg/L and threshold concentration C_t of 10 mg/L as a function of flow and runoff duration

Affected length increases as discharge and runoff duration increase. Because the degradation rate is small (0.05 d^{-1}), reducing the concentration by just a factor of 2 takes large distances—tens to hundreds of kilometers.

For toxicity, this finding is troubling because any effects would remain for large distances; however, the experiments covered in Chapter 4 show little effect of KAc on microbial activity even at deicer levels higher than those observed in the two field collection seasons. For DO consumption, this finding implies that deficits should be small; this intuition is supported with the results that follow.

Of course, at these distances, the assumption that the channel geometry and flow rate do not change is unrealistic. Rehmann et al. (2021) encountered a similar challenge in predicting the length of a stream affected by an intrusion of fire retardant; the researchers implemented an approach that accounts for the change in the order of the stream (Strahler 1957) using mean widths and lengths from Downing et al. (2012) and hydraulic geometry relations from Leopold (1960). In this case, the watershed modeling of the U of M team provides a fuller view of the stream network that will remove the need for assumptions about the network.

5.3.3.2 Dissolved Oxygen Deficit

The model allows the DO deficit to be predicted as a function of distance from the runoff site and time after runoff begins. These results can provide the maximum DO deficit occurring at any position in the stream (Figure 5.4).

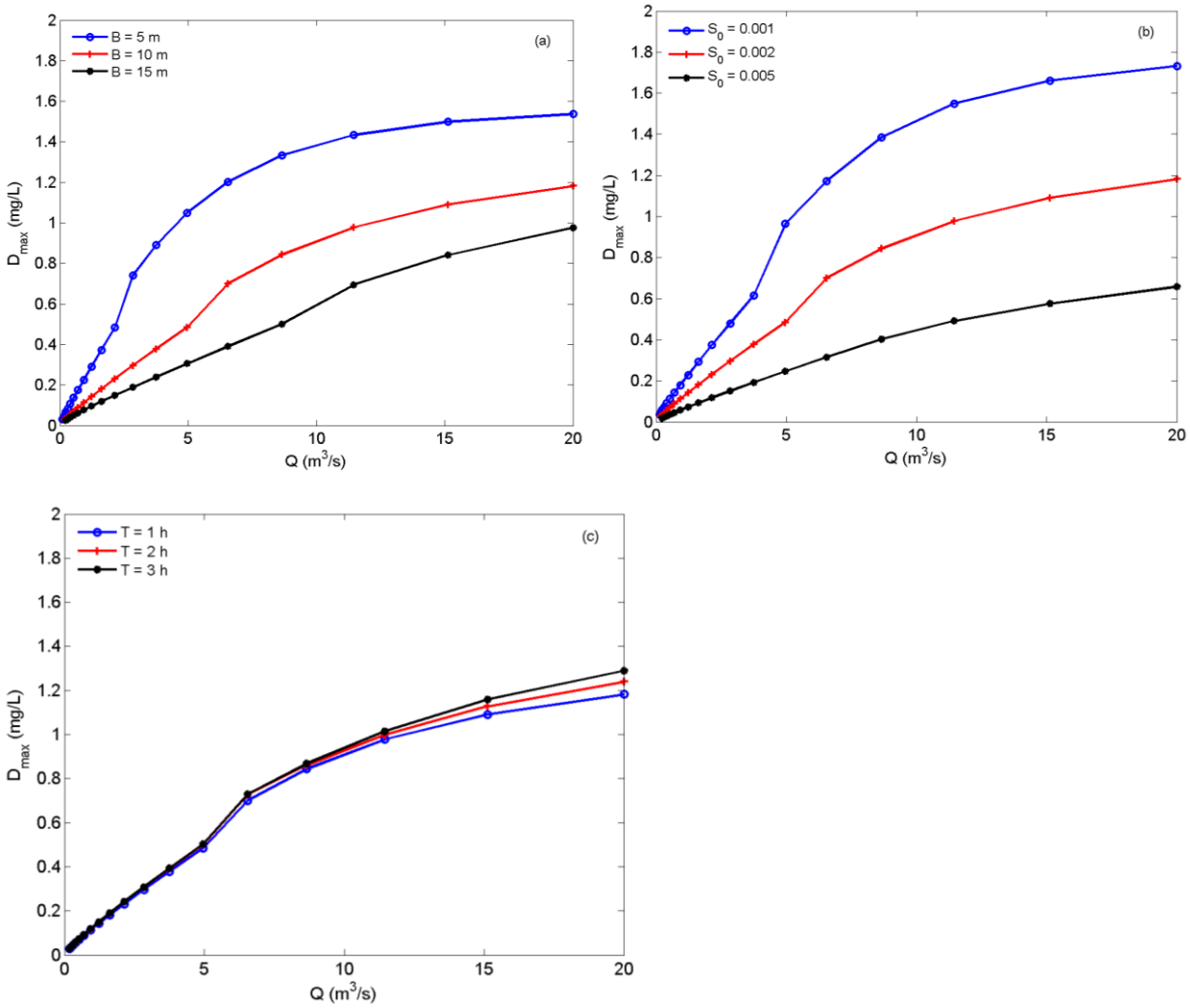

BOD in the runoff is 100 mg/L, and a temperature of 1°C is used

Figure 5.4. Maximum DO deficit as a function of discharge with secondary dependence on (a) channel width, (b) channel slope, and (c) runoff duration

The DO deficit increases with discharge, and it decreases with channel width and slope. It also increases slightly as the runoff duration increases. A key finding is that, for the conditions listed in the previous Table 5.1, the maximum DO deficit is less than 2 mg/L, or less than 15% of the DO concentration at saturation at 1°C. At higher temperatures, upon which the degradation rate decreases (Revitt and Worrall 2003), the maximum DO deficit is smaller. Also, the input BOD concentration of 100 mg/L exceeds the values that the U of M team measured at the I-35 and CE sites during the first sampling season. The DO deficit is directly proportional to the input BOD concentration; therefore, the DO deficit is likely to be even less than that illustrated in Figure 5.4.

5.4 FATE AND TRANSPORT OF KAC IN LAKES

5.4.1 Developing the Model

In contrast to the model for streams, the model for lakes focuses on setting boundaries on the transport of KAc in a lake. The transport processes in lakes—which can include internal waves, currents, effects of the earth's rotation, penetrative convection, vertical mixing from various sources of turbulence, and horizontal dispersion—are too complex in general to comprehensively model inexpensively, especially for a large lake like Lake Superior. Instead, the model for lakes attempts to estimate the extent of the spreading by horizontal dispersion and vertical mixing.

The concentration, *C,* of a contaminant was computed using a three-dimensional version of equation (2), ignoring advection:

$$\frac{\partial C}{\partial t} = K_x \frac{\partial^2 C}{\partial x^2} + K_y \frac{\partial^2 C}{\partial y^2} + K_z \frac{\partial^2 C}{\partial z^2} - \lambda C \qquad \textbf{(11)}$$

where K_x and K_y are the horizontal dispersion coefficients, and K_z is the vertical eddy diffusivity. Analogous to equation (2), equation (11) applies for any contaminant undergoing three-dimensional spreading and first-order decay. For a mass, *M,* input on the shore at the surface of a lake, equation (7) predicts the concentration to be as follows:

$$C = \frac{Me^{-\lambda t}}{(4\pi t)^{3/2}(K_x K_y K_z)^{1/2}} \exp\left(-\frac{x^2}{4K_x t} - \frac{y^2}{4K_y t} - \frac{z^2}{4K_z t}\right) \qquad \textbf{(12)}$$

Thus, given the mass of contaminant and coefficients of degradation, horizontal dispersion, and vertical mixing, one can compute the concentrations at any point and time.

Unlike applications in river mixing, in which the dispersion coefficient *K* is usually taken to be constant, dispersion in lakes depends on the scale L_c of the contaminant cloud, which can be defined in terms of the major and minor axes σ_{ma} and σ_{mi} and the size (i.e., area σ^2) of the elliptical cloud as follows:

$$L_c = 3\sigma = 3(2\sigma_{ma}\sigma_{mi})^{1/2} \qquad \textbf{(13)}$$

Peeters and Hofmann (2015) summarized several data sets that follow the relation as follows:

$$K = aL_c^b \qquad \textbf{(14)}$$

where *a* and *b* are coefficients. The exponent *b* is zero for Fickian diffusion (i.e., constant dispersion coefficient). However, measurements show that, in lakes $b > 0$ because, as the cloud grows, motions of larger size can disperse the contaminant. The exponent is 4/3 for homogeneous isotropic turbulence in the inertial subrange (Okubo 1971). Of the values from Peeters and Hofmann (2015), which come from experiments with drifters in Lake Constance, Switzerland, three are smaller and one is larger (Figure 5.5(a)).

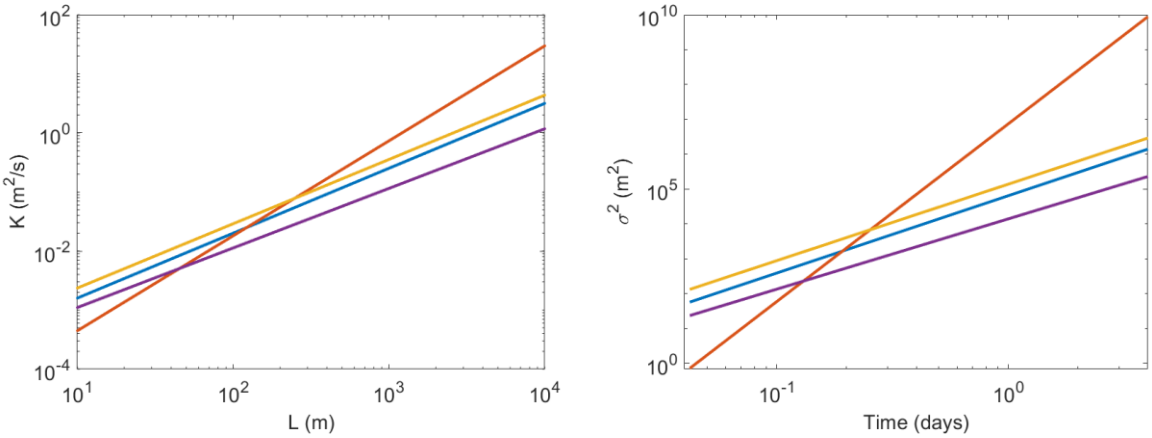

Parameters taken from four experiments in Peeters and Hofmann 2015

Figure 5.5. Examples of horizontal dispersion in a lake: (a) dependence of the dispersion coefficient on length scale and (b) growth of the contaminant cloud as a function of time

Analyzing the spatial moments of a contaminant cloud as in Fischer et al. (1979, Ch. 2) gives a relationship between the growth of the size of the cloud and the dispersion coefficient as follows:

$$K = \frac{1}{4}\frac{d\sigma^2}{dt} \tag{15}$$

Combining equations (13) through (15) yields the following:

$$\sigma^2 = \alpha t^{\frac{2}{2-b}} \tag{16}$$

with $\alpha = 3^{2b/(2-b)}\left(4a\right)^{2/(2-b)}$. Equation (15) recovers results from previous work as follows: if *b* =0, the cloud size grows linearly with time (Fischer et al. 1979, Ch. 2), and, if *b* = 4/3, $\sigma^2 \propto t^3$ (Okubo 1971). Three of the values from Peeters and Hofmann (2015) give a cloud with a mean diameter of about 300 m after 4 days, while the other gives a much larger cloud (Figure 5.5(b)).

The theory of diffusion relates the variance to time and the dispersion coefficient as $\sigma_x^2 = 2K_x t$, for example. If the horizontal spreading is taken to be equal in the two horizontal directions, equation (12) becomes equation (17):

$$C = \frac{4Me^{-\lambda t}}{2\pi^{3/2}\sigma^2\sqrt{K_z t}}\exp\left(-\frac{r^2}{\sigma^2}-\frac{z^2}{4K_z t}\right) \tag{17}$$

where $r = \left(x^2 + y^2\right)^{1/2}$ is the horizontal distance from the input point. Then, from equation (16) and the relation for α, the peak concentration, which occurs at (*r*, *z*) = (0, 0) is as follows:

$$C_p = \frac{2Me^{-\lambda t}}{\alpha \pi^{3/2} K_z^{1/2}} t^{-(b+2)/(4-2b)} \quad \textbf{(18)}$$

The mass, *M,* was estimated from runoff from two lanes (i.e., *N* = 2) to an inlet on a bridge using equation (19):

$$M = f_r f_s \rho_s R N L_r \quad \textbf{(19)}$$

where f_r is the fraction of applied KAc appearing in the runoff, f_s is the fraction of active ingredient in the deicer solution (50%), ρ_s is the density of the deicer solution (1,280 kg/m^3), *R* is the application rate, and L_r is the length of highway running off to the inlet. For an application rate of 30 gal/lane-mile (or 7.1×10^{-5} m^3/lane-m) and a length of 200 ft (or 61 m), the mass is 2.8 kg.

5.4.2 Parameterizing the Model

Horizontal dispersion coefficients measured in lakes vary widely. Values from Okubo (1971), Murthy (1976), and Lawrence et al. (1995) are similar to those from Peeters and Hofmann (2015) but slightly larger because of vertical shear dispersion. Peeters and Hofmann (2015) attributed large differences between their values of *K* and the measurements of Stocker and Imberger (2003) and Stephens et al. (2004) to internal wave motions in the latter cases. Such motions should be less important in the winter when the stratification of Minnesota lakes is small. Furthermore, using equation (16) to estimate the cloud size should be conservative because other horizontal motions, such as currents, are ignored: this approach will give a lower bound on the size and upper bound on the concentrations at any time. To estimate concentrations given the input amount and the horizontal spread, vertical mixing also needs to be estimated.

Values of the coefficients *a* and *b* from several studies are listed, roughly in order of increasing horizontal scale, in Table 5.3.

Table 5.3. Values of the coefficients in equation (16) for the horizontal area of a contaminant cloud in a lake

Water body	Reference	Length range (m)	*a*	*b*
L. Constance	Peeters and Hofmann 2015	30–620	1.08×10^{-4}	1.01
L. Constance	Peeters and Hofmann 2015	200–1,200	1.27×10^{-4}	1.1
L. Michigan	Choi et al. 2020	190–1,460	3.5×10^{-2}	0.2
L. Constance	Peeters and Hofmann 2015	100–2,000	1.92×10^{-4}	1.09
L. Constance	Peeters and Hofmann 2015	130–3,700	1.1×10^{-5}	1.61
L. Michigan	Choi et al. 2020	950–2,900	2×10^{-3}	0.97
L. Michigan	Choi et al. 2020	1,460–8,000	1.1×10^{-4}	1.09
L. Ontario	Murthy 1976	324–15,261	6.65×10^{-4}	1.22
Gulf of Mexico	Poje et al. 2014	430–76,000	2.68×10^{-4}	1.2
Ocean	Okubo 1971	64–110,000	3.7×10^{-4}	1.2

Source: Adapted from Choi et al. 2020

Most of the exponents are between 1 and 1.2, and the values of the coefficient a are mostly on the order of 10^{-4}. Two of the cases differ substantially: one of the experiments from Peeters and Hofmann (2015) had a contaminant cloud whose area increased more quickly (i.e., higher b), while, at large time, the cloud in the experiments of Choi et al. (2020) grew more slowly (i.e., lower b).

Table 5.3 also omits the experiments of Stocker and Imberger (2003) and Stephens et al. (2004) because significant internal wave motions affected the dispersion they observed (Peeters and Hofmann 2015). For this study, such motions should be less important in the winter when the stratification of Minnesota lakes is small. The data in Table 5.3 guide the estimates of horizontal spread for lakes of various sizes.

As with horizontal dispersion, estimating vertical mixing in a lake involves striking a balance between tradeoffs. Simple models could be easily constructed and used widely, but they might omit important processes and factors. More complex models approach realistic cases, but they might require too many data or too much experience to be easily used. With the view of developing a model that is easy to use, the research team adopted the vertical mixing coefficient of $K_z = 10^{-3}$ m^2/s from the experiments of Fer et al. (2002) in a deep lake in winter.

5.4.3 Evaluating the Model

Some example calculations illustrate the behavior to be expected. Peak concentrations in the lake start high and drop quickly given the spreading in three dimensions (Figure 5.6).

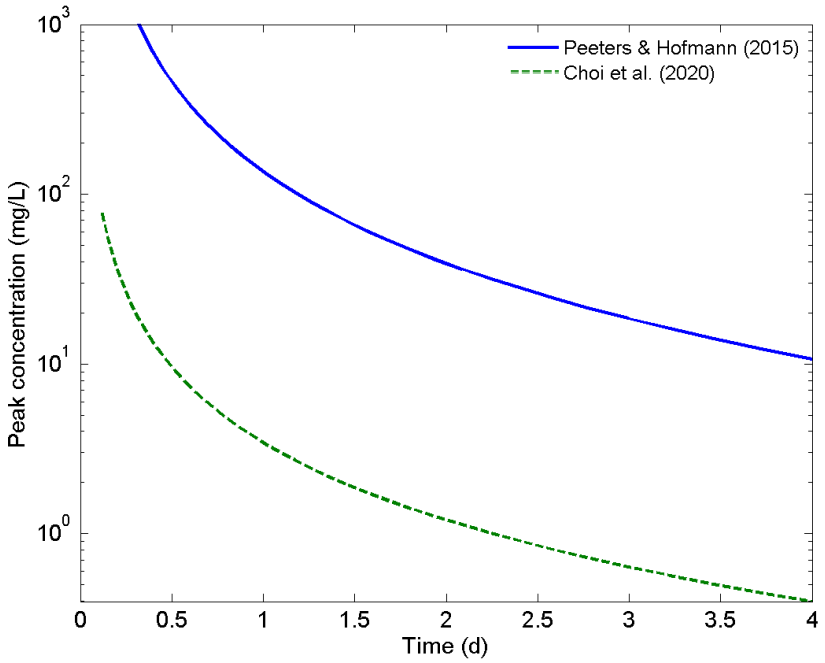

Input mass is 2.8 kg and vertical eddy diffusivity is 10^{-3} m^2/s (Fer et al. 2002)

Figure 5.6. Decrease in peak concentration caused by spreading in a lake, with curves computed for $a = 1.27\times10^{-4}$ and $b = 1.1$ (Peeters and Hofmann 2015) and $a = 2\times10^{-3}$ and $b = 0.97$ (Choi et al. 2020)

Using the coefficients from Peeters and Hoffman (2015) in the model yields concentrations over 1,000 mg/L within 0.5 d of the input. Field measurements from the first sampling campaign gave potassium and acetate concentrations of about 800 mg/L and 3,500 mg/L in late January 2020. The predicted concentrations in Figure 5.6 drop to about 10 mg/L after 4 d. These predictions strongly depend on the coefficients adopted for the spreading model: the coefficients from Choi et al. (2020) give much smaller concentrations because the value of *a* is about 20 times smaller than in Peeters and Hoffman (2015).

The horizontal and vertical spread of KAc is indicated in Figure 5.7.

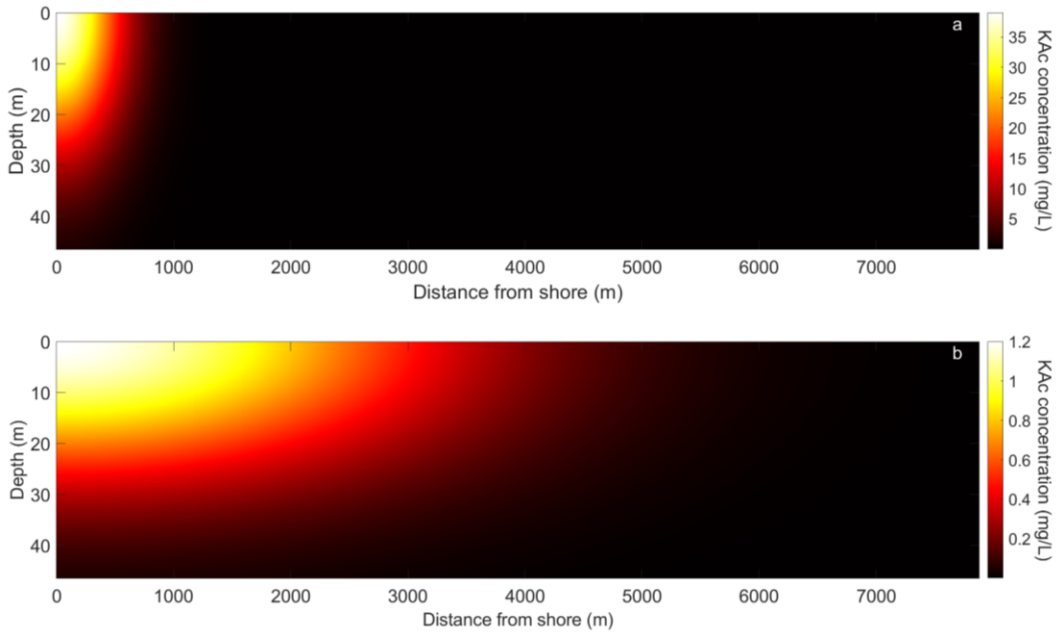

Vertical eddy diffusivity of 10^{-3} m^2/s

Figure 5.7. KAc concentrations in a horizontal-vertical plane 2 d after runoff of 2.8 kg, with spreading parameters *a* and *b* taken from Peeters and Hofmann 2015 and Choi et al. 2020, respectively

Again, differences arising for the choice of the parameters *a* and *b* are apparent: At 2 d after the input, the length scale $\Lambda = 3\sigma/2$ is 830 m for the Peeters and Hofmann (2015) values (Figure 5.7(a)) and about 4,700 m for the Choi et al. (2020) values (Figure 5.7(b)). The difference in peak concentrations from the previous Figure 5.6 is reflected in the *x*-*z* slices of the concentration field; at t = 2 d, the peak concentration in Figure 5.7(a) is about 30 times larger than that in Figure 5.7(b).

With 10 sets of *a* and *b* in the previous Table 5.3, one must ask which to choose. Each of the observations pertains to a range of flow lengths. For example, the values from Peeters and Hofmann (2015) apply to a range of 200–1,200 m; whereas, the values from Choi et al. (2020) apply to a range of 950–2,900 m. In this case, the Peeters and Hofmann (2015) values apply better for the initial evolution of the contaminant cloud because they were developed for smaller length scales. The values from Choi et al. (2020) could be applied once the cloud has grown beyond 1,200 m. As noted at the outset of the modeling for lakes, this analysis helps to establish bounds on likely concentrations to be observed.

5.5 SUMMARY

The results from these versions of the models allow the following observations to be summarized:

- The tracer-response curves provide the spatial and temporal information needed to assess exposure to contaminants, including KAc and BOD. Once threshold concentrations are identified for KAc and BOD, affected lengths and exposure times can be computed.
- Affected reaches are likely to be long. Small degradation rates lead to substantial distances needed to reduce the concentrations by dispersion. As a result, more precise prediction of the affected length requires attention to the full stream network.
- The DO deficit from KAc is likely to be small compared to the DO concentration at saturation. For a wide range of conditions tested here, the deficit was less than 2 mg/L, or 15% of the concentration at saturation.
- KAc concentrations from runoff in lakes can reach high values initially and drop sharply because of spreading in three dimensions.

CHAPTER 6: CONCLUSIONS

This project assessed KAc's persistence in soil and water, its effects on water quality, and its toxicity to microorganisms. This assessment was addressed with field measurements, laboratory experiments, and modeling.

Between the ISU and U of M teams, field sites were selected to investigate a range of conditions, and sampling characterized KAc concentrations in soil and water as well as measured DO, BOD, pH, and other water quality parameters. Laboratory experiments investigated the persistence of KAc and its microbial toxicity at higher resolution than possible in the field sampling.

Two models of the fate and transport of KAc in runoff to streams and lakes were constructed: KAcStream predicted the decrease in dissolved oxygen concentrations caused by BOD from KAc in streams, and KAcLake estimated the spread of KAc in a lake. These models complemented the watershed modeling of the U of M team.

6.1 MAJOR FINDINGS

Results from field sampling in Duluth during the winters of 2019–2020 and 2020–2021 showed that, while KAc deicers impacted some water-quality parameters, the observed effects were relatively small. When applied on its own without mixing with chloride-based deicers, the KAc deicer appeared to have little effect on the concentrations of aqueous nitrogen species (e.g., ammonia, nitrite, nitrate) or heavy metals. While KAc deicer application resulted in elevated TOC and sulfate concentrations, the elevated TOC was likely from the acetate in the deicer, and the CF7 KAc-based deicer (Cryotech) used by MnDOT has also been reported to include high sulfate concentrations.

Unsurprisingly, KAc deicer application led to greater potassium concentrations in runoff water. The runoff samples from KAc-applied areas also tended to have higher sodium and calcium concentrations, which was unexpected. Further discussion with MnDOT and city of Duluth staff revealed the likelihood that these areas still received some chloride-based deicer either directly or in the immediate vicinity, which may have resulted in the presence of Na, Ca, and Cl in the samples. However, these elevated concentrations of TOC, sulfate, Na, Ca, and Cl observed in runoff appeared to have limited impact on surface waters in the surrounding areas. Similarly, the application of KAc deicers resulted in limited effects on soil quality (i.e., only elevated potassium concentrations), especially compared to areas with chloride-based deicer application.

Contrary to some published studies, there was no observable aerobic biodegradation of KAc by representative surface water and soil microorganisms at room temperature up to 28 days. Soil slurries composed of soil from sites receiving KAc deicer application (e.g., the I-35, Rice's Point, and Blatnik Bridge sites) and Duluth surface waters from Lake Superior and Lester River showed no change in acetate concentrations even when exposed to pure KAc chemicals.

These observations suggest that KAc biodegradation is unlikely or will occur at a very slow rate around Duluth (i.e., by native microbial communities) under aerobic and spring/summer conditions. These

results are supported by literature that indicates acetate, while used for critical cellular mechanisms, is often not biodegraded at all or, at most, removed at very slow rates under aerobic conditions. Furthermore, laboratory experiments with model bacterial species showed that the KAc deicer had limited impact on bacterial metabolism even at high concentrations (e.g., 3.5 g/L, which is similar to acetate concentrations measured in runoff water samples). However, the deicer resulted in slightly lower metabolism in model bacteria compared to comparable concentrations of pure KAc, pointing to the potential impact of deicer additives. These results suggest that the presence of KAc deicer (either as acetate or potassium) does not exhibit toxicity toward bacteria at the concentrations observed in the runoff samples.

Two models of KAc fate and transport in streams and lakes were developed. The KAcStream model provides a way to estimate the DO deficit from KAc. This deficit is likely to be small compared to the DO concentration at saturation. For a wide range of conditions tested in this project, the deficit was less than 2 mg/L, or 15% of the concentration at saturation. The KAcLake model provides a way to estimate the concentrations as a cloud of KAc spreads in a lake. KAc concentrations from runoff in lakes can reach high values initially and drop sharply because of spreading in three dimensions. Initial simulations using these models suggest that the direct impact of KAc on dissolved oxygen levels in streams and lakes would be relatively small overall. The models were made available to MnDOT as an openly accessible MATLAB Runtime application, in which initial conditions can be manipulated by users to better predict KAc fate and transport in aquatic environments of interest.

6.2 SUMMARY RECOMMENDATIONS

The results from this project indicate that, while KAc deicers can have immediate impacts on water quality from field application, these impacts appear to be relatively small especially to larger bodies of water. Although larger fauna were not assessed, the impact of KAc on aerobic bacteria appeared to be small. The fate and transport models further suggest that the impact of KAc deicers on DO levels in the water would be limited. However, these impacts would likely be magnified in sensitive water bodies, so caution should be exercised before applying KAc deicers in these areas.

The researchers recommend that MnDOT use the two models, KAcStream and KAcLake, to guide its choice of sites and concentrations of KAc deicer applications. These models allow for initial estimates of the environmental impact of KAc applications.

REFERENCES

Axler, R., C. Kleist, G. Host, C. Hagley, M. Lonsdale, J. Reed, J. Schomberg, N. Will, J. Henneck, G. Sjerven, E. Ruzycki, T. Carlson, B. Munson, and C. Richards. 2009. Lake Superior Streams: Community Partnerships for Understanding Water Quality and Stormwater Impacts at the Head of the Great Lakes. Data accessed December 28, 2020, http://lakesuperiorstreams.org/streams/stream_data.html.

Bahadur, R. and W. B. Samuels. 2015. Modeling the Fate and Transport of a Chemical Spill in the Elk River, West Virginia. *Journal of Environmental Engineering*. Vol. 141, No. 7, pp. 05014007-1–05014007-9.

Barton, C. D. and A. D. Karathanasis. 2002. Clay Minerals. In *Encyclopedia of Soil Science*. Springer Science & Business Media, Dordrecht, The Netherlands.

Bravo, H. R. 1997. Modeling DO Conditions in Streams using Lagrangian Advection Method. *Journal of Hydraulic Research*. Vol. 35, No. 5, pp. 643–658.

Cetin, B., A. H. Aydilek, and Y. Guney. 2012. Leaching of Trace Metals from High Carbon Fly Ash Stabilized Highway Base Layers. *Resources, Conservation and Recycling*. Vol. 58, pp. 8–17.

Chapra, S. C. 1997. *Surface Water-Quality Modeling*. McGraw-Hill, New York, NY.

Chapra, S. C., G. J. Pelletier, and H. T. Lu. 2008. *QUAL2K: A Modeling Framework for Simulating River and Stream Water Quality*. Version 2.11. Civil and Environmental Engineering Dept., Tufts University, Medford, MA.

Choi, J., C. Troy, N. Hawley, M. McCormick, and M. Wells. 2020. Lateral Dispersion of Dye and Drifters in the Center of a Very Large Lake. *Limnology and Oceanography*. Vol. 65, No. 2, pp. 336–348.

Chun, C. L., K. Cassidy, J. Henneck, and J. S. Gulliver. 2021. *Environmental Field Evaluation and Persistence of KAc in Meltwater, Runoff, and Receiving Water Body--Year 2*. Report for Task 7: submitted to the Minnesota Department of Transportation under project 1034767.

Churchill, M. A., H. L. Elmore, and R. A. Buckingham. 1962. The Prediction of Stream Reaeration Rates. *Journal of the Sanitary Engineering Division*. Vol. 88, No. 4, pp. 1–46.

Corsi, S. R., D. Mericas, and G. T. Bowman. 2012. Oxygen Demand of Aircraft and Airfield Pavement Deicers and Alternative Freezing Point Depressants. *Water Air and Soil Pollution*. Vol. 223, No. 5, pp. 2447–2461.

Covar, A. P. 1976. *Selecting the Proper Reaeration Coefficient for Use in Water Quality Models*. Presented at the U.S. EPA Conference on Environmental Simulation and Modeling, April 19–22, Cincinnati, OH.

Defourny, C. 2000. *Environmental Risk Assessment of Deicing Salts*. 8th World Salt Symposium, May 7–11, Hague, The Netherlands, pp. 767–770.

Demars, B. O. L. and J. R. Manson. 2013. Temperature Dependence of Stream Aeration Coefficients and the Effect of Water Turbulence: A Critical Review. *Water Research*. Vol. 47, No. 1, pp. 1–15.

Downing, J. A., J. J. Cole, C. M. Duarte, J. J. Middelburg, J. M. Melack, Y. T. Prairie, P. Kortelainen, R. G. Striegl, W. H. McDowell, and L. J. Tranvik. 2012. Global Abundance and Size Distribution of Streams and Rivers. *Inland Waters*. Vol. 2, No. 4, pp. 229–236.

Fay, L. and X. M. Shi. 2012. Environmental Impacts of Chemicals for Snow and Ice Control: State of the Knowledge. *Water Air and Soil Pollution*. Vol. 223, No. 5, pp. 2751–2770.

Fer, I., U. Lemmin, and S. A. Thorpe. 2002. Observations of Mixing Near the Sides of a Deep Lake in Winter. *Limnology and Oceanography*. Vol. 47, No. 2, pp. 535–544.

Fischer, H. B., E. J. List, R. C. Y. Koh, J. Imberger, and N. H. Brooks. 1979. *Mixing in Inland and Coastal Waters*. Academic Press, New York, NY.

French, H. K., S. Van der Zee, and A. Leijnse. 2001. Transport and Degradation of Propyleneglycol and Potassium Acetate in the Unsaturated Zone. *Journal of Contaminant Hydrology*. Vol. 49, No. 1–2, pp. 23–48.

Gonzalez-Pinzon, R., R. Haggerty, and M. Dentz. 2013. Scaling and Predicting Solute Transport Processes in Streams. *Water Resources Research*. Vol. 49, pp. 4071–4088.

Gulliver, J. S. 2007. *Introduction to Chemical Transport in the Environment*. Cambridge University Press, Cambridge, England.

Henderson, F. M. 1966. *Open Channel Flow*. MacMillan, New York, NY.

Iwasa, Y. and S. Aya. 1991. Predicting Longitudinal Dispersion Coefficient in Open-Channel Flows. In *Environmental Hydraulics*. Vols. 1 and 2, pp. 505–510.

Kosson, D. S., H. A. van der Sloot, F. Sanchez, and A. C. Garrabrants. 2002. An Integrated Framework for Evaluating Leaching in Waste Management and Utilization of Secondary Materials. *Environmental Engineering Science*. Vol. 19, No. 3, pp. 159–204.

Koussis, A. D. and J. Rodríguez-Mirasol. 1998. Hydraulic Estimation of Dispersion Coefficient for Streams. *Journal of Hydraulic Engineering*. Vol. 124, No. 3, pp. 317–320.

Lawrence, G. A., K. I. Ashley, N. Yonemitsu, and J. R. Ellis. 1995. Natural Dispersion in a Small Lake. *Limnology and Oceanography*. Vol. 40, No. 8, pp. 1519–1526.

Leopold, L. B. 1960. Rivers. *American Scientist*. Vol. 50, No. 4, pp. 511–537.

Liu, H. 1977. Predicting Dispersion Coefficient of Streams. *Journal of Environmental Engineering Division*. Vol. 103, No. 1, pp. 59–69.

Murthy, C. R. 1976. Horizontal Diffusion Characteristics in Lake Ontario. *Journal of Physical Oceanography*. Vol. 6, No. 1, pp. 76–84.

NIH. 2020. *Acetic Acid*. National Institutes of Health. https://webwiser.nlm.nih.gov/substance?substanceId=402&identifier=Acetic%20Acid&identifierType=name&menuItemId=76&catId=115 Last accessed December 28, 2020.

Novotny, E. V., D. Murphy, and H. G. Stefan. 2008. Increase of Urban Lake Salinity by Road Deicing Salt. *Science of The Total Environment*. Vol. 406, No. 1–2, pp. 131–144.

O'Connor, D. J. and W. E. Dobbins. 1958. Mechanism of Reaeration in Natural Streams. *Transactions of the American Society of Civil Engineers*, Vol. 123, No. 1, pp. 641–684.

Okubo, A. 1971. Oceanic Diffusion Diagrams. *Deep Sea Research and Oceanographic Abstracts*. Vol. 18, No. 8, pp. 789–802.

Owens, M., R. W. Edwards, and J. W. Gibbs. 1964. Some Reaeration Studies in Streams. *International Journal of Air and Water Pollution*. Vol. 8, pp. 469–486.

Peeters, F., A. Wuest, G. Piepke, and D. M. Imboden. 1996. Horizontal Mixing in Lakes. *Journal of Geophysical Research: Oceans*. Vol. 101, No. C8, pp. 18361–1837.

Peeters, F. and H. Hofmann. 2015. Length-Scale Dependence of Horizontal Dispersion in the Surface Water of Lakes. *Limnology and Oceanography*. Vol. 60, No. 6, pp. 1917–1934.

Pinhal, S., D. Ropers, J. Geiselmann, and H. de Jong. 2019. Acetate Metabolism and the Inhibition of Bacterial Growth by Acetate. *Journal of Bacteriology*. Vol. 201, No. 13, e00147-19.

Poje, A. C., T. M. Ozgokmen, B. L. Lipphardt, Jr., B. K. Haus, E. H. Ryan, A. C. Haza, G A. Jacobs, A. J. H. M. Reniers, M. J. Olascoaga, G. Novelli, A. Griffa, F. J. Beron-Vera, S. S. Chen, E. Coelho, P. J. Hogan, A. D. Kirwan, Jr., H. S. Huntley, and J. Mariano 2014. Submesoscale Dispersion in the Vicinity of the Deepwater Horizon Spill. *Proceedings of the National Academy of Sciences*. Vol. 111, No. 35, pp. 12693–12698.

Rehmann, C. R., P. R. Jackson, and H. J. Puglis. 2021. Predicting the Spatiotemporal Exposure of Aquatic Species to Intrusions of Fire Retardant in Streams with Limited Data. *Science of The Total Environment*. Vol. 782, No. 146879, pp. 1–10.

Reichert, P. and O. Wanner. 1991. Enhanced One-Dimensional Modeling of Transport in Rivers. *Journal of Hydraulic Engineering*. Vol. 117, No. 9, pp. 1165–1183.

Revitt, D. M. and P. Worrall. 2003. Low Temperature Biodegradation of Airport De-Icing Fluids. *Water Science and Technology*. Vol. 48, No. 9, pp. 103–111.

Rutherford, J. C. 1994. *River Mixing*. Wiley, New York, NY.

Schmalle, G. F. and C. R. Rehmann. 2014. Analytical Solution of a Model of Contaminant Transport in the Advective Zone of a River. *Journal of Hydraulic Engineering*. Vol. 140, No. 7, pp. 04014029-1–04014029-8.

Stephens, C. L., G. A. Lawrence, and P. F. Hamblin. 2004. Horizontal Dispersion in the Surface Layer of a Long Narrow Lake. *Journal of Environmental Engineering and Science*. Vol. 3, pp. 413–417.

Stocker, R. and J. Imberger. 2003. Horizontal Transport and Dispersion in the Surface Layer of a Medium-Sized Lake. *Limnology and Oceanography*. Vol. 48, No. 3, pp. 971–982.

Strahler, A. N. 1957. Quantitative Analysis of Watershed Geomorphology. *Eos, Transactions of the American Geophysical Union*. Vol. 38, pp. 913–920.

U.S. EPA. 2018. *2018 Edition of the Drinking Water Standards and Health Advisories*. United States Environmental Protection Agency, Washington, DC.

Weiss, P. T. and J. S. Gulliver. 2019. *Potassium Acetate as a Road Salt Alternative*. Task 3 report submitted to the Minnesota Department of Transportation, Minneapolis, MN.

APPENDIX A: MODEL USER MANUAL

OBJECTIVES

This appendix provides training materials for the models described in Chapter 5 to predict fate and transport of KAc in lakes and streams. The models have been encapsulated in two MATLAB apps, KAcStream and KAcLake, which can be run from any computer as long as MATLAB Runtime, which is freely available, is installed.

KAcStream allows the user to explore the effects of KAc on the dissolved oxygen deficit downstream of a runoff point, and KAcLake plots concentrations as a function of depth and distance from shore.

This appendix provides guidance for running the apps. In particular, it explains how to install MATLAB Runtime and run KAcStream and KAcLake.

INSTALLING MATLAB RUNTIME

The apps were developed in the computational software MATLAB. Although the researchers will gladly share the source code, they assumed that most users would not have access to MATLAB. Therefore, the apps were developed as standalone executable files. Running the apps requires installing MATLAB Runtime version 9.9. If you try to run either of the applications without MATLAB Runtime version 9.9, the error message in Figure A.1 appears.

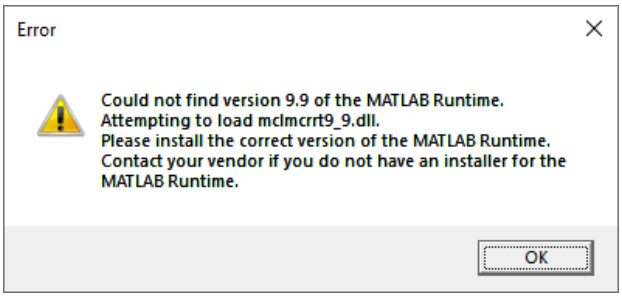

Figure A.1. Error message resulting from not having MATLAB Runtime version 9.9

To install MATLAB Runtime version 9.9, follow these steps:

1. Go to https://www.mathworks.com/products/compiler/matlab-runtime.html.
2. Choose the correct link for R2020b (version 9.9) corresponding to your operating system (i.e., Windows, Mac, or Linux). Be sure to choose version 9.9. Do not choose the most recent version.
3. Extract the files from the downloaded archive.
4. Launch the Setup application. You should see a window that says MATLAB Runtime Installer.
5. Click Next.
6. Accept the terms of the license agreement and click Next.
7. Choose the installation folder and click Next and Install.
8. Click Finish when the Installation is complete window appears.

RUNNING KAcSTREAM

KAcStream estimates the maximum dissolved oxygen (DO) deficit resulting from runoff of KAc. That is, at each point downstream of the runoff point, it computes the DO deficit as a function of time and chooses and plots the maximum value. To run the app, follow these steps:

1. Ensure that version 9.9 of MATLAB Runtime is installed on your computer. If not, see Installing MATLAB Runtime previously.
2. Launch the current version of KAcStream. At the time of this writing the current version is 06.
3. Wait 5–10 seconds for the window to appear.
4. Enter the six required input values:
5. Enter the initial biochemical oxygen demand (BOD) in the runoff in mg/L.
6. Enter the duration of the runoff in hours.
7. Enter the discharge (or flow) of the stream in cubic feet per second (cfs).
8. Enter the width of the stream in feet.
9. Enter the channel slope (i.e., the slope in the direction of flow).
10. Enter the temperature in degrees Fahrenheit. The temperature must be between 23 and 68°F.
11. Click Calculate.
12. View the plot of maximum DO deficit as a function of distance from the point of runoff on the right side of the window.

For example, with the default values in Table A.1, the model produces the output shown in Figure A.2.

Table A.1. Default values for KAcStream

Parameter (units)	Default value
Initial BOD (mg/L)	100
Runoff duration (h)	2
Flow (cfs)	10
Width (ft.)	5
Slope	0.001
Temperature (°F)	32

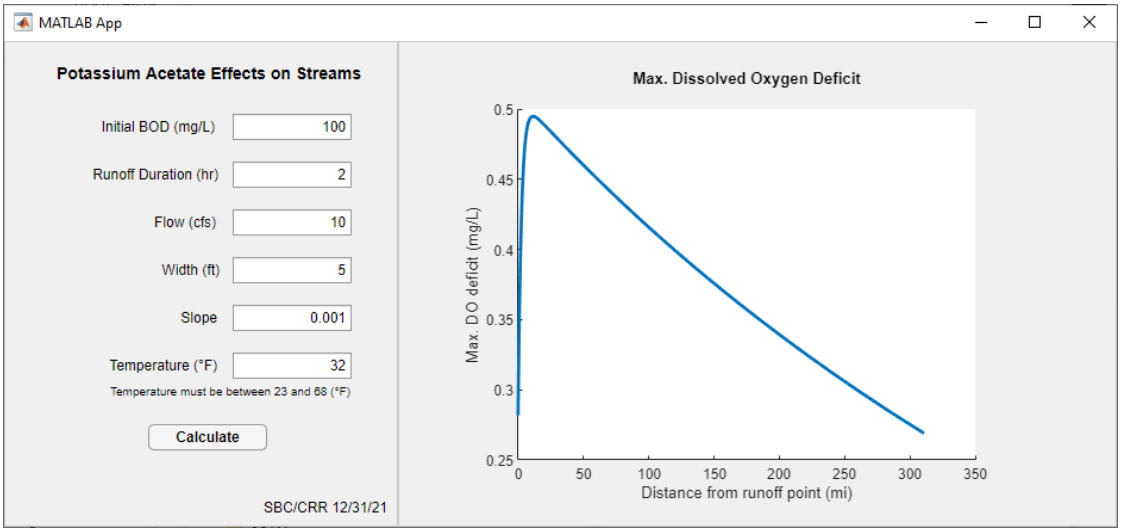

Figure A.2. Result of running KAcStream with the default values of the parameters

In this case, the maximum DO deficit increases from small values near the runoff point to a maximum of about 0.49 mg/L at a distance of 11.8 miles downstream of the runoff point and then decreases slowly with further distance. If the cursor is placed on the plot, five controls will appear in the upper right corner: copy/save, pan, zoom in, zoom out, and restore view. For example, to zoom in, click the magnifying glass with the plus sign and click and drag on the plot to select a rectangle to zoom.

RUNNING KAcLAKE

KAcLake computes concentrations of KAc resulting from runoff near the shore of a lake. It plots concentrations as a function of depth and distance from the shore. To run the app KAcLake, follow these steps:

1. Ensure that version 9.9 of MATLAB Runtime is installed on your computer. If not, see Installing MATLAB Runtime previously.
2. Launch the current version of KAcLake. At the time of this writing the current version is 03.
3. Wait 5-10 seconds for the window to appear.
4. Enter the six required input values:
5. Enter the length (in feet) of highway lane contributing to the runoff. Notice that the number of lanes will be entered separately; that is, do not account for the number of lanes in the contributing length.
6. Enter the number of lanes contributing to the runoff.
7. Enter the application rate in gal/lane-mile.
8. Enter the temperature in degrees Fahrenheit. The temperature must be between 23 and 68ºF.
9. Enter the time (in days) after the runoff occurs for which you want the plot of concentrations.
10. Use the slider to set the fraction of applied KAc that appears in the runoff.
11. Click Calculate.
12. View the concentration plot on the right side of the window.

For example, with the default values in Table A.2, the model produces the output shown in Figure A.3.

Table A.2. Default values for KAcLake

Parameter (units)	Default value
Contributing lane length (ft.)	200
Number of lanes	2
Application rate (gal/lane-mi)	30
Temperature (°F)	32
Final time for plotting (d)	4
Runoff fraction	1.0

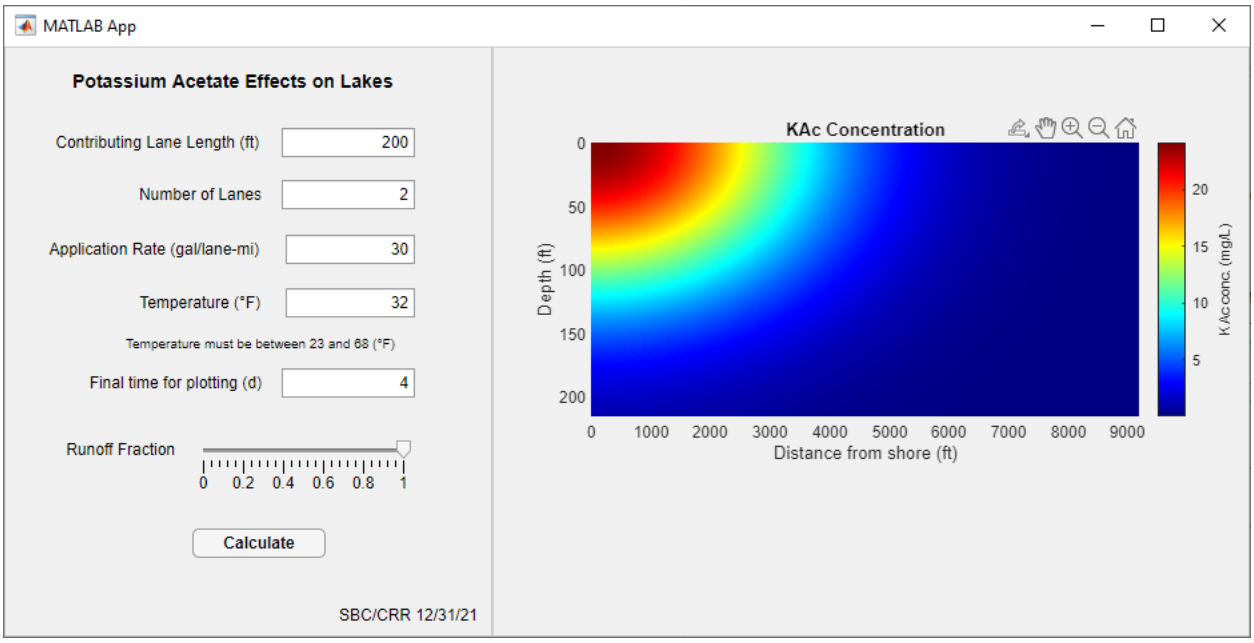

Figure A.3. Result of running KAcLake with the default values of the parameters

The color bar on the right of the plot gives the scale for concentration; as the parameters are changed, be sure to note any changes in the color bar scale. As with KAcStream, the user can adjust the plot with the controls that appear in the upper right corner when the cursor is placed on the plot.

FURTHER DETAILS ON ASSUMPTIONS

Most of the assumptions involved in the models that form the basis of KAcStream and KAcLake have been outlined in Chapter 5. Three additional points will be discussed here: the choice of degradation coefficient, the selection of initial BOD in KAcStream, and the spreading parameters in KAcLake.

The degradation of KAc is complicated by its dependence on temperature, concentration, and perhaps other factors. Revitt and Worrall (2003) measured the degradation coefficient for Clearway, a product with KAc, at temperatures of 1, 4, and 8°C. No observable degradation of acetate after 24 hours was reported in Chapter 4, whereas the report for the U of M team's Task 7 shows that at high concentrations, degradation begins after a lag time (Chun et al. 2021). Degradation coefficients were

highest for the lowest initial concentrations. In both apps, the degradation coefficient was linearly interpolated as a function of temperature using the U of M measurements for non-filtered samples at 4 and 20–23°C and an initial concentration of 100 mg/L and the Revitt and Worrall (2003) measurements for 1 and 8°C. The value at 1°C was assumed to apply to -5°C. Therefore, the user of KAcStream and KAcLake is told to keep the temperature between 23 and 68°F (i.e., -5 and 23°C). The larger values of degradation coefficients yield a conservative (i.e., high) estimate of the maximum dissolved oxygen deficit.

KAcStream requires an estimate of the initial biochemical oxygen demand. The default value of 100 mg/L represents an approximate upper bound of BOD_5 in runoff from the Rice's Point and I-35 sampling sites in the winter of 2020–2021, although the value at the Blatnik Bridge sites was 10–20 times higher (Chun et al. 2021). Figure 27 of U of M's Task 7 report shows that BOD_5 increases with acetate concentration (Chun et al. 2021). However, instead of implementing a relationship between acetate concentration and initial BOD, KAcStream requests that input from the user.

KAcLake computes concentrations using an empirical relationship for the horizontal dispersion of a contaminant in lakes. As described in Chapter 5, several values of the spreading parameters are available from lake measurements, and they depend on the scale of the contaminant cloud. Figure 5.7 shows the difference in the growth of the horizontal size of the contaminant cloud for different experiments, and Table 5.4 lists eight sets of parameters a and b for lake measurements. Peeters and Hofmann (2015) give $a = 1.27\times10^{-4}$ and $b = 1.1$ for length scales between 200 and 1,200 m, while Choi et al. (2020) give $a = 1.1\times10^{-4}$ and $b = 1.09$ for length scales between 1,460 and 8,000 m. Therefore, KAcLake uses average values of $a = 1.2\times10^{-4}$ and $b = 1.1$ for all cases.

APPENDIX B: STANDARD OPERATING PROCEDURES FOR FIELD SAMPLING

Standard Operating Procedure for Field Sampling

December 17, 2019

Safety

- Dress warmly and bring extra footwear and clothes.
- Wear safety vests.
- Deploy traffic cones and a safety light.
- Ensure phones are charged.
- Bring hand warmers, a shovel, and a first aid kit.

Equipment checklist

- First aid kit
- One 2-liter bottle for each site plus extra (12)
- ISCO bottles
- Tools (+ drill)
- Labels
- Sharpies
- Bucket and rope
- Cooler with ice
- YSI sonde
- ISCO 2150 and 6700 manuals
- Towels
- Batteries for the ISCO samplers
- Shovels
- Automobile window scraper and brush
- Car charger/inverter
- Crow bar
- Pick
- Keys for the sampler boxes
- Multimeter
- Hot water
- Soil sampler
- Standard operation procedure
- Gas meter
- Ladder
- Safety vests
- Traffic cones
- Safety light
- Laptop with FlowLink
- Lab book and pen

Sampling at Brewery Creek and Lake Superior

1. Label bottles according to the protocol below.
2. Rinse bottle and cap three times and dump downstream before taking sample.
3. Collect the sample at Lake Superior with the rope and bucket.
4. Store samples on ice.
5. Measure pH, dissolved oxygen, and conductivity with the YSI sonde. At the lake, measure in one of the samples to avoid danger from icy rocks.

Sampling in storm sewers

Preparing for sampling

1. Remove manhole cover and take out the ISCO 2150 data logger.
2. Check life of the batteries in the ISCO equipment and change if necessary.
3. Program ISCO 2150.
4. Record field notes on the program. Include field time, start time, and pacing.

   Example: Visited site at 2:00 pm, set it to start at 5:00 pm, 2 samples/bottle, 500 mL every 3 hours.

5. Change manhole sampler battery + add handwarmers.
6. Place samplers and ISCO 2150s in the drain (or lock the box).

Retrieving the data and samples

1. Clear snow from site and solar panel.
2. Remove manhole cover and take out the ISCO 2150 datalogger.
3. Download the flow data from the ISCO 2150.
4. Check life of batteries in the ISCO equipment and change if necessary.
5. Either remove ISCO from the storm drain or open the sampler box.
6. Recover samples and place lids with numbered labels on them.
7. Store samples on ice.
8. Check notes from pre-event and record samples collected.

Labeling

Label samples with “Location-site-MM/DD/YY” where

Location = I35, BB (Blatnik Bridge), or CE (Central Entrance)

Site = KAc, Cl, BC (Brewery Creek), RP (Rice Point) or LS (Lake Superior)

For processed samples (in falcon tubes), indicate filtered (F) or non-filtered (NF) and acidified (A) or not acidified (NA). List the acid and concentration. For example, a filtered and acidified sample from the KAc site for I-35 would be labeled.

I35-KAc-11/27/19

F/A 1% HNO_3

A sample from the site downstream of Central Entrance (i.e., Brewery Creek) that is acidified and not filtered would be labeled as follows:

CE-BC-11/27/19

NF/A 0.5% HCl

A sample from the bucket underneath Blatnik Bridge that was neither filtered nor acidified would be labeled as follows:

BB-KAc-11/27/19

NF/NA

Samples from grab samples should include A, B, or C to indicate the grab sample from which it was taken. For example:

I35-LS-11/27/19 A

F/A 1% HNO_3

Samples collected by programming the ISCO sampler should include field notes indicating the time and volume of each sample.

Example: Visited site at 2:00 pm, set it to start at 5:00 pm, 2 samples/bottle, 500 mL every 3 hours.

Then, if the sampler is programmed as in this example on 12/2 at the NaCl Central Entrance site (Pecan), the first three samples would be labeled as follows:

- CE-Cl-12/2/19 A: The first and second 500 mL samples, collected at 5:00 pm and 8:00 pm.
- CE-Cl-12/2/19 B: The third and fourth 500 mL samples, collected at 11:00 pm and 2:00 am (12/3).
- CE-Cl-12/3/19 C: The fifth and sixth 500 mL samples, collected at 5:00 am and 8:00 am on 12/3.

Notice that the date on the label is the date of the earliest sample collected—e.g., 12/2 on sample B but 12/3 on sample C.

APPENDIX C: CLOUD SIZE IN A LAKE

The size of the contaminant cloud in a lake is defined in terms of the moments of the concentration distribution *C* (Peeters et al. 1996). The mass *M* of contaminant is given by

$$M = \int_V C dV \tag{C.1}$$

where the integral is computed over the volume *V* of the lake. The center of mass in the i^{th} coordinate direction is

$$\bar{x}_i = \frac{1}{M} \int_V x_i C dV \tag{C.2}$$

and the covariance is

$$\sigma_{ij}^2 = \frac{1}{M} \int_V (x_i - \bar{x}_i)(x_j - \bar{x}_j) C dV \tag{C.3}$$

The variances in the directions of the major and minor principal axes of the elliptical cloud can then be computed as

$$\sigma_{ma}^2 = \frac{\sigma_1^2 + \sigma_2^2}{2} + \sqrt{\frac{\left(\sigma_1^2 + \sigma_2^2\right)^2}{4} - \sigma_1^2 \sigma_2^2 + \sigma_{12}\sigma_{21}}$$
$$\sigma_{mi}^2 = \frac{\sigma_1^2 + \sigma_2^2}{2} - \sqrt{\frac{\left(\sigma_1^2 + \sigma_2^2\right)^2}{4} - \sigma_1^2 \sigma_2^2 + \sigma_{12}\sigma_{21}} \tag{C.4}$$

where the subscripts 1 and 2 indicate the two horizontal directions. With these definitions, the contaminant cloud is modeled as an ellipse with lengths of $2\sigma_{ma}$ and $2\sigma_{mi}$ along the major and minor principal directions, respectively. Then, the cloud size can be computed as

$$\sigma^2 = 2\sigma_{ma}\sigma_{mi} \tag{C.5}$$

As noted in the report for task 5a, the model for large lakes will focus on the horizontal extent of the contaminant cloud. An estimate of the concentrations can be obtained by noting that if the concentrations are normally distributed (i.e., they follow Gaussian distributions in the horizontal directions), then 86% of the mass is contained within the ellipse (Peeters and Hofmann 2015).